

Copyright Warning & Restrictions

The copyright law of the United States (Title 17, United States Code) governs the making of photocopies or other reproductions of copyrighted material.

Under certain conditions specified in the law, libraries and archives are authorized to furnish a photocopy or other reproduction. One of these specified conditions is that the photocopy or reproduction is not to be “used for any purpose other than private study, scholarship, or research.” If a user makes a request for, or later uses, a photocopy or reproduction for purposes in excess of “fair use” that user may be liable for copyright infringement,

This institution reserves the right to refuse to accept a copying order if, in its judgment, fulfillment of the order would involve violation of copyright law.

Please Note: The author retains the copyright while the New Jersey Institute of Technology reserves the right to distribute this thesis or dissertation

Printing note: If you do not wish to print this page, then select “Pages from: first page # to: last page #” on the print dialog screen

The Van Houten library has removed some of the personal information and all signatures from the approval page and biographical sketches of theses and dissertations in order to protect the identity of NJIT graduates and faculty.

ABSTRACT

APPLICATION OF SIGNAL PROCESSING TECHNIQUES FOR MEASUREMENT OF MUSCLE FIBER CONDUCTION VELOCITY

by

Satheesh Kumar Swaminathan

The objectives of this study were to evaluate if muscle fiber conduction velocity (MFCV) could be used as a reliable indicator of fatigue and to characterize the recovery of MFCV after a fatiguing contraction. The decline of MFCV with fatigue was modelled using linear regression and compared with the decline in median frequency (MF). It was found that the percent decline in MF with fatigue was greater than that of MFCV with fatigue and that the decline of MFCV was consistent in all subjects tested. It was thus determined that MFCV could be used as a reliable indicator of fatigue. Possible explanations for the recovery of MFCV after fatigue were given. The recovery curves for all subjects were curve fit using the exponential peeling technique. A comparison of the time constants showed that 8 out of 9 subjects had values between 2-4 minutes, indicating that the recovery process had a similar response in these 8 subjects.

Decomposition of the EMG is a useful tool which helps us better understand the functioning of the neuromuscular system. An algorithm was developed to decompose the EMG into its constituent motor units based on the work done by Deluca et al. Preliminary results were obtained. However, further research is needed in this area.

**APPLICATION OF SIGNAL PROCESSING TECHNIQUES
FOR MEASUREMENT OF MUSCLE FIBER CONDUCTION VELOCITY**

by
Satheesh Kumar Swaminathan

**A Thesis
Submitted to the Faculty of
New Jersey Institute of Technology
in Partial Fulfillment of the Requirements for the Degree of
Master of Science in Biomedical Engineering**

Biomedical Engineering Committee

May 1995

Blank Page

APPROVAL PAGE

**APPLICATION OF SIGNAL PROCESSING TECHNIQUES
FOR MEASUREMENT OF MUSCLE FIBER CONDUCTION VELOCITY**

Satheesh Kumar Swaminathan

Dr. Stanley Reisman, Thesis Advisor Date
Professor of Electrical Engineering
and Associate Chair for Graduate Studies, NJIT

Dr. David Kristol, Committee Member Date
Professor of Chemistry and Director of the
Biomedical Engineering Program, NJIT

Dr. Thomas Findley, Committee Member Date
Associate Professor of Medicine, UMDNJ and
Director of Research, Kessler Institute for Rehabilitation

BIOGRAPHICAL SKETCH

Author: Satheesh Kumar Swaminathan

Degree: Master of Science in Biomedical Engineering

Date: May 1995

Undergraduate and Graduate Education:

- Master of Science in Biomedical Engineering,
New Jersey Institute of Technology, Newark, NJ, 1995
- Bachelor of Engineering in Electronics and Communication Engineering,
University of Madras, Madras, India, 1993

Major: Biomedical Engineering

Presentations and Publications:

S. K. Swaminathan, H. Gage and D. Kristol, “ The Man Machine Interaction in Central Nursing Stations,” 20th Annual Northeast Bioengineering Conference, Massachusetts, U.S.A, March 1994.

This thesis is dedicated to my parents
Ramaswamy Meenakshi and Annaswamy Swaminathan,
my beloved grandmother Ramaswamy Muthulakshmi,
my family, friends and colleagues.

ACKNOWLEDGMENT

The author wishes to express his sincere gratitude to his thesis advisor Dr. Stanley Reisman. He provided more guidance, encouragement and support than was his obligation, without which this thesis could not have been completed.

The author thanks Dr. Thomas Findley for having provided the infrastructure for doing research at Kessler Institute for Rehabilitation and for serving as a member of the committee.

A big thank you to Dr. David Kristol for his continued support and encouragement to the author's research and for serving as a member of the committee.

Special thanks to Dr. Kozo Hanayama, who worked with the author on this project and provided valuable medical information. The author also thanks John Andrews, for taking interest in his project, and offering innovative and creative solutions to the various problems encountered during this research.

Last but not the least, the author thanks all his colleagues and the administrative staff at Kessler Institute for Rehabilitation. Their encouragement and support is greatly appreciated.

TABLE OF CONTENTS

Chapter	Page
1 INTRODUCTION.....	1
1.1 Physiology of the Muscle.....	1
1.1.1 Resting and Action Potential.....	1
1.1.2 Mechanism of Contraction of Muscle.....	6
1.1.3 The Motor Unit.....	11
1.2 Anatomical Details of the Muscle Under Study.....	13
1.2.1 Skeleton of the Wrist and the Hand.....	13
1.2.2 The Abductor Digiti Minimi Muscle.....	13
1.3 EMG.....	16
1.4 Muscle Fiber Conduction Velocity.....	18
1.4.1 Literature Review.....	19
1.4.2 Signal Processing (The Correlation Function).....	22
1.5 Mathematical Techniques.....	27
1.5.1 Linear Regression.....	27
1.5.2 The Exponential Peeling Technique.....	29
1.6 Precision Decomposition of the EMG Signal.....	31
1.6.1 Literature Review.....	33
1.6.2 Signal Processing (Precision Decomposition).....	34
1.7 Scope of Thesis.....	37

TABLE OF CONTENTS
(Continued)

Chapter	Page
2 METHODS.....	39
2.1 Experimental Protocol.....	39
2.2 Electrode Placement and Configuration.....	42
2.3 Data Acquisition.....	44
2.4 Data Analysis (Signal Processing).....	45
2.4.1 Estimation of Muscle Fiber Conduction Velocity.....	45
2.4.2 Precision Decomposition of the EMG.....	46
3 RESULTS AND DISCUSSION.....	47
3.1 Muscle Fiber Conduction Velocity (MFCV).....	47
3.1.1 MFCV (Fatigue).....	47
3.1.2 MFCV (Recovery).....	53
3.2 Precision Decomposition of the EMG Signal.....	61
(Preliminary Results)	
3.2.1 Discussion of Results.....	61
APPENDIX A REMAINING RESULTS A.1 Muscle Fiber Conduction Velocity.....	82
A.2 MFCV (Recovery).....	85
A.3 Precision Decomposition.....	97
APPENDIX B INSTRUMENTATION B.1 Precision Load Cells	100

TABLE OF CONTENTS
(Continued)

Chapter	Page
B.2 Instrumentation Amplifier.....	102
B.3 Isolated Preamplifier..... (Model 13-5407-58)	104
B.4 Data Acquisition Board..... (Keithley Das1601)	105
APPENDIX C DATA ACQUISITION.....	106
APPENDIX D FLOWCHARTS AND PROGRAMMING DETAILS	109
D.1 Muscle Fiber Conduction Velocity..... (MFCV)	109
D.2 Precision Decomposition.....	117
REFERENCES.....	129

LIST OF FIGURES

Figure	Page
1.1a Diffusion Potential.....	4
1.1b Establishment of Resting Membrane Potentials in Muscle fibers.....	5
1.2 A Typical Action Potential.....	6
1.3a Basic Structure of Human Skeletal Muscle.....	7
1.3b Two Chains of Troponin in a Thin Filament Block the Cross Bridge Binding Sites on Actin.....	7
1.4 Sequence of Events Leading to the Contraction of Muscle.....	8
1.5 Effect of Ca ++ Ions on Troponin and Tropomyosin Molecules.....	9
1.6 Relaxed and Contracted Conditions of the Sarcomere.....	9
1.7 Structure of a Motor Unit.....	12
1.8 Dorsal View of the Bones of the Wrist and the Hand.....	14
1.9a Anatomy of the Abductor Digiti Minimi Muscle.....	15
1.9b Location of the ADM Muscle in the Palm (Ventral View).....	16
1.10 A Typical EMG Recorded from the ADM Muscle.....	17
1.11 Power Spectrum of EMG Signal in Figure 1.10	18
1.12 Two Sine Waves Shifted in Time.....	23
1.13 Correlogram of Two Sine Waves.....	24
1.14a Four Channels of the Typical EMG signal.....	25
1.14b Correlogram Between Channel 1 and Channel 2.....	25
1.16 Method for Decomposition of the Myoelectric Signal.....	31
2.1 Flowchart Explaining Protocol.....	41

LIST OF FIGURES
(Continued)

Figure	Page
2.2 Schematic of the Active Electrode.....	43
3.1 Decline of MFCV with Fatigue.....	48
3.2 Decline of Median Frequency with Fatigue.....	49
3.3 MFCV Decline with Fatigue.....	51
3.4 Decline of Median Frequency with Fatigue.....	52
3.5 Graphical Illustration of MFCV (Recovery) of Subject 4.....	54
3.6 Curve Fitted MFCV Data (subject 4).....	56
3.7 Peeled MFCV Data (Subject 4).....	56
3.8 Graphical Illustration of MFCV (recovery): Subject 6.....	58
3.9 Curve Fitted MFCV Data (Subject 6).....	60
3.10 Peeled MFCV Data.....	60
3.11 Original Filtered Signal.....	61
3.12 Amplitude Thresholded Signal.....	61
3.13 Decomposed Signal (Unit I).....	62
3.14 Decomposed Signal (Unit II).....	62
3.15 Template (Unit I).....	62
3.16 Template (Unit II).....	62
3.17 Decomposed Signal (Unit I).....	63
3.18 Template (Unit I).....	63
3.19 Three Channels of the Filtered Original Signal.....	65

LIST OF FIGURES
(Continued)

Figure	Page
3.20 Amplitude Thresholded Signal (TS).....	65
3.21 Decomposed Signal (Unit I).....	65
3.22 Decomposed Signal (Unit II).....	65
3.23 Template (Unit I).....	66
3.24 Template (Unit II).....	66
3.25 Filtered Original EMG Signal (Subject B).....	69
3.26 Amplitude Thresholded Signal (Subject B).....	69
3.27 Decomposed Signal (Unit I).....	69
3.28 Decomposed Signal (Unit II).....	69
3.29 Template 1 (Unit I).....	69
3.30 Template 2 (Unit II).....	69
3.31 Decomposed Signal (Decision Criterion: 0.35).....	70
3.32 Template I (Unit I).....	70
3.33 Subject B: Original Filtered Signal (1.024 secs.).....	71
3.34 Amplitude Thresholded Signal (TS).....	71
3.35 Decomposed Signal (Unit I).....	71
3.36 Template I (Unit I).....	71
3.37 Original Signal (1.35 seconds).....	71
3.38 Amplitude Thresholded Signal (TS).....	71
3.39 Decomposed Signal (Unit I).....	72

LIST OF FIGURES
(Continued)

Figure	Page
3.40 Decomposed Signal (Unit II).....	72
3.41 Decomposed Signal (Unit III).....	72
3.42 Template I (Unit I).....	72
3.43 Template II (Unit II).....	72
3.44 Template III (Unit III).....	72
A.1.1 Decline of MFCV with Fatigue (Subject 8).....	82
A.1.2 Decline of Median Frequency with Fatigue (Subject 8).....	83
A.1.3 Decline of MFCV with Fatigue (Subject 3).....	84
A.1.4 Decline of Median Frequency with Fatigue (Subject 3).....	84
A.2.1 Curve Fitted MFCV Data (Subject 1).....	86
A.2.2 Peeled MFCV Data (Subject 1).....	86
A.2.3 Curve Fitted MFCV Data (Subject 2).....	88
A.2.4 Peeled MFCV Data (Subject 2).....	88
A.2.5 Curve Fitted MFCV Data (Subject 3).....	90
A.2.6 Peeled MFCV Data (Subject 3).....	90
A.2.7 Curve Fitted MFCV Data (Subject 5).....	91
A.2.8 Peeled MFCV Data Points (Subject 5).....	91
A.2.9 Curve Fitted MFCV Data (Subject 7).....	93
A.2.10 Peeled MFCV Data (Subject 7).....	93
A.2.11 Curve Fitted MFCV Data (Subject 8).....	95

LIST OF FIGURES
(Continued)

Figure	Page
A.2.12 Peeled MFCV Data (Subject 8).....	95
A.2.13 Curve Fitted MFCV Data (Subject 9).....	96
A.2.14 Peeled MFCV Data (Subject 9).....	96
A.3.1 Filtered Original Signal (0.58 secs.).....	97
A.3.2 Amplitude Thresholded Signal (55 mV).....	97
A.3.3 Unit I	97
A.3.4 Decomposed Signal (Unit II).....	97
A.3.5 Template 1 (Unit I).....	97
A.3.6 Template 2 (Unit II).....	97
A.3.7 Amplitude Threholded Signal (55 mV).....	98
A.3.8 Decomposed Signal (0.35) (Unit I).....	98
A.3.9 Decomposed Signal (Unit II).....	98
A.3.10 Template I (Unit I).....	98
A.3.11 Template II (Unit II).....	98
A.3.12 Original Filtered Signal (300 Hz).....	99
A.3.13 Amplitude Thresholded Signal (55 mV).....	99
A.3.14 Decomposed Signal (Unit I).....	99
A.3.15 Decomposed Signal (Unit I).....	99
A.3.16 Ttemplate I (Unit I).....	99
A.3.17 Template II (Unit II).....	99

LIST OF FIGURES
(Continued)

Figure	Page
B.1 The SENSOTEC Load Cell (Model 31).....	101
B.2 Dimensions of the SENSOTEC Load Cell.....	101
B.3a Settings available in GOULD Amplifier (13-4615-58).....	103
B.3b A Typical Experimental Configuration of the GOULD (13-4615-58) Amplifier..	103
B.4 The Isolated Preamplifier.....	104
D.1 Flowchart Showing the Steps Involved in the Computation of MFCV.....	111
D.2 Flowchart Outlining the Steps to be Carried Out During the Precision Decomposition Technique.....	118

LIST OF TABLES

Table	Page
3.1 MFCV (Fatigue) and Median Frequency (Subject 4).....	48
3.2 MFCV (Fatigue) and Median Frequency (Subject 5).....	51
3.3 A Comparison between the Percent Change in MFCV to that of MF.....	52
3.4 MFCV (Recovery): Subject 4	54
3.5 Smoothed MFCV Data Points Plotted using the Exponential Peeling Method (Subject 4).....	55
3.6 MFCV (Recovery): Subject 6	58
3.7 Smoothed MFCV Data Points Plotted using the Exponential Peeling Method (Subject 6).....	59
3.8 Time Constants of the Subjects Tested.....	59
A.1.1 MFCV (Fatigue) and Median Frequency (Subject 8).....	82
A.1.2 MFCV (Fatigue) and Median Frequency (Subject 3).....	83
A.1.3 MFCV (Fatigue): Subject 7.....	84
A.1.4 MFCV (Fatigue): Subject 2.....	85
A.2.1 MFCV Recovery (Subject 1).....	85
A.2.2 Smoothed MFCV Data Points Plotted using the Exponential Peeling Technique (Subject 1).....	85
A.2.3 MFCV Recovery (Subject 2).....	87
A.2.4 Smoothed MFCV Data Points Plotted using the Exponential Peeling Technique (Subject 2).....	87
A.2.5 MFCV Recovery (Subject 3).....	87

LIST OF TABLES
(Continued)

Table	Page
A.2.6 Smoothed MFCV Data Points Plotted using the Exponential Peeling Technique (Subject 3).....	89
A.2.7 MFCV Recovery (Subject 5).....	89
A.2.8 Smoothed MFCV Data Points Plotted using the Exponential Peeling Technique (Subject 5).....	89
A.2.9 MFCV Recovery (Subject 7).....	92
A.2.10 Smoothed MFCV Data Points Plotted using the Exponential Peeling Technique (Subject 7).....	92
A.2.11 MFCV Recovery (Subject 8).....	92
A.2.12 Smoothed MFCV Data Points Plotted using the Exponential Peeling Technique (Subject 8)	94
A.2.13 MFCV Recovery (Subject 9).....	94
A.2.14 Smoothed Data Points Plotted using the Exponential Peeling Technique (Subject 9).....	94

CHAPTER 1

INTRODUCTION

Biomedical Engineering is an interdisciplinary field. It requires inputs from physicians, physiologists and engineers. The contribution of each of the three groups of people is essential to the understanding of certain pathological problems in the human body. As an engineer in the field of Biomedical Engineering, I have used engineering tools to estimate and characterize the myoelectric signal, namely the electrical signal that is picked up from electrodes, as a result of the activity of the underlying muscle fibers. The following document describes the research conducted in, developing a method for estimating the conduction velocity of the muscle fiber using the technique of cross correlation, and developing and implementing a method for decomposing a myoelectric signal into its constituent motor units.

1.1 Physiology of the Muscle

Muscles are tissues that tend to shorten upon chemical and electrical stimulation [4]. The underlying mechanisms of contraction of the muscle and certain fundamental concepts will be discussed below.

1.1.1 Resting and Action Potential

A cell (muscle or nerve cell) has two environments namely, the internal environment and the external environment [1]. A muscle/nerve cell contains a high concentration of

potassium ions and a lower concentration of sodium and chloride ions in its internal environment. Conversely, the external environment of the muscle cell/nerve cell contains a larger concentration of sodium and chloride ions and a lesser concentration of potassium ions.

The cell membrane of a muscle cell (sarcolemma) is selectively permeable. This means that the membrane is more permeable to certain ions and less permeable to others. There are other mechanisms which are responsible for the establishment of the resting membrane potential. One of these is active transport and in the case of muscle cells the active transport pump (Na - K- ATP ase Pump) transports 3 sodium ions out of the cell (into the interstitial fluid) in exchange for 2 potassium ions (into the intracellular fluid) at the expense of 1 molecule of ATP (Adenosine Triphosphate) [1]. As a result of this pump we have a charge separation across the plasma membrane of the muscle cell i.e greater concentration of sodium ions outside the plasma membrane and larger concentration of potassium ions inside the membrane (inside the cytosol). A definition of equilibrium potential at this point will help us better understand the establishment of the resting and action potential. The equilibrium potential is that potential at which the electric force is equal to the concentration force (gradient) across the membrane. At the equilibrium potential there is no net movement of the ion, because the opposing forces acting on it are exactly balanced [1].

With these concepts in mind we can go into the mechanisms which are responsible for establishment of the resting and action potential. As described earlier a muscle cell has a larger intracellular concentration of potassium ions and a larger

extracellular concentration of sodium and chloride ions. It is also known that the plasma membrane of the muscle cell is 75 times more permeable to potassium than to that of sodium. Hence the inner side of the plasma membrane is negative as compared to the outside due to the increased concentration of the K^+ ions inside the cell and Na^+ ions outside the cell. Due to the increased permeability of the plasma membrane to the K^+ ions, the resulting potential across the membrane, which is often referred to as the resting membrane potential, is closer to the equilibrium potential of the K^+ ions than that of the Na^+ ions. The role of the chloride ions is relatively minor because the cell membrane is permeable to chloride ions and so the equilibrium potential of the chloride ions is equal to the resting membrane potential of the plasma membrane[1].

A typical value for the resting membrane potential is -90 mv, the inside of the membrane being more negative than the outside. The equilibrium potential of potassium is -94 mV and that of sodium is +61mV [1]. Referring to figure 1.1b we observe that there is a diffusion of K^+ and Na^+ ions into and out of the cell. The net equilibrium potential (EP) across the cell membrane depends upon the EPs of all the interacting ions. Hence the resting membrane potential or the net equilibrium potential (measured with respect to the inside of the cell) has a value closer to that of the EP of potassium, owing to the higher concentration of potassium ions inside the cell membrane.

Whenever the plasma membrane is subjected to a stimulus eg. electrical, the permeability of the membrane changes due to the opening up of voltage gated sodium channels. This causes an influx of sodium ions into the cell thereby changing the membrane potential of the plasma membrane from its resting potential value. As a result the potential of the

membrane rises rapidly in the positive direction. The normal polarized state of -90 mV is lost and in most cases the potential overshoots beyond the zero level and becomes positive, a typical range being $20 - 35\text{ mV}$ [2]. This rapid change in the potential of the membrane from a value of -90 mV to $+20\text{ mV}$ is called **depolarization** and it is the depolarization which results in an **action potential**. Following the depolarization (within 0.0001 seconds) the sodium channels begin to close and potassium channels open more than normally. Then, rapid diffusion of potassium ions to the exterior re-establishes the normal negative resting membrane potential. This is called **repolarization** of the membrane [2]. The typical duration of a muscle action potential is 1 millisecond. Figure 1.2 illustrates a typical action potential.

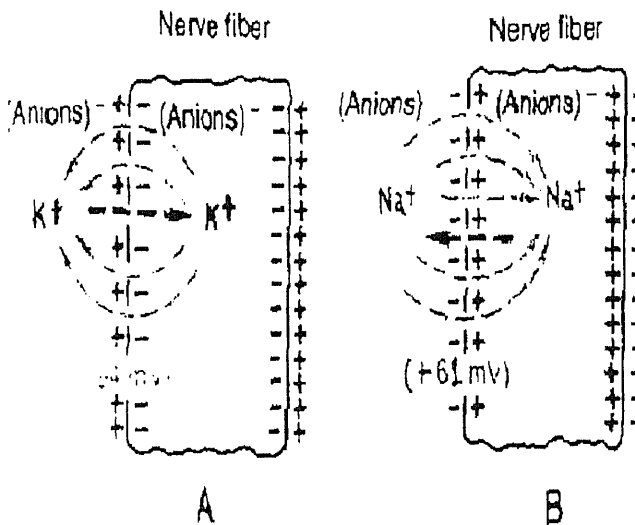


Figure 1.1 a

Diffusion Potential

- A) Establishment of Diffusion Potential due to Potassium ions diffusing from inside the Cell to the outside through a membrane that is permeable only to potassium.
- B) Establishment of Diffusion Potential when the membrane is permeable only to Sodium ions.

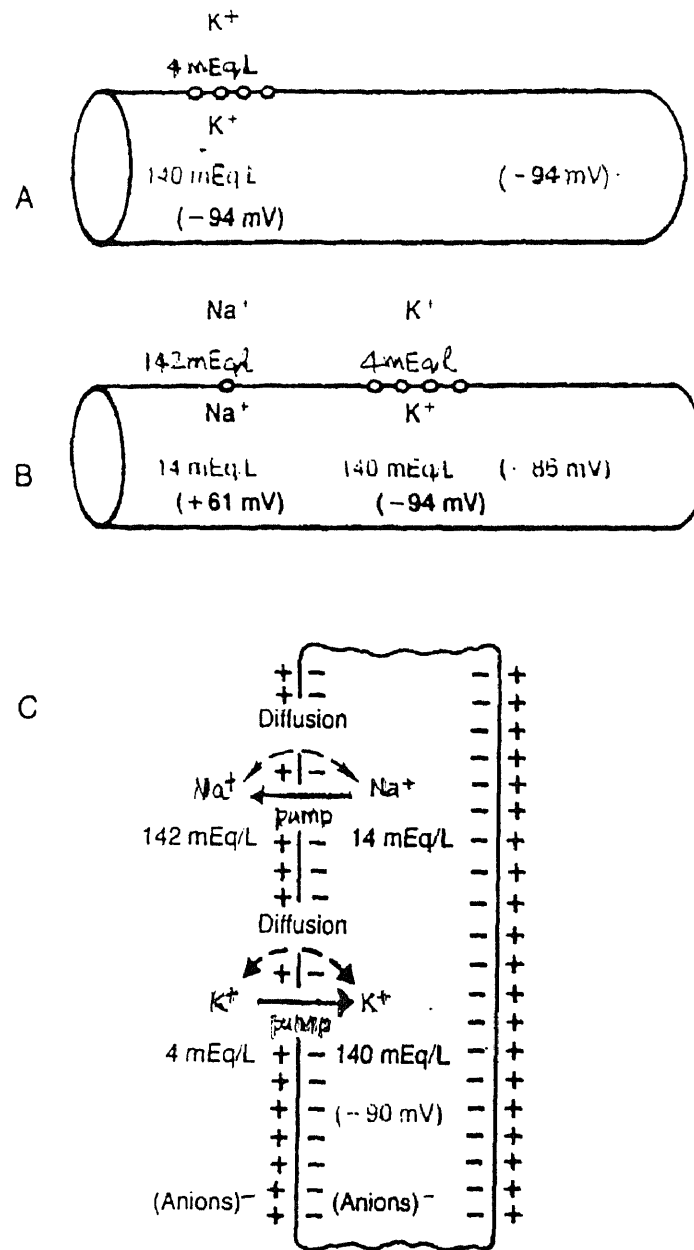


Figure 1.1b

Establishment of Resting Membrane Potentials in Muscle Fibers

- A) When the Membrane Potential is caused by Potassium diffusion alone.
 B) When the Membrane Potential is caused diffusion of both Sodium and Potassium ions.
 C) When the membrane potential is caused by the diffusion of both Potassium and Sodium ions and the pumping of the ions by the Na - K -ATP ase Pump.

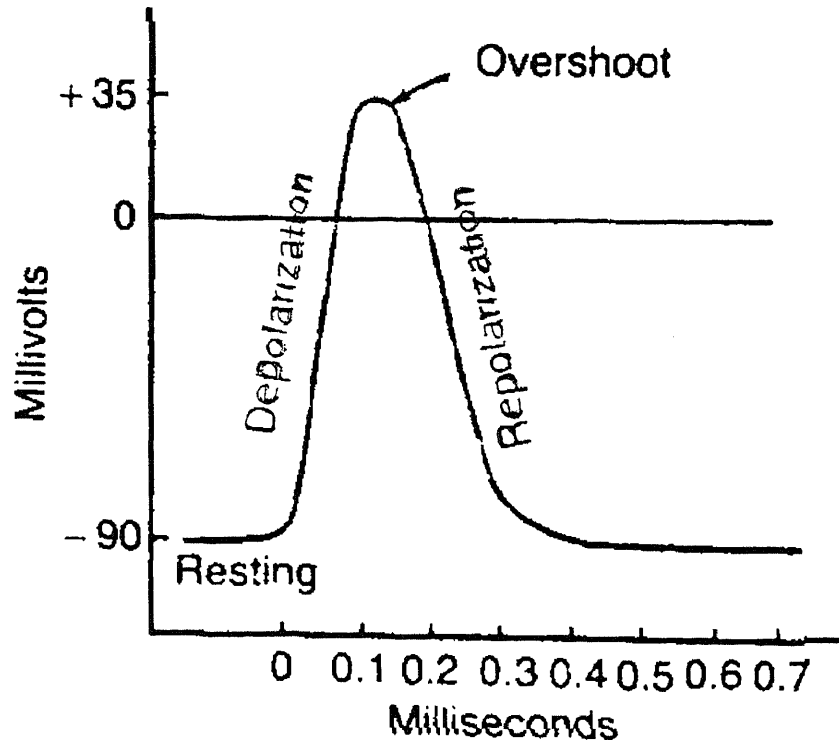


Figure 1.2
A Typical Action Potential

1.1.2 Mechanism of Contraction of Muscle

Figure 1.3 gives the basic structure of a muscle and its constituent elements. As seen in the figure, a muscle is composed of several muscle fibers. Each muscle fiber in turn is made up of a number of **myofibrils** which are cylindrical elements located perpendicular to the axis of the muscle fiber [1]. Each myofibril in turn is composed of number of thick and thin filaments arranged in a repeating pattern along the length of a myofibril. One unit of this repeating pattern is referred to as a **sarcomere**. The **thick filaments** are composed entirely of a contractile protein **myosin** and the **thin filaments** contain the contractile protein **actin** as well as two other proteins **troponin** and **tropomyosin**.

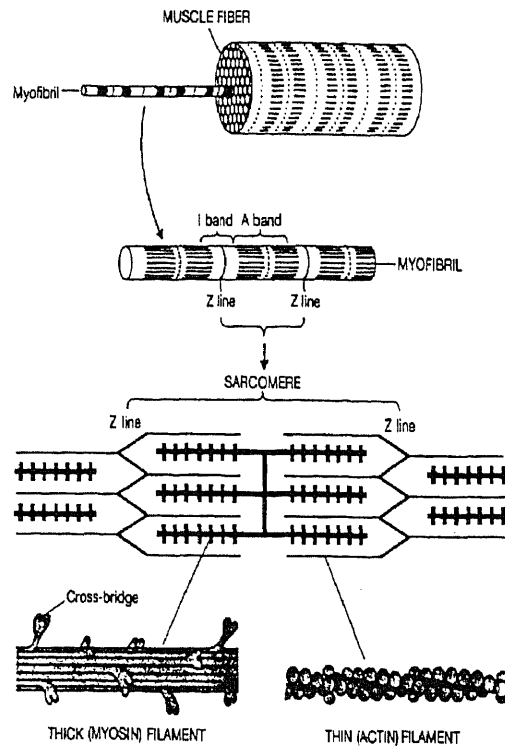


Figure 1.3a
Basic Structure of the Human Skeletal Muscle

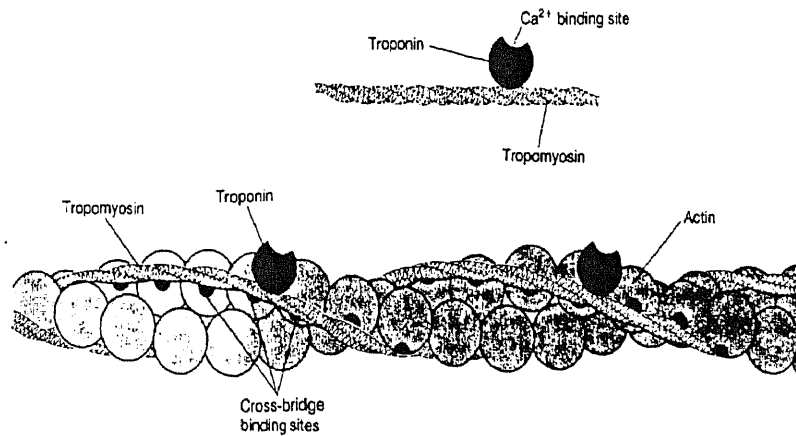


Figure 1.3 b
Two Chains of Troponin in a Thin Filament Block the Cross Bridge Binding Sites on Actin

The thick filaments are located in the center of each sarcomere and their orderly parallel arrangement produces the A band. One end of each actin filament is covered is anchored to a network of interconnecting proteins known as the Z line whereas the other end overlaps a portion of the thick filaments. The H zone is a relatively light band produced in the center of the A band. This region represents only the central part of the thick filaments. The narrow dark band in the center of the H zone is referred to as the M line and is produced by all proteins that bind all the thick filaments in a sarcomere together. Finally, and most important of all the space between adjacent thick and thin filaments is bridged by projections, called **cross bridges** which are portions of myosin molecules that extend from the surface of thick filaments toward thin filaments.

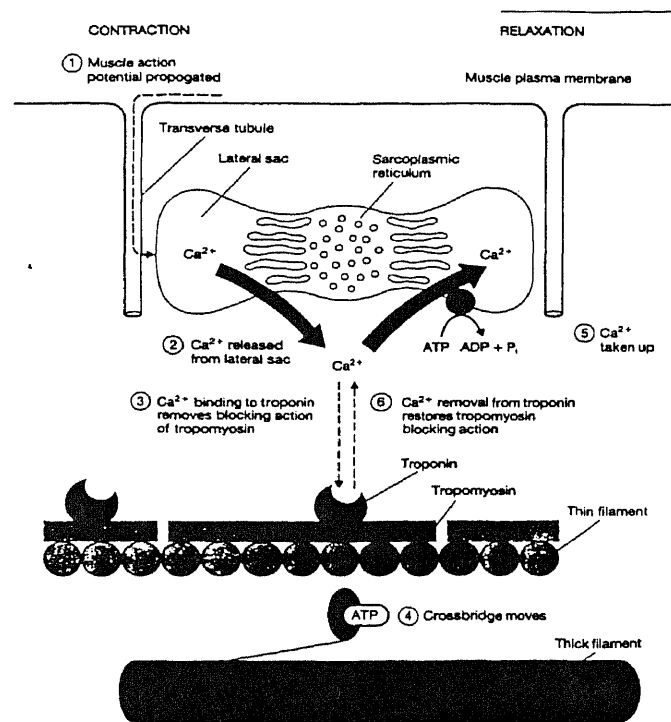


Figure 1.4
Sequence of Events Leading to the Contraction of Muscle

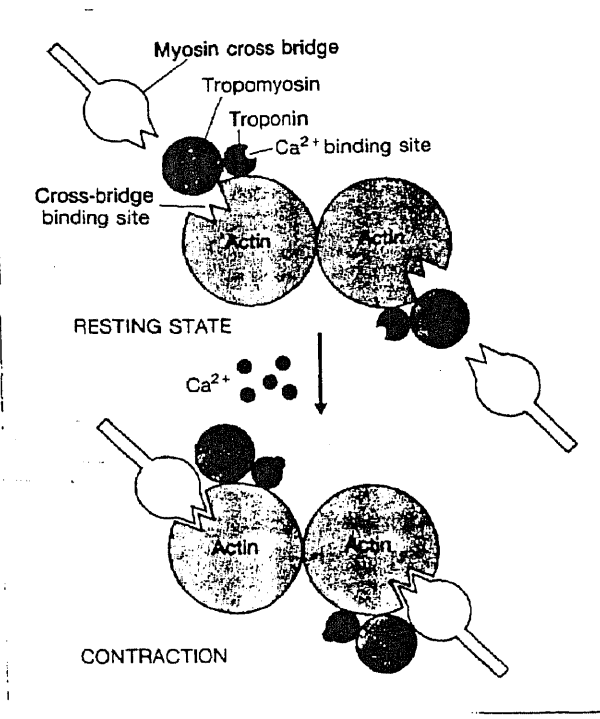


Figure 1.5
Effect of Ca ++ Ions on Troponin and Tropomyosin Molecules.

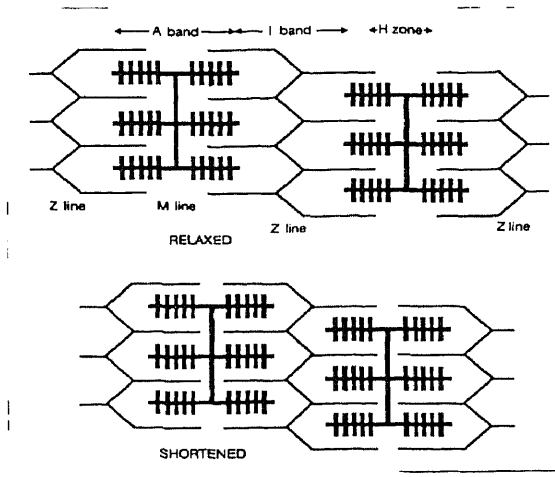


Figure 1.6
Relaxed and Contracted Conditions of the Sarcomere

All the above mentioned contractile proteins play a very important part in the contraction of a muscle fiber as will be explained below. When a nerve impulse i.e action potential from a nerve ending activates the muscle fiber the cross bridges bind to the thin filaments and exert a force on them [1]. Figure 1.4 illustrates the sequence of events which lead to the contraction of a muscle.

When an action potential arrives from a nerve, it propagates along the plasma membrane of the muscle fiber, and is conducted very rapidly along the membrane of the transverse tubules. The propagation of the action potential along the t - tubule triggers the release of Ca^{++} ions from the lateral sacs of the sarcoplasmic reticulum (endoplasmic reticulum in a muscle cell). The free calcium ions then bind to the binding sites on the protein molecule troponin. The activated troponin molecule then pulls the tropomyosin molecules, so that the myosin binding sites on each actin molecule are exposed. Figure 1.5 illustrates the action of the Ca^{++} ion on the troponin and tropomyosin molecules.

Simultaneously, once the muscle fiber receives the nerve impulse, the force generation mechanisms are activated. The overlapping thick and thin filaments of a sarcomere move past each other propelled by the movement of the cross bridges.

During the contraction of the skeletal muscle, the cross bridges (the head of the myosin protein molecule) which are energized by the phosphorylation of the ATP attach to the now opened actin binding sites. Each bound cross bridge then executes a swivelling motion, which forces the thin filaments at either end of the A band toward the M line thereby resulting in a shortening of the sarcomere. This condition is clearly illustrated in figure 1.6.

1.1.3 The Motor Unit

The nerve cells whose axons innervate skeletal muscle fibers are known as motor neurons. The cell bodies of these motor neurons are located either in the brainstem or in the spinal cord. The motor neurons also have the largest axons in the body which enables them to propagate action potentials at high velocities, thereby allowing signals to be transmitted from the central nervous system to the skeletal muscle fibers with minimal delay [1].

Within a muscle, the axon of each motor neuron divides into many branches, each branch forming a single junction with a muscle fiber. Hence, a single motor neuron controls many muscle fibers. However each muscle fiber has only one nerve junction and is therefore controlled by only one motor neuron. A motor neuron plus the fibers that it innervates is called a **motor unit**.

The muscle fibers belonging to a single motor unit although located in one muscle, are scattered throughout the muscle. The important point to be noted is that when an action potential is produced in a single motor neuron, all the muscle fibers belonging to its motor unit contract. Figure 1.7 illustrates the organization of a motor unit.

When a motor neuron fires, it triggers the depolarization of the muscle fiber. The depolarization propagates toward the ends of the muscle fiber, generating two action potentials [3]. The final result of an action potential is the contraction of the muscle fiber. The spatial-temporal superposition of the action potentials for all the muscle fibers of one motor unit is referred to as a motor unit action potential. The sequence of motor unit action potentials through time is the motor unit action potential train[3].

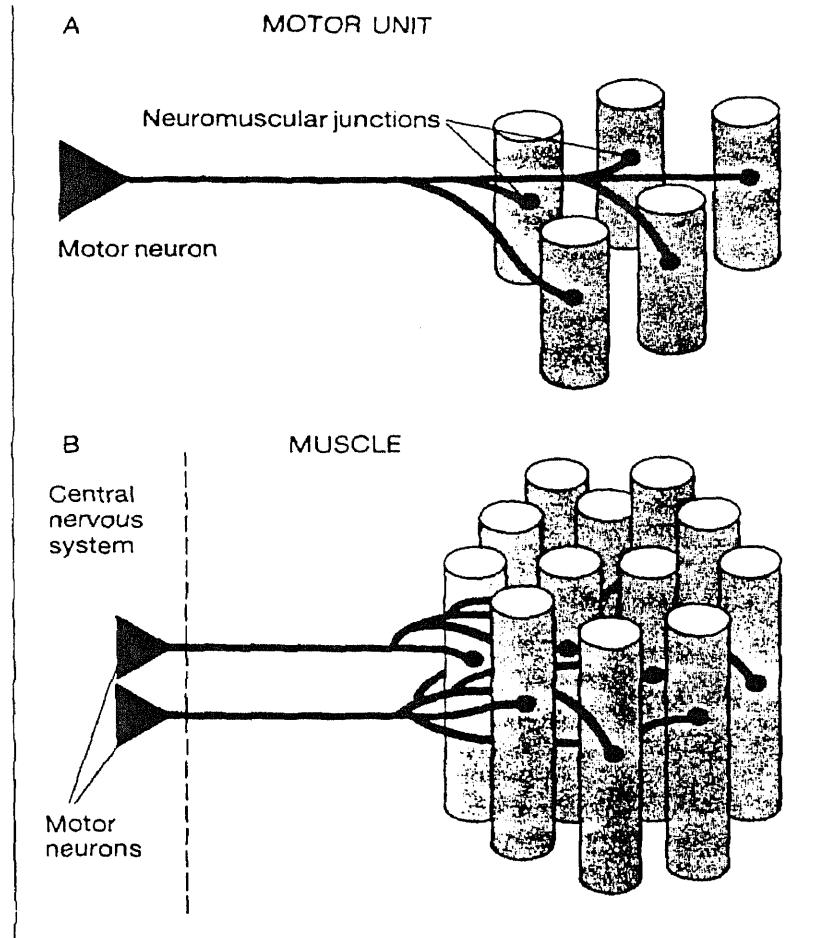


Figure 1.7

Structure of a Motor Unit

- A) Single motor unit consisting of one motor neuron and the fibers that it innervates
- B) Two motor units and their intermingled fibers in a muscle

An electrode placed over the muscle fibers or within the muscle will detect the electromyogram(EMG) which is the summation of the motor unit action potential trains in its vicinity.

1.2 Anatomical Details of the Muscle under Study

1.2.1 Skeleton of the Wrist and the Hand

The skeleton of the carpus or the wrist is composed of eight carpal bones arranged in two rows of four each. In the proximal row, beginning on the radial side, the scaphoid, the lunate and the triquetral bones articulate proximally with the radius and the articular disc of the ulna to form the radiocarpal or wrist proper. They articulate transversely with each other and distally with the distal row of carpals. The distal row, starting on the radial side is made up of the trapezium, trapezoid, capitate and hamate bones. The **pisiform** bone i.e the fourth bone in the proximal row, lies on the anterior surface of the triquetral and articulates with that bone only. The pisiform bone bears posteriorly, a facet for articulation of the triquetral. Figure 1.8 shows the arrangement (dorsal view) of the bones of the wrist and the hand.

1.2.2 The Abductor Digiti Minimi Muscle

The abductor digiti minimi (ADM) muscle was chosen for this research study and hence the anatomy of this muscle will be described in some detail. Figure 1.9 illustrates the attachments of the abductor digiti minimi muscle. The ADM arises from the pisiform bone and often from the adjacent tendon of the flexor carpi ulnaris (described as flexor in figure 1.9) and joins the flexor digiti minimi to insert into the medial side of the base of the proximal phalanx of the little finger. It frequently sends a slip of insertion around the ulnar of the finger to attach into the extensor tendon. The ADM muscle abducts the little finger and helps flex the metacarpophalangeal joint[4].

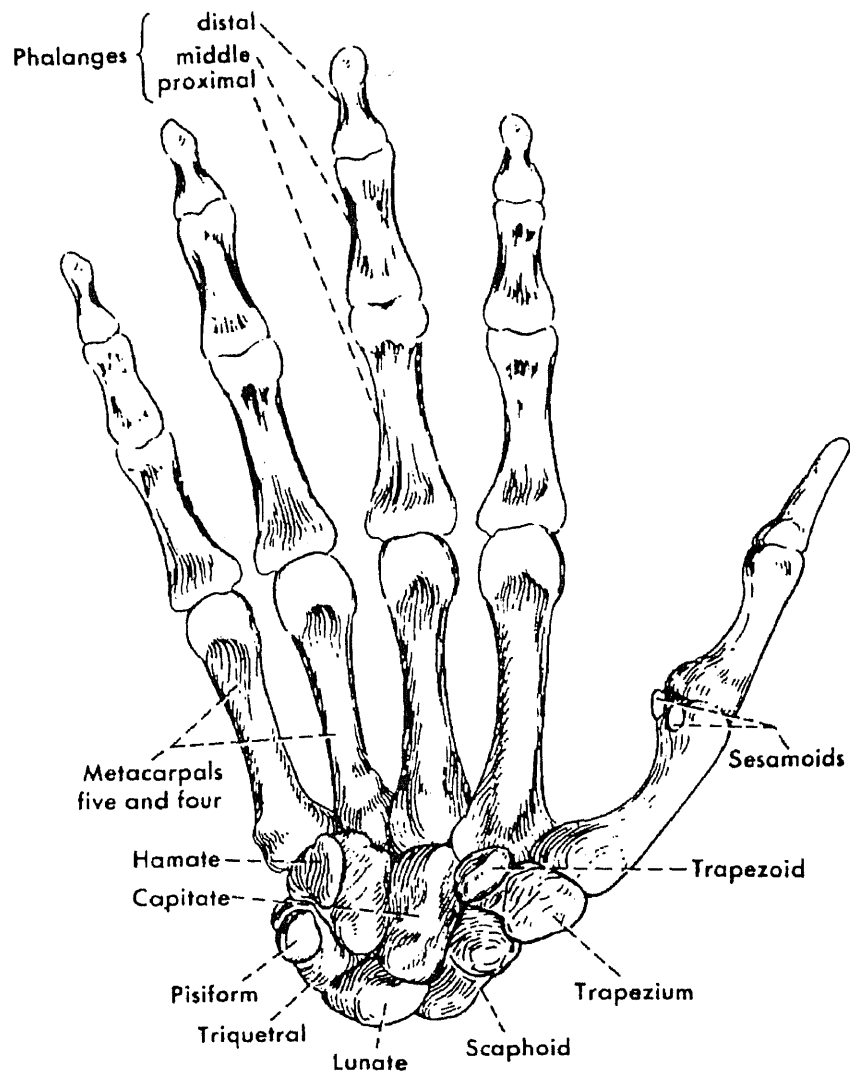


Figure 1.8
Dorsal View of the Bones of the Wrist and the Hand

Any study of conduction velocity requires long muscles consisting of long parallel muscle fibers. This requirement helps to minimize the errors in the measurement of distance between the electrodes. Another reason for the selection of the ADM muscle is

that it has no synergists for contraction of the little finger. Hence this permits us to associate any changes in muscle fiber conduction velocity (MFCV) only to this isolated muscle and this was an important consideration which influenced the selection of this muscle for this study.

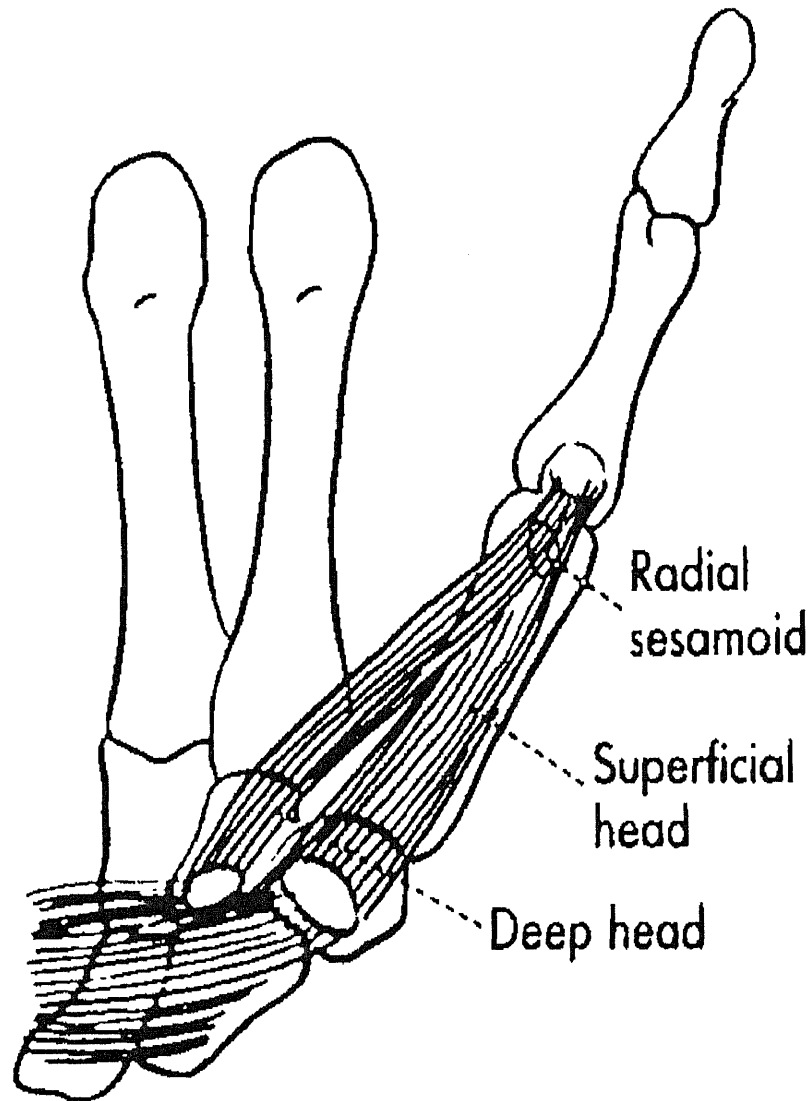


Figure 1.9 a
Anatomy of the Abductor Digiti Minimi Muscle

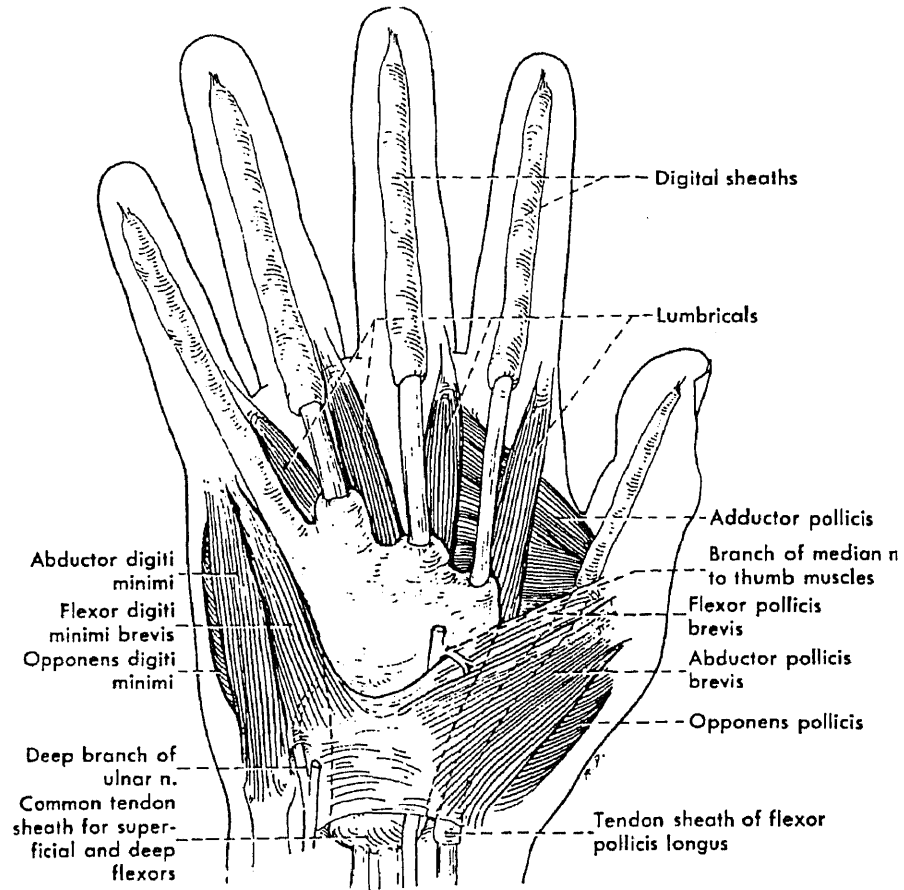


Figure 1.9 b
Location of the ADM Muscle in the Palm (Ventral View)

1.3 EMG

The bioelectric potentials associated with muscle activity constitute the **electromyogram** (EMG). Formally stated the EMG is the name given to the total signal detected by an electrode. It is the algebraic summation of all motor unit action potential trains from all active motor units, within the pickup area of the electrode [5]. These bioelectric potentials may be measured on the surface of the body near a muscle of interest or directly from the muscle, by penetrating the skin with needle electrodes. Since EMG

measurements are usually intended to provide an indication of the amount of activity of a given muscle or a group of muscles, rather than of an individual muscle fiber, the pattern is usually a summation of the individual action potentials from the fibers constituting the muscle, or muscles being measured [6].

The surface EMG electrodes pick up potentials from all the muscles within the range of the electrodes. This implies that potentials from nearby large muscles may interfere with attempts to measure the EMG from smaller muscles, even though the electrodes are placed directly over the smaller muscles.

The amplitude of the EMG signal changes depending on the amount of muscle activity. The amplitude of a typical EMG signal can vary between $50 \mu\text{V}$ to 500mV and the frequency of the EMG can vary between 10Hz to 3000Hz , depending on the type of electrode, the placement of the electrode and the activity of the muscle[7]. A typical EMG recorded from the abductor digiti minimi muscle is shown in figure 1.10 and the power spectrum of this EMG signal is represented in figure 1.11.

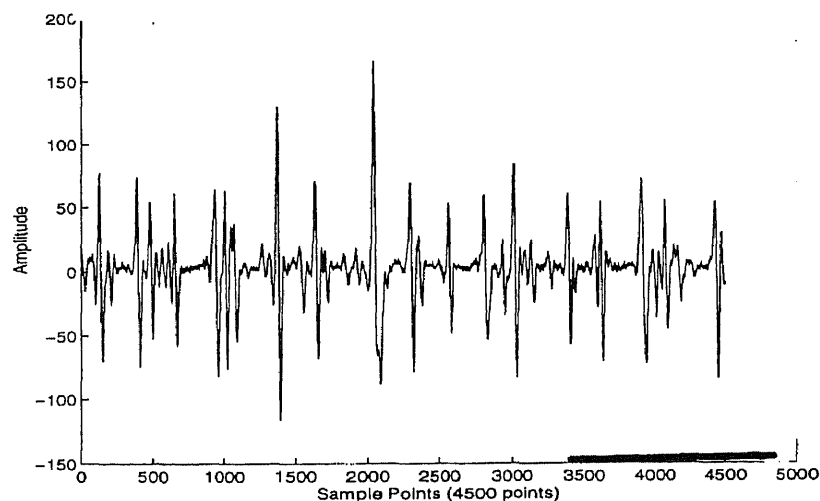


Figure 1.10
A Typical EMG Recorded from the ADM Muscle

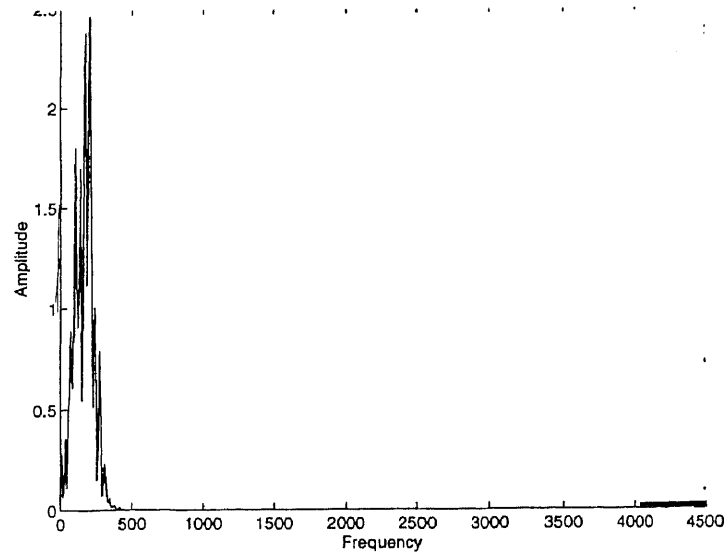


Figure 1.11
Power Spectrum of EMG Signal in Figure 1.10
(Amplitude Units vs Frequency (Hz))

Figure 1.11 gives us the range of frequencies associated with a typical EMG signal.

1.4 Muscle Fiber Conduction Velocity

When an action potential from a motor neuron lands on a motor end plate, this action potential propagates along all the muscle fibers that this motor neuron innervates.

However there is a time delay in the propagation of this action potential between muscle fibers belonging to the same motor unit. The velocity at which this action potential is propagated along the muscle fiber is the muscle fiber conduction velocity.

It is known that median frequency or mean frequency decrease with muscle fatigue. However the causes for the decline in the mean /median frequency are not clearly known. It is suspected that one of the determinants of the decline in the median /mean frequency is muscle fiber conduction velocity (MFCV), others being associated with the

central nervous drive like synchronization of motor units, firing rate, phasic behavior of units rotating between periods of activity and periods of quiescence, temperature, shortening of muscle fiber and accumulation of various metabolites. It has been reported [25], that an increase in temperature is accompanied by an increase of MFCV. The temperature of the dorsal side of the palm was recorded continuously, throughout the experiment. This was done so that the relationship between temperature and MFCV could be better understood and explained. Thus we see that MFCV is an indicator of the state and the physical properties of the muscle and hence it can be used as a diagnostic tool for determining the state and condition of a muscle.

1.4.1 Literature Review

Various studies have been carried out to estimate and quantify the influence of MFCV and the correlation of MFCV with median frequency and mean frequency. Studies were also carried out to isolate and determine the possible factors causing a change in conduction velocity. Nielson, Mills et al. [12], studied the changes in muscle fiber conduction velocity and its influence on mean/median frequency. Their study has a lot of importance to the present work as they made an attempt to quantify the relation between MFCV and median frequency/median frequency. They found that during contraction levels of 10% and 20 % of the maximal voluntary contraction (MVC), the conduction velocity rose as the contraction progressed. This, they hypothesize, could be due to two important factors. During submaximal contractions, there is a recruitment of motor units having faster fiber velocities. This could therefore increase the average muscle fiber

conduction velocity. However at contraction levels above 30% of MVC the conduction velocity was found to decrease owing to the following reasons. Motor units with slow conduction velocities and large twitch tensions and which are usually more resistant to fatigue are recruited during these contraction levels. In this context a twitch is defined as brief contractile response of a skeletal muscle, which is elicited by a single maximal volley of impulses in the motor neuron supplying it [2]. Hence this could cause a decrease in the average conduction velocity. The other explanation for the decline in conduction velocity at contraction levels above 30% MVC could be that certain intramuscular metabolites accumulate during muscle fatigue thereby slowing the velocity in currently active units hence reducing the conduction velocity in the muscle fiber. They also found that there was a strong correlation between the increase in conduction velocity and that of median/mean frequency at 30 and 40% MVC contractions.

Broman et al.[13], conducted a study to evaluate a non-invasive method to measure muscle fiber conduction velocity. They found that by using a double differentiation technique they could eliminate some of the interference that would be introduced due to the cross talk between the two channels. It was also found that the cut off frequency of the (signal) input analog filters could be set such that superimposed action potentials obtained as a result of the reflection at the ends of the muscle could be eliminated. The filter settings were determined as follows. Any action potential train which has a wavelength greater than the length of the muscle itself will be reflected at the ends of the muscle. Taking an empirical value of muscle fiber conduction velocity i.e. 5 m/s (for the biceps), as a first measure we can eliminate these superimposed signals by

setting the input (signal) analog filters to a frequency that corresponds to a wavelength, less than the length of the muscle.

Hilfiker et al.[14], used a 30 by 3 matrix surface electrode arrangement to record the muscle fiber conduction velocity. They tried to establish that the MFCV obtained using a multielectrode/multichannel arrangement could be used as a diagnostic tool for detecting certain myopathic conditions. They could also locate the neuromuscular junction by looking at 30 channels of propagating muscle fiber action potentials.

Broman, De Luca et al. [15], studied the influence of MFCV on spectral parameters like median/mean frequency. They established that at large contraction levels i.e 40 - 60 % MVC the conduction velocity decreased along with the spectral parameters like mean/median frequency. However it was found that the spectral parameters decreased twice as much as that of conduction velocity. Hence it was found that there were other factors like synchronization and firing rates of motor units which were influencing the spectral parameters at these contraction levels.

Naije and Zorn [16], developed a method for estimating the MFCV in the biceps brachii using the cross correlation technique. They found that the clear narrow cross correlation peak at a particular time lag corresponded to an action potential conduction time between the electrodes. This indicated that muscle fiber action potentials were propagated with velocities which varied within a very narrow range.

1.4.2 Signal Processing (The Correlation Function)

Various types of correlation measures have been used in conduction velocity studies. Two of the most important ones are the Pearsons correlation coefficient and the correlation function. In this study a correlation function ρ_{12} was used.

$$\rho_{12}(\tau) = \frac{R_{12}(\tau)}{\sqrt{R_1(0) * R_2(0)}} \quad (1.1)$$

Equation (1.1) gives us the formula for the normalized correlation function ρ_{12} .

Here $R_{12}(\tau)$ is the cross correlation function which is calculated as follows.

$$R_{12}(\tau) = \int X_1(t) * X_2(t + \tau) dt \quad (1.2)$$

where $X_1(t) \rightarrow \text{SignalNumberOne}$

$X_2(t + \tau) \rightarrow \text{SignalNumberTwo}$

and $R_n(0) = \int X_n(0) * X_n(0) dt$

where $n = 1, 2, \dots, m$ values.

$R_n(0)$ is defined as the autocorrelation function of the nth signal. This is basically the cross correlation function evaluated at a zero lag. The correlation function was found to be an ideal tool for determining the conduction velocity for reasons mentioned below. The correlation function is calculated as follows.

Consider two sine waves where one sine wave is shifted in time with respect to the other.

$$y1 = \sin(t) \text{ where } t \text{ is a time vector.} \quad (1.3)$$

$$y_2 = \sin(t-1) \text{ where } y_1 \text{ is delayed by 1 time unit.} \quad (1.4)$$

Each point of y_1 is multiplied with the corresponding point in y_2 . Then the vector y_2 is shifted by one index point and then multiplied with y_1 . This proceeds until the entire length of y_2 is exhausted. Therefore the computation of the cross correlation function involves the shift, multiplication and an integration (continuous signals) or a summation (discrete signals) of the two signals being correlated. The result is a correlation function vector which contains a set of values, each value corresponding to a product obtained at a certain shift or lag. Note that the correlation of a signal at zeroth lag is referred to as the auto correlation.

In the calculation of the cross correlation (equation 1.2) note that $X_2(t)$ is delayed by a time shift of τ with respect to $X_1(t)$. Figures 1.12 and 1.13 show two sine waves $y_1(t)$ and $y_2(t-1)$ and their resulting correlogram. A correlogram is a plot of amplitude vs time of a cross correlation function.

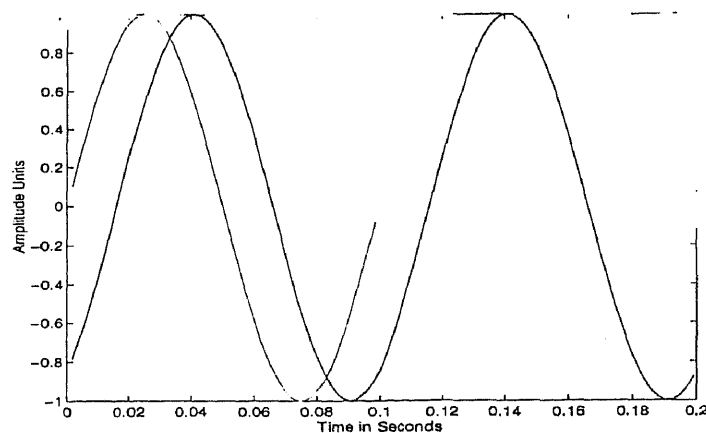


Figure 1.12
Two Sine Waves Shifted in Time

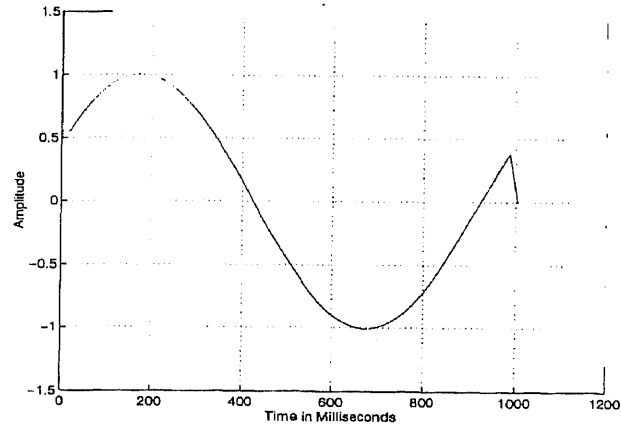


Figure 1.13
Correlogram of Two Sine Waves

The time delay (τ) between any two signals can be obtained directly from the correlogram. The time delay is the value of the x coordinate in the correlogram, at which the amplitude of the correlation function is a maximum. Hence by looking at figure 1.13 we can infer that the time delay between the two time shifted sine waves is 90 milliseconds .

The discrete form of the correlation function is represented below.

$$R_{12}(\tau) = \sum_{m=0}^{M-1} X_1(m) * X_2(t - m) \quad (1.5)$$

All the terms have the same meaning as in equation (1.5) except that a summation of the product of the shifted signals is taken in this case. In equation (1.6) m represents the shift value or the lag. The sum of the product of the two signals $X_1(t)$ and $X_2(t - m)$ is taken over the range of values for the lag m i.e from 0 to M-1.

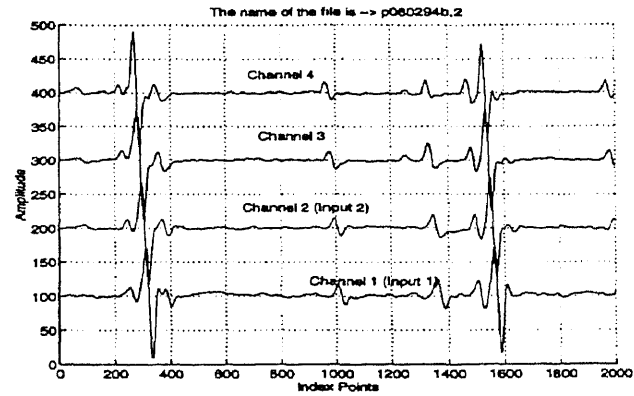


Figure 1.14a
Four Channels of the Typical EMG Signal

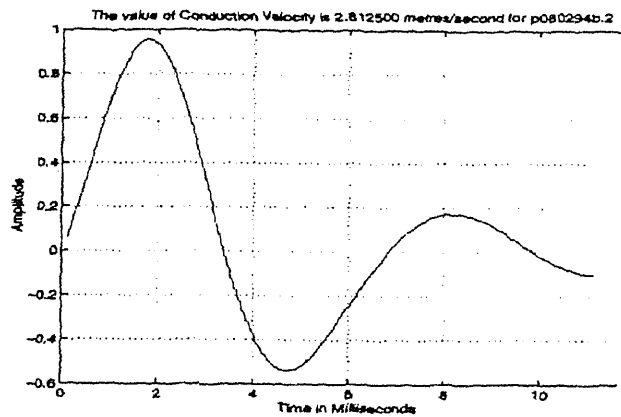


Figure 1.14b
Correlogram between Channel 1 and Channel 2

Hence the length of the correlation function is equal to the number of shift values, namely 'M' in this case.

Figure 1.14a shows 4 channels of a typical EMG signal (1-2000 points). Two channels of this signal were correlated using the above mentioned algorithm and the resulting correlogram is shown in figure 1.14b. The maximum amplitude of the correlogram gives us an indication as to how closely the two signals are correlated and

the time instant at which the amplitude of the correlogram is a maximum. This time instant directly gives us the time lag or the time delay between the two signals, which in this case are the two action potentials obtained from two different channels.

There were two advantages of using the correlation function for the given application. First, the correlogram has a maximum amplitude where the two signals exactly superimpose on each other and have lower amplitude at all other values of lag. Second, the lag/shift value which corresponds to the maximum amplitude of the correlogram gives us the time delay between the two signals.

The cross correlation function can therefore be used as a powerful tool for estimating the time delay and the similarity of any two signals. This was the technique used for estimating the conduction velocity of the muscle fiber. More details regarding the actual computation and implementation of the software for calculating the conduction velocity can be found in Appendix D. In Appendix D details of the algorithm and the actual MATLAB™ source code used to calculate the conduction velocity have been provided.

1.5 Mathematical Techniques

1.5.1 Linear Regression

The behavior of median frequency and MFCV with respect to time can be best studied by performing a regression analysis. Regression analysis is a statistical tool, which models the relationship between two or more quantitative variables, so that one variable may be predicted from the other or others [30]. The linear regression function is given in equation (1.7).

$$Y = A + BX \quad (1.8)$$

Here X is the independent variable, Y is the dependent variable, A is the Y intercept of the regression line and B is the slope [30]. The regression parameters A and B are unknown and can be estimated from sample data. X and Y can then be plotted once the data points are available. A good estimator of the regression parameters is obtained by the method of least squares [30]. Using the least square estimation, the estimates for the slope, y -intercept and the correlation coefficients are calculated as shown below.

$$\text{Slope} = \text{Numtr} / \text{Dentr} \quad (1.9)$$

$$\text{Numtr} = \sum_{t=0}^b XY - \frac{(\sum_{t=0}^b X * \sum_{t=0}^b Y)}{n} \quad (1.10)$$

$$\text{Dentr} = (\sum_{t=0}^b X^2) - \frac{(\sum_{t=0}^b X)^2}{n} \quad (1.11)$$

In the above equations we observe that all the summations are done from $t=0$ to b . This variable “ t ” denotes the time instants at which the MFCV was computed and this increases in steps of two, since the MFCV values were calculated at each 2 minute time

instant starting from $t=0$. The upper limit of "t" which is indicated as "b" varies between subjects as different subjects have different fatigue endurance times. For example for subject 4 (table 3.1), "b" takes the value of 20 minutes, whereas for subject 5 (table 3.2), it is 8 minutes.

The Y intercept is given as follows

$$Y \text{ intercept} = \text{Num1} / \text{Dentr} \quad (1.12)$$

where Num1 is calculated as given in equation 1.12.

$$\text{Num1} = \frac{\sum_{t=0}^b X^2 * \sum_{t=0}^b Y - \sum_{t=0}^b X * \sum_{t=0}^b XY}{n} \quad (1.13)$$

In the above equations n denotes the number of data points. Hence with the data points, y-intercept values and slope a regression line can be obtained [30]. Note that all the symbols used in equations 1.13 have the same meaning as in equations 1.10 and 1.11.

To estimate the degree of association between the variables (data points), the correlation coefficient was computed. The correlation coefficient is a number between -1 and +1, and it indicates how closely two variables are related to each other. The correlation coefficient is calculated as follows.

$$r = \frac{\sum_{t=0}^b XY - \frac{\sum_{t=0}^b X \sum_{t=0}^b Y}{n}}{\sqrt{\left[\left(\sum_{t=0}^b X^2 - \frac{(\sum_{t=0}^b X)^2}{n} \right) \left(\sum_{t=0}^b Y^2 - \frac{(\sum_{t=0}^b Y)^2}{n} \right) \right]}} \quad (1.14)$$

A positive value of r indicates the existence of a positive relationship while a negative value of 'r' implies that there exists an inverse relationship between the two variables

being correlated. If the modulus of 'r' is 1 , it indicates that there is an exact match between the two variables that were correlated.

1.5.2 The Exponential Peeling Technique

One of the objectives of this research was to study the recovery curve of the MFCV. It has been reported [24] that the recovery curve of the MFCV consists of components of exponentials. Thus an exponential curve fitting technique was used in this study. The exponential peeling technique, a curve fitting method, was used to fit the recovery curve of the MFCV.

The response of a linear system to a step input is a sum of decaying exponentials. In most practical applications the order of the system is not known and it is in such cases that the peeling technique is of great importance.

Suppose we were given an exponential function $f(t)$ which was plotted as a function of time. We will attempt to fit a sum of exponentials to the function $f(t)$. We begin by assuming that this function has a first order solution as given in equation (1.14).

$$f(t) = Ke^{-\frac{t}{\tau}} \quad (1.15)$$

where τ is the time constant. Taking the natural logarithm on both sides of equation 1.14 we arrive at equation 1.15.

$$\ln(f(t)) = \ln(K) - \frac{t}{\tau} \quad (1.16)$$

We find that equation 1.15 represents the equation of a straight line having an intercept of $\ln(K)$ and a slope of $-\frac{1}{\tau}$. Therefore if $f(t)$ is a first order equation, then the complete solution of $f(t)$ can be obtained from the plot of $\ln(f(t))$ Vs t where 't' is time.

The situation is more complex when we have a function $f(t)$ which belongs to a second order system i.e. one which has a solution consisting of two exponentials. In such a case we know that one of the exponentials decays faster than the other. Thus after the first exponential dies out there remains only one other exponential whose solution can be found as described above. Therefore this slower decaying exponential can be 'peeled' from the function $f(t)$ resulting in $\{f(t) - Ke^{-\frac{t}{\tau}}\}$ which is then plotted Vs time 't'. The same procedure may be repeated for systems having an order greater than 1 i.e. having a solution consisting of more than one exponential.

In practical applications the function $f(t)$ is plotted Vs time on semilog paper and the peeling technique is used to characterize the system completely i.e. calculating the time constant, coefficients and the order.

1.6 Precision Decomposition of the EMG Signal

The term decomposition has been commonly used to describe the process whereby individual motor unit action potentials are identified and uniquely classified from a set of superimposed action potential trains belonging to concurrently active motor units. The concept of decomposition is depicted in Figure 1.16.

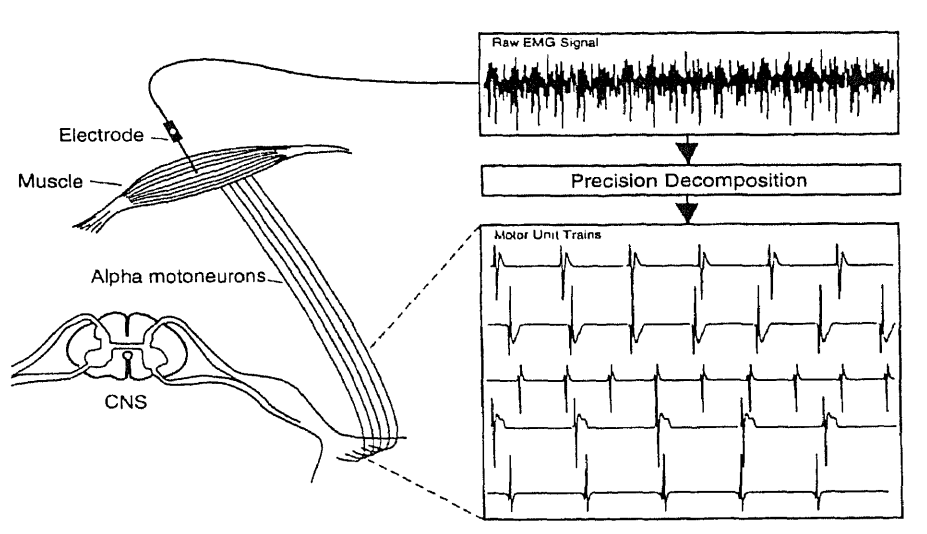


Figure 1.16
Method for Decomposition of the Myoelectric Signal

Identification refers to the categorization of the times of occurrences of the motor unit action potentials (MUAP) as well as the description of its morphological characteristics [8]. Precision decomposition involves the extraction of the timing information and the morphological characteristics from the myoelectric signal. The timing information provides us a complete description of the inter pulse interval, firing rate, and synchronization characteristics. Furthermore the availability of all the motor unit action

potentials discharged by a specific motor unit enables a more consistent expression of the shape by averaging the shape over a set of discharges.

The precision decomposition technique can be applied to both clinical and research environments. It can be used as a tool to explore the working of the nervous system in normal and dysfunctional modalities. In the field of neurology the ability to measure the behavior of the firing rates and synchronization of the motor unit discharges holds the promise of being used to more analytically classify the dysfunctions of CNS origin. The other important advantage is that the precision decomposition technique could provide a more accurate basis for the diagnosis of patients, based on the morphological measurements.

The morphology (as referred to in this document) describes the parameters related to the MUAP shape. These are peak to peak amplitude, time duration, the number of phases and the area of the myoelectric signal [8]. The morphology of the MUAP

1.6.1 Literature Review

During the past decade, the clinical community has made several attempts to extract as many motor unit action potentials as possible from the EMG signal. The work of Buchthal and his colleagues during the 1950s and the 1960s [8], paved the way for quantitative measurements and application of the EMG signal. Their work involved the quantification of the morphological characteristics of individually detected motor unit action potentials (MUAPs) obtained from a needle electrode. Their study established the painstaking manual approach of graphically measuring the morphological characteristics of individually detected MUAPs. Gerstein and Clark [9] simultaneously studied the firing patterns of several neurons. Keehn [10] developed an iterative spike separation technique for separation of a motor unit action potential train into individual MUAPs. These studies were considered as pioneering attempts at characterizing the discharge times of neural activity and identifying individual action potentials using shape discrimination.

Applications for separation of the EMG signals did not appear until a full decade later when the works of LeFever and Deluca [8] and [11], Andreassen [17] and Guihenec et al.[18] and McGill and Dorfman [19] became known. Andreassen [17] developed a computerized analysis of motor unit firings. Guihenec et al.[18] developed a procedure for automatic detection and pattern recognition of single motor unit potentials in needle electrodes. LeFever and Deluca [11] developed a procedure for decomposing the myoelectric signal into its constituent action potentials. They used a distance measure to compare any two action potentials, thereby transforming the signal to a signal space

representation. More about this study will be described in section 1.6.2, as the method developed in this thesis is based on LeFever and Deluca's technique for decomposing the myoelectric signal. Stashtuk and De Bruin [20] developed a technique for automatic decomposition of the myoelectric signal. Their technique was based on spectral measures. A Fourier transform of the digitized signal was performed and the power spectrum coefficients were then used as features to represent the MUAPs in the decomposition algorithm. The advantage of using the power spectrum coefficients as opposed to the time domain distance measure was that the alignment errors introduced during the decomposition procedure could be eliminated. On the other hand if phase information were being used in the decomposition technique then this technique cannot be used as phase information is lost during the estimation of the power spectrum coefficients.

1.6.2 Signal Processing (Precision Decomposition)

As described in section 1.5.1 attempts have been made to decompose the myoelectric signal into its constituent motor units. The importance of this is to better characterize the myoelectric signal in terms of its morphology (peak to peak amplitude, time duration, number of phases and the area of the MUAP) and the control properties of the motor units (firing characteristics and synchronization of motor units).

The technique used by the author for developing the precision decomposition technique was based on the work by LeFever and Deluca [11]. Before describing the technique in detail terms used in this discussion will be explained. A template is defined as the exact waveform that would be received in the absence of noise [11]. The squared signal space

distance between two waveform vectors (sampled and digitized) v_1 and v_2 is the square of the absolute value of the difference between v_1 and v_2 and is represented as $|\vec{v}_1 - \vec{v}_2|^2$.

The motor unit action potential trains (MUAPTs) obtained from the sampled and digitized EMG signal were decomposed into their constituent motor units. The steps in the algorithm used for decomposition were as follows.

Step 1: Reconstruct the original myoelectric signal (ME) into one which has fewer motor unit action potentials (MUAPTs) by setting an amplitude threshold of 55 mV.

This allows only dominant motor units to remain and all others to be eliminated.

The resulting signal will be referred to as the thresholded signal (TS).

Step 2: Pick the first MUAPT in the TS. We make an assumption that this is the template for the first motor unit. This signal will be referred to as \vec{s}_1 .

Step 3: Pick the next MUAPT in the TS. We will refer to this as \vec{r} .

Step 4: The squared signal space distance (SSSD) between the two signals is computed.

Subsequently the SSSD is normalized with respect to the signal power since the absolute change in a MUAP waveform was roughly proportional to the waveform amplitude. The resulting mathematical expression is given below.

$$\frac{|\vec{r} - \vec{s}_1|^2}{|\vec{s}_1|^2} \quad (1.6)$$

where all the terms have the same meanings as discussed in steps 2 and 3. The above equation thus represents the normalized squared signal space distance (NSSSD).

Step 5: After the calculation of the NSSSD, this value was then compared against an empirical value of 0.15 which was obtained from LeFever and Deluca [11]. The comparison is illustrated mathematically in equation 1.17.

$$\frac{|\bar{r} - \bar{s}|^2}{|\bar{s}|^2} < 0.15 \quad (1.7)$$

Step 6 : If this condition was satisfied, the MUAP (denoted as \bar{r} in this case) is assigned to the same motor unit as the template. Otherwise a new template \bar{s}_2 is created and now each new MUAP is compared with both the templates before assigning it to a new motor unit.

Steps 2 to 6 were repeated up to the entire length of the ME. The ME was thus decomposed into individual MUAPTs (motor unit action potential trains) and the templates of each motor unit were also obtained as a result of the decomposition procedure. A myoelectric signal (ME) consisting of 5200 sample points, the TS, the constituent motor units of the ME and the templates corresponding to the ME are indicated from figure 3.7 to figure 3.12 (chapter 3; section 3.2), so that the process of decomposition can be better understood.

Thus it can be seen from figures 3.7 to 3.12 that the ME has been completely characterized into its constituent motor units with the templates representing the signature of their corresponding motor units.

1.7 Scope of Thesis

The author and his colleague at Kessler Institute for Rehabilitation wanted to investigate if muscle fiber conduction velocity (MFCV) could be used as a reliable indicator of fatigue. They also wanted to study the recovery of MFCV after fatigue, as information regarding the recovery of MFCV is very scant. A customized software was developed in MATLAB™ to calculate the muscle fiber conduction velocity (MFCV). The program was written with several other user friendly features so that physicians could use this software without getting involved into the signal processing algorithms for measurement of the MFCV. Thus this provided an automatic method for the estimation of MFCV. Data analysis was done using this software and the results obtained were critically reviewed.

A technique was developed to decompose the myoelectric signal into its constituent motor units and a method was developed to perform a precision decomposition of the myoelectric signal . A brief overview of the importance of decomposition of the myoelectric signal is given below.

Attempts to study the behavior of the central nervous system have been consistently pursued over the years. Precision decomposition of the EMG signal using the template matching technique, could be a new tool which enables one to look into the working of the nervous system in normal and dysfunctional modalities [8]. Furthermore the ability to obtain more reliable representations of motor unit action potential (MUAP) shapes by averaging over several correctly identified MUAPs of an individual motor unit,

provides a more accurate basis for any diagnosis based on morphological measurements[8].

Several previous studies were used as a guideline by the author to develop the software for implementing the decomposition technique. Gertein et al.[9], studied the simultaneous firing patterns of several neurons and their work is considered as a pioneering work in this field. Keehn [10] developed an iterative spike technique for the decomposition of the myoelectric signal. However it was Deluca and LeFever [11] who developed a sophisticated algorithm for the decomposition of the EMG signal into its constituent motor units.

The author developed a user friendly software in MATLAB™ based on the technique suggested by Deluca and Le Fever et al.[11], for precision decomposition of the EMG signal. Certain modifications were made to the decomposition technique and the reasons for the modification have been described in detail in section 1.4.2. Section 3.2 discusses some preliminary results that were obtained using this decomposition technique. The developed software and algorithm were tested on a sample of the collected data.

CHAPTER 2

METHODS

2.1 Experimental Protocol

Twenty subjects between the ages of 25 - 45 were tested using the protocol which will be described below. After the required setup, which will be described in detail in sections 2.2 and 2.3 , the subjects were asked to contract their abductor digiti minimi muscle (by moving their little finger in the dominant hand) to their maximal voluntary contraction (MVC). The MVC was recorded using a load cell (SENSOTEC Load Cell #31 and GM signal conditioning display unit).

The subjects were then allowed to rest for 10 minutes. Following this they were asked to perform a contraction of 5% of their MVC. 8 channels of EMG data were then recorded at a sampling rate 2500 Hz per channel. This sampling frequency (for each channel) was chosen to be 5 times the highest frequency in the EMG signal i.e the highest frequency being around 500 Hz. The objective of this recording was to examine eight channels of the EMG data in an attempt to determine the position of the neuromuscular junction. The location of the neuromuscular junction in turn assists the investigator in picking the channels to be correlated, as the shape of an action potential near a junction is usually distorted. After this another file containing 4 channels of EMG data was recorded at a sampling rate of 9000Hz per channel. Such a high sampling rate was required in order to enhance the resolution of the recorded EMG data thereby improving the overall accuracy in the measurement of muscle fiber conduction velocity(MFCV). As discussed

in section 1.4.2 the cross correlation function was used for estimating the time delay between any two channels of the EMG signal.

Figure 2.1 illustrates the protocol that was used for recording EMG data during this research. The subjects were asked to perform a 20% MVC. Data were acquired continuously at 2 minute intervals, while the subject maintained the 20 % MVC. When the subject's contraction level, indicated as a dc voltage on the oscilloscope, fell below the 20% MVC value for more than 3 seconds, the subject was asked to stop the contraction. Data were immediately collected at this stage. This represented the fatigue condition. Following the fatigue condition, collection of data proceeded at 1 minute intervals for 6 minutes with the subject maintaining a 5% maximum voluntary contraction at each recording. Following this data were recorded at 2 minute intervals up to 12 min at 5% MVC. Data was acquired at 3 minute intervals from this time instant up to 25 minutes, and the last recording was taken after a 5 minute interval. The reason for recording data at unequal time intervals was as follows. As mentioned in section 1.4 one of the objectives of this study was to examine the recovery of strength (MVC) of the subject and if possible plot the time course of the strength (MVC), based on the values of MVC recorded at 3, 6, 12, 18 and 30 minutes. It has been reported that the recovery of strength (MVC) is a much slower process than that of fatiguing of the muscle. This explains the wider time intervals in recording the data 8 minutes after the subject performed a 20 % MVC up to his endurance limit.

The influence of temperature and the possible effects that temperature has on the MFCV have been explained in section 1.4. Hence temperature data (temperature of the

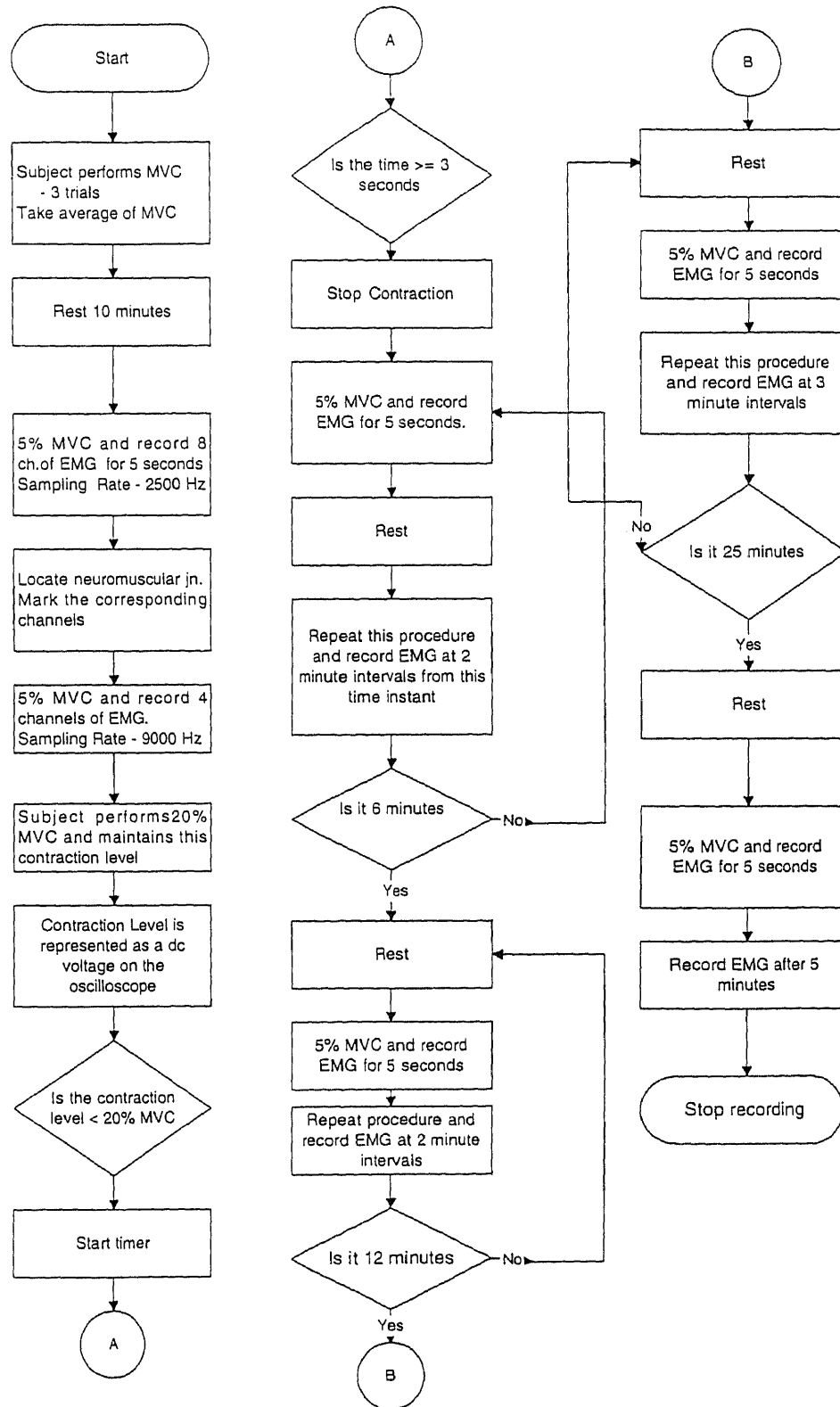


Figure 2.1
Flowchart Explaining the Protocol

palm; dorsal side) was collected continuously throughout the experiment. This would help the investigator to examine the influence of temperature on MFCV and thereby better characterize the change in MFCV during fatigue and during recovery.

2.2 Electrode Placement and Configuration

An 8 channel active surface electrode was used to record the surface electromyogram of the subject . The electrode was mounted such that the metal contacts of the electrodes were flush with the abductor digiti minimi muscle. The impedance of the skin is typically between 10-100 Kiloohms [21]. When passive electrodes were used, skin cleaners had to be used beforehand to reduce the impedance offered by the skin. The most important drawback in using skin cleaners is that, if the interelectrode distance is small, then a short could result between any two electrodes by accident. The advantages of using an active electrode were as follows. An active electrode uses operational amplifiers in voltage follower configurations thereby acting as an impedance transformer between the skin and the active electrode. An active electrode hence eliminates the need skin preparation before positioning the electrode to the skin surface [21]. Movement artifacts of the electrode were reduced by using clinical cloth tapes(Kendall-Curasilk) to strap the electrode and keep it in place. The schematic of a typical electrode is shown in figure 2.2.

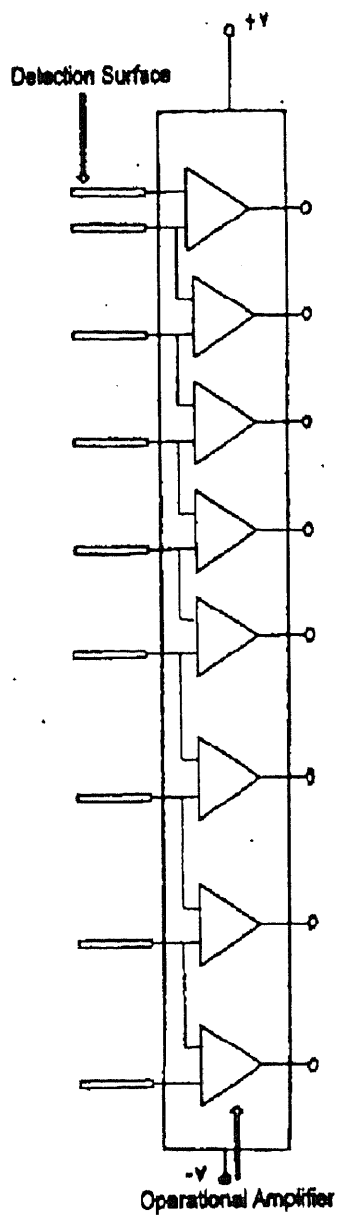


Figure 2.2
Schematic of the Active Electrode

2.3 Data Acquisition

The 8 channel EMG signal which was acquired from the active electrode was then given as an input to an isolated preamplifier (Gould #11-5407-58). The preamplifier was connected to an instrumentation amplifier (Gould #13-4615-58) where the signal was bandpass filtered between 30 Hz and 1000 Hz and amplified. The gain of the amplifier was adjusted for each trial and for each subject by changing the value of the full scale setting in the instrumentation amplifier. As the amplitude of the EMG signal recorded in this study was typically between 100 - 200 millivolts (figure 1.10), the amplifier gain was set to 300 and 125 corresponding to a full scale setting of '1' and '2.5' respectively. The conditioned analog data were then given to a 12 bit resolution analog to digital interface board (Keithley Metrabyte #Das 1601) through a screw terminal accessory board (Keithley Metrabyte # STA-16). The sampling rate of the analog signal was 9000 Hz, which was needed to improve the resolution and accuracy of the cross correlation technique which has been described in detail in section 1.4.2. This converted digital data was then stored in binary form, on an IBM 286 PC using data acquisition software (KeithleyMetrabyte #Streamer v3.25). The output of the signal conditioner was also monitored using a 4 channel digitizing oscilloscope (Tektronix #TDS455A) during the experiment, to detect and observe noise, and other interference due to motion artifacts.

The digitized EMG signal was then transferred from the data acquisition PC to offline computers (IBM 486/586) for data analysis, using Netware™ (A Network Software).The digitized, binary data files were then converted to ASCII using UNPACK™ (STREAMER v3.5 Unpack) which converts the binary data into n channels

(as specified by the user) of ascii data . Once the ascii data file was obtained it was in a form suitable for data analysis by the signal processing software MATLAB™. Appendix C can be referred to for more details regarding data acquisition.

2.4 Data Analysis (Signal Processing)

2.4.1 Estimation of Muscle Fiber Conduction Velocity (MFCV)

The software, MATLAB™, was used for Signal Processing. As discussed in section 1.4.2, the objective of this project was to measure the conduction velocity of the muscle fiber and this was achieved using a cross correlation technique. In this application the correlation function was used as a powerful tool to achieve two objectives: to determine the similarity and the time lag between the two signals.

A program was thus developed to implement the cross correlation between two channels of EMG data at a time and the **correlogram** was obtained. The standard algorithm in MATLAB™ for computing the cross correlation was improved so that a user friendly program could perform the normalized cross correlation/ autocorrelation for both periodic and aperiodic signals. The program was then tested with different sets of data obtained from different subjects. The outputs of this program were as follows.

- 1) Plots of the input signals
- 2) Plot of the correlogram
- 3) The value of the muscle fiber conduction velocity (MFCV) which was calculated using the following formula

$$\text{Velocity} = \text{Distance} / \text{Time Lag}$$

Distance :- Distance between the Electrodes

Time :- Time Lag between the two Signals (from Correlogram)

Appendix D contains the algorithm and the program used for calculation of the conduction velocity using the cross correlation technique.

2.4.2 Precision Decomposition of the EMG Signal

A customized software was developed for template analysis of the myoelectric signal.

The objective of this analysis as discussed in section 1.5.2 was to decompose the myoelectric signal into its constituent motor units, thereby characterizing the shape and form of the individual motor units. The EMG data (ASCII form) was then fed as the input to the program and the following outputs where obtained.

- 1) A plot of the original myoelectric signal with several motor unit potentials.
- 2) Plots of the templates that were formed by the software during decomposition.
- 3) Plots of individual motor units with the timing of the action potentials preserved.

Appendix D contains a more detailed description of the algorithm and the software used to decompose the myoelectric signal, while Appendix A contains the plots obtained as a result of the precision decomposition.

CHAPTER 3

RESULTS AND DISCUSSION

This chapter presents the results that were obtained from two studies conducted by the author, namely, muscle fiber conduction velocity (MFCV) and the precision decomposition study.

3.1 Muscle Fiber Conduction Velocity (MFCV)

As mentioned in section 1.4 the objective of this study was twofold. One objective was to investigate if MFCV could be used as a reliable indicator of fatigue and the second objective was to characterize the recovery of MFCV after the subject performed a maximum voluntary contraction upto his/her endurance limit.

3.1.1 MFCV (Fatigue)

One of the objectives of this study was to determine if MFCV could be used as a reliable indicator of fatigue. As discussed in section 2.1, the subject was asked to maintain a 20% MVC until he/she could no longer maintain this contraction level. Data were collected at 2 minute intervals during the fatiguing contraction (20% MVC). The MFCV was calculated at each two minute time instant and the following results were obtained for one subject. From table 3.1 we observe that at fatigue (0 min.), the MFCV of subject 4 is higher than the pre-fatigue value of 2.65 meters/second and this is believed to be due to the recruitment of the type II fibers (faster MFCV and faster twitch). These muscle fibers

have higher conduction velocities as compared to type I fibers which are recruited during the initial stages of a contraction. This is because the type I fibers have more excitable

Table 3.1 MFCV(Fatigue) and Median Frequency (Subject 4)
Prefatigue value of MFCV: 2.65 metres/second

Subject 4	Time	MFCV	Median frequency	Temperature
Condition	minutes	metres/second	Hertz	centigrade
during fatigue	0	2.8	116	30.5
during fatigue	2	2.7	111	30.3
during fatigue	4	2.5	118	30.5
during fatigue	6	2.4	90	30.6
during fatigue	8	2.4	88	31.0
during fatigue	10	2.3	90	31.2
during fatigue	12	2.1	83	31.1
during fatigue	14	2.1	76	31.4
during fatigue	16	2.0	74	31.3
during fatigue	18	2.3	81	31.3
during fatigue	20	2.0	77	31.1

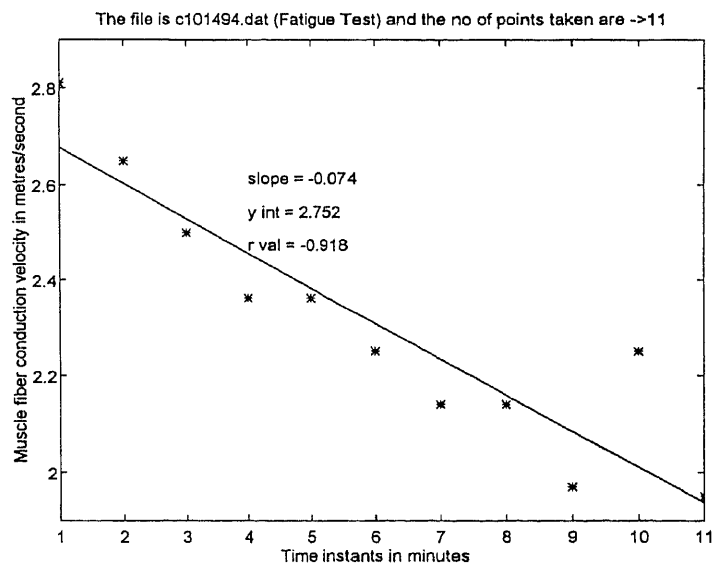


Figure 3.1

Decline of MFCV with Fatigue (plot and a linear regression line)
(MFCV vs Time Instants (0, 2, 4, 6, 8, 10, 12, 14, 16, 18, 20 min., shown in Table 3.1))

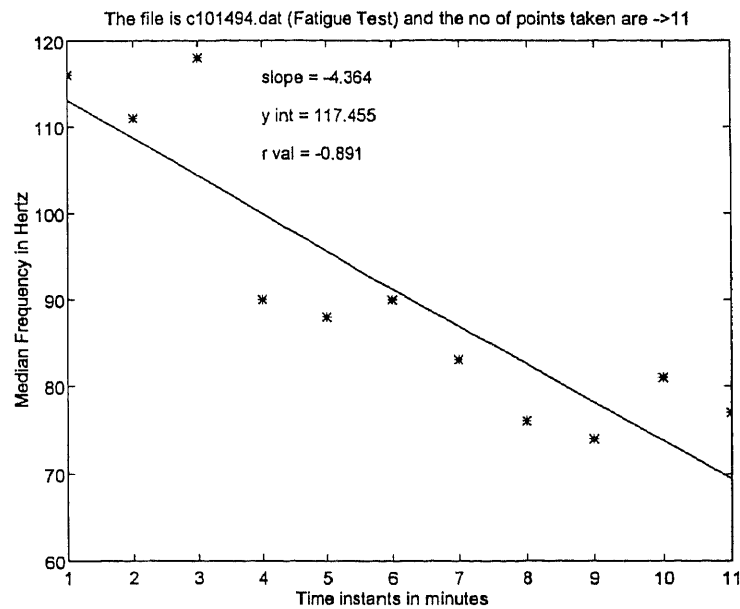


Figure 3.2

Decline of Median Frequency with Fatigue (plot and linear regression line)
Median frequency vs Time Instants, shown in Table 3.1

cell membranes as compared to type II fibers. As the contraction progresses there is a decline in the MFCV with fatigue. This is due to two factors. First, the type II fibers which are recruited during the contraction (20% MVC) are fast fatiguable. This means that they can maintain a given force level only for a certain period of time (varies between subjects). Once the type II fibers are fatigued the type I fibers (slow MFCV) continue firing and contract. Second, as the type II fibers contract, lactic acid (a metabolite) builds up. Wim et al. [25] and Toshio [26] have reported that the buildup of lactic acid is predominantly due to the contraction of the type II fibers. The accumulation of lactic acid results in a reduction of the pH of the interstitial fluid surrounding the muscle thereby causing the cell membranes of the muscle cells to be less excitable. This

in turn reduces the MFCV. The other effect that is produced by the buildup of lactic acid is that the shape of the action potentials become wider which means corresponding decline in the frequency of the myoelectric signal. This is seen as a decline in median frequency which is also computed in this study.

Figures 3.1 and 3.2 show the plots of MFCV and median frequency calculated at each 2 minute instant of time as shown in table 3.1. Table 3.1 also indicates the values of MFCV and MF. Examining figures 3.1 and 3.2 we can simultaneously compare the decline of MFCV and median frequency with fatigue.

The data obtained from another subject (subject 5) also shows a decline in the MFCV with fatigue. Referring to table 3.2 we once again find that the MFCV at fatigue (0 minutes) has a higher value than the prefatigue value i.e. 3 meters/second due to the recruitment of type II fibers. There is a subsequent decline in MFCV because the type II fibers become fatigued as the contraction progresses. The simultaneous buildup of lactic acid lowers the MFCV and alters the shape of the action potentials, thereby decreasing the median frequency during the progression of the contraction. These factors are complemented by the recruitment of type I fibers, which have slower MFCVs and have lower frequency components. Therefore it is observed that there is a decline in MFCV with fatigue for both subjects 4 and 5. This decline in MFCV with fatigue was also seen in the other 7 subjects whose results are shown in Appendix A.2.

Table 3.2 MFCV (Fatigue) and Median Frequency (subject 5)
Prefatigue value of MFCV: 3 metres/second

Subject 5				
Condition	Time	MFCV	Median frequency	Temperature
	minutes	metres/second	Hertz	centigrade
during fatigue	0	3.8	131	27.3
during fatigue	2	3.8	117	27.3
during fatigue	4	3.0	107	27.6
during fatigue	6	2.8	90	28.4
during fatigue	8	2.7	79	28.6

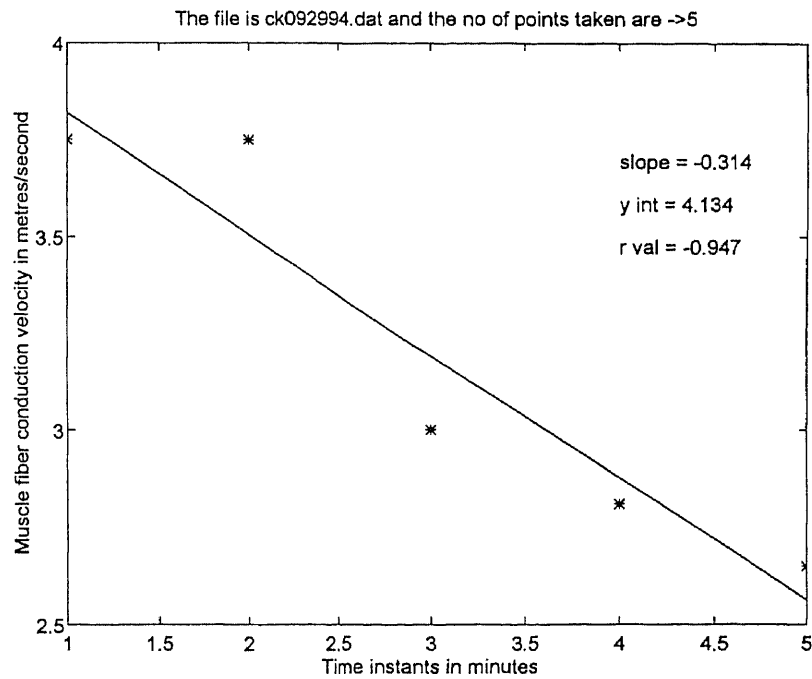


Figure 3.3
MFCV Decline with Fatigue
(MFCV vs Time Instants (0, 2, 4, 6, 8 min.) as shown in Table 3.2)

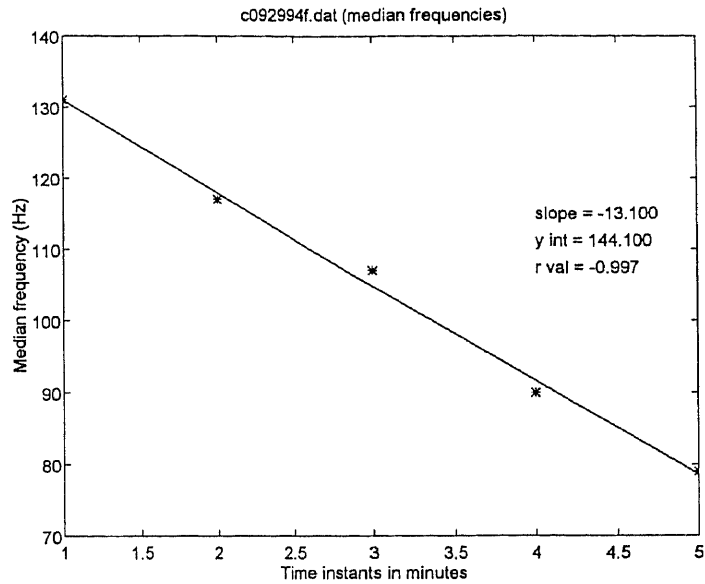


Figure 3.4
Decline of Median Frequency with Fatigue
Median Frequency vs Time Instants, shown in Table 3.2

Table 3.3 A Comparison between the Percent Change in MFCV to that of MF

Subject No.	% Change in MFCV	% Change in Median Frequency (MF)
4	44.44%	39.47%
5	32.89%	40.4%
8	16.1%	37%
3	15.98%	22.2%

Table 3.3 gives a comparison of the decline of MFCV to that of the MF, for each of the four subjects for whom the MF was calculated. The comparison of MFCV and the MF was carried out only for 4 out of the 6 subjects tested, because the endurance times and the number of data files recorded were more for these four subjects. This in turn meant that there was more fatigue data available for these four subjects. It is observed that with

the exception of subject 4 the percentage drop in median frequency is more pronounced than that of the MFCV. This in turn conforms with our expectation that median frequency is influenced by other factors like synchronization, recruitment and the firing rate of motor units and not by MFCV alone.

3.1.2 MFCV (Recovery)

The other objective of this study was to characterize the recovery curve of the MFCV after a fatiguing contraction. Two representative results are presented and discussed in this section.

As discussed in section 2.1 the subjects were asked to perform a 20% MVC until they could no longer maintain this contraction level. Following this the subject was asked to perform a 5% MVC and data were collected at subsequent instants of time as described in section 2.1. These data represented the recovery phase of the MFCV.

Referring to table 3.4 we find that the MFCV of subject 4 at post fatigue(0 min.) is 2.05 m/s. It can also be observed that the MFCV at post fatigue (0 min.) is lower than that at prefatigue. At 1 min. post fatigue, the MFCV of the subject rises. This could be due to two reasons. First, there could be a strength recovery of type II muscle fibers which were exhausted as a result of the fatigue contraction (20% MVC) that preceded the recovery phase. Second, the breakdown of lactic acid which reduces the pH of the interstitial fluid surrounding the muscle cells, makes the cell membranes less excitable and thereby reduces the MFCV. Looking at table 3.4 we find that subject 4 recovers the original value of MFCV at 3 min. (post fatigue). Subsequently there is an overshoot in

the values of MFCV from the prefatigue value as shown in table 3.4. The overshoot of MFCV after a fatiguing contraction has been reported by Van der Hoeven et al.[24] and this is observed in subject 4 from 15 min. (post fatigue) to the end of the test (30 min.post fatigue).

Table 3.4 MFCV(Recovery): Subject 4

Subject 4			
Condition	Time (minutes)	MFCV	Temperature
	(with respect to fatigue)	metres/second	centigrade
prefatigue	before fatigue	2.65	30.5
post fatigue	0	2.05	31.3
post fatigue	1	2.40	31.3
post fatigue	2	2.50	31.2
post fatigue	3	2.65	31.1
post fatigue	4	2.65	31.0
post fatigue	6	2.65	30.8
post fatigue	10	2.65	31.1
post fatigue	15	2.81	31.0
post fatigue	21	2.81	31.0
post fatigue	30	2.81	30.8

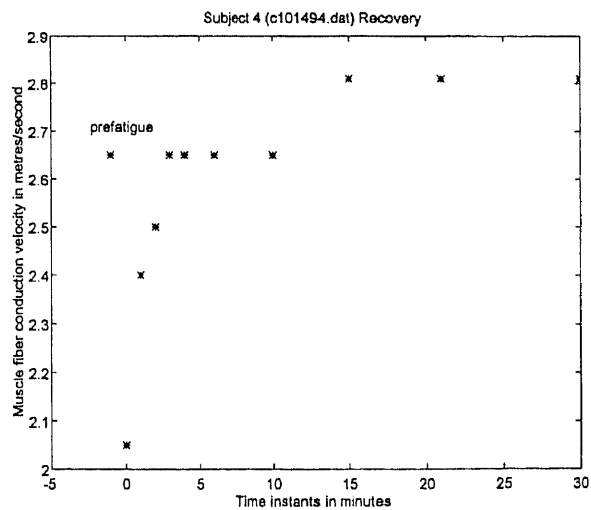


Figure 3.5

Graphical Illustration of MFCV (Recovery) of Subject 4

Table 3.5 Smoothed MFCV Data Points Plotted using the Exponential Peeling Method (Subject 4)

Subject 4 Recovery										
F(t)	2.25	2.39	2.51	2.61	2.64	2.72	2.78	2.8	2.8	2.8
F1(t)	-0.55	-0.41	-0.29	-0.19	-0.16	-0.08	-0.02			
t (minutes)	0.00	1.00	2.00	3.00	4.00	6.00	10.00	15.00	21.00	30.00

This supernormal overshoot in the MFCV can be attributed to the increase in the muscle fiber (MFIB) diameter caused by the increase in water content during dynamic exercise conditions. Furthermore it has been reported [24], [28], [29] that there is a dependence between MFCV and muscle fiber radius i.e. MFCV increases with an increase in muscle fiber radius due to a decreased internal resistance of the MFIB.

Although temperature has an influence on the MFCV and increases in temperature result in increases in MFCV, for subject 4 we find that at 15 min. post fatigue, the temperature of the palm (dorsal surface) remains at a relatively constant value of 31 degrees centigrade, the peak temperature recorded being 31.3 degrees centigrade. It was also observed that in subjects 3,6,8 and 9 (Appendix A.2) an increase in temperature (2-6 min., post fatigue) was accompanied by increases in MFCV and a subsequent decline in temperature produced no significant effect on the MFCVs. However in subjects 1,2,4,5 and 7 (Appendix A.2) such a clear association between temperature and MFCV was not found.

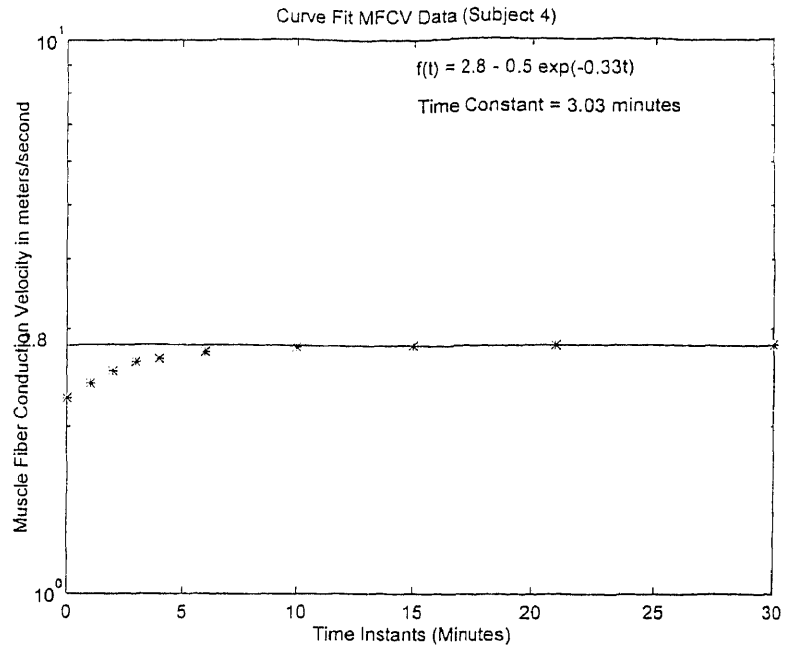


Figure 3.6
Curve Fitted MFCV Data (Subject 4)

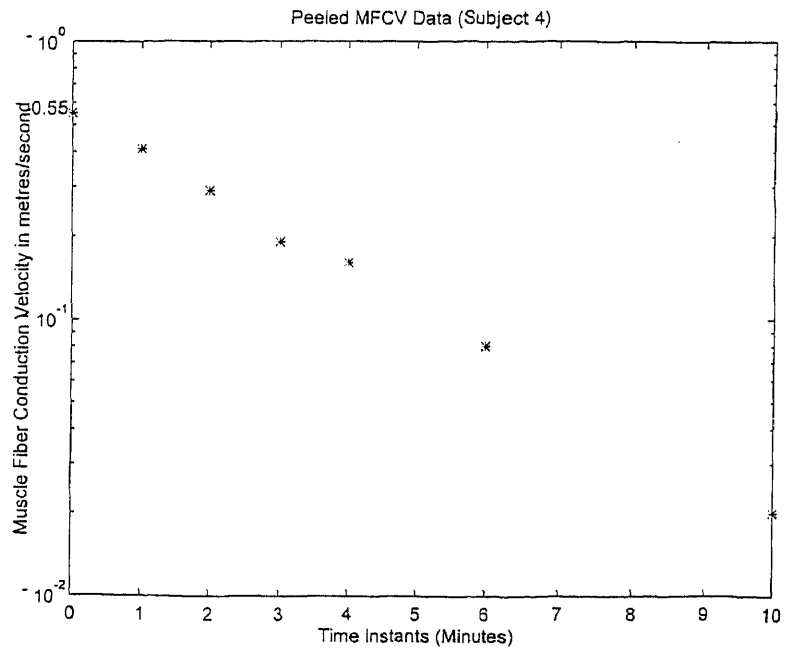


Figure 3.7
Peeled MFCV Data (Subject 4)

Attempts have been made to model the recovery curve of the MFCV after a fatiguing contraction[24]. The recovery curves of the MFCV of all the 9 subjects tested during the course of this research were modelled using the exponential peeling technique discussed in section 1.5.2. The data points, which were the values of MFCV at each two minute time instant, were smoothed using the S Plus™ smooth function. These smoothed data points were then fitted to an exponential using the exponential peeling technique. More details about the smoothing function have been attached in Appendix D.

The order and the time constant of the each of the recovery curves were also determined using this technique. Referring to table 3.4, and figures 3.6 and 3.7, we observe that the recovery curve(RC) consists of a dc component and one exponential component. The time constant of the RC for subject 4 was 3.03 minutes which meant that it took 3.03 minutes for subject 4 to recover 63 % of the final value of his/her MFCV.

Table 3.6 gives us the values of temperature and MFCV during the recovery phase for subject 6. Referring to table 3.6 we find that the MFCV of subject 6 at 0 min. (post fatigue) is lower than the prefatigue value of MFCV. At 1 min., post fatigue, subject 6 shows an increase in MFCV and this can be explained by the recovery of type II muscle fibers and the breakdown of lactic acid, as discussed earlier in this section.

Furthermore it is found that subject 6 recovers the prefatigue value of MFCV at 4min., post fatigue as compared to subject 4 (3 min., post fatigue).From this time instant the MFCV of subject 6 increases above the prefatigue value, and stabilizes at 21 min., post fatigue. As observed in subject 4 this stabilized value of MFCV of subject 6, at 21

min., post fatigue, represents the overshoot in MFCV and can be explained by the swelling of the muscle fiber, as discussed earlier in this section.

The recovery curve (RC) of MFCV, of subject 6, was also modelled using the exponential peeling technique. Referring to table 3.6 and figures 3.9 and 3.10 it may be observed that the RC of subject 6 consists of a dc component and an exponential component. The time constant of the RC, for subject 6, is 3.29 minutes. This meant that

Table 3.6 MFCV (Recovery): Subject 6

Subject 6			
Condition	Time (minutes) (with respect to fatigue)	MFCV metres/second	Temperature centigrade
prefatigue	before fatigue	2.2	26.3
post fatigue	0	1.1	26.7
post fatigue	1	1.8	26.8
post fatigue	2	2.1	27.0
post fatigue	3	2.1	27.3
post fatigue	4	2.3	27.5
post fatigue	6	2.4	27.8
post fatigue	10	2.8	28.4
post fatigue	15	2.7	28.1
post fatigue	21	2.5	27.7
post fatigue	30	2.5	26.7

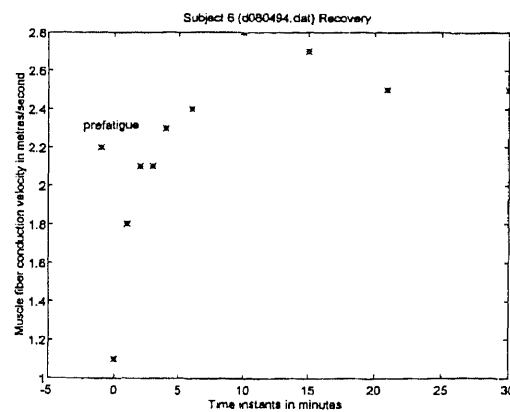


Figure 3.8
Graphical Illustration of MFCV(Recovery): Subject 6

Table 3.7 Smoothed MFCV Data Points Plotted using the Exponential Peeling Method (Subject 6)

Subject 6 Recovery										
F(t)	1.56	1.78	1.97	2.13	2.28	2.43	2.55	2.6	2.6	2.6
F1(t)	-1.04	-0.82	-0.63	-0.47	-0.32	-0.17	-0.05			
t minutes	0.00	1.00	2.00	3.00	4.00	6.00	10.00	15.00	21.00	30.00

Table 3.8 Time Constants of the Subjects Tested
(Determined from the Exponential Peeling Technique)

Subject No.	Time Constant minutes
1	3.85
2	2.64
3	2.5
4	3.03
5	3.47
6	3.29
7	1.19
8	4.17
9	2.28

subject 6 took 3.29 minutes to recover 63 % of his/her final value of MFCV. It was found that the time constants of 8 subjects out of 9 tested, ranged between 2.28 minutes to 4.17 minutes, with the exception of subject 7 who had a time constant of 1.19 minutes. Hence, it may be inferred that the recovery process in 8 out of 9 subjects had similar response times. Table 3.8 shows the time constants obtained from the recovery curves of all the 9 subjects tested. It can be observed that the time constants of the recovery process of 8 subjects ranged between 2 - 4 minutes (approximately). The stabilized overshoot of MFCV above the pre-fatigue value was observed in all subjects, except subjects 2, 7 and 9 (Appendix A.2). Appendix A.2 contains remaining results of the recovery phase.

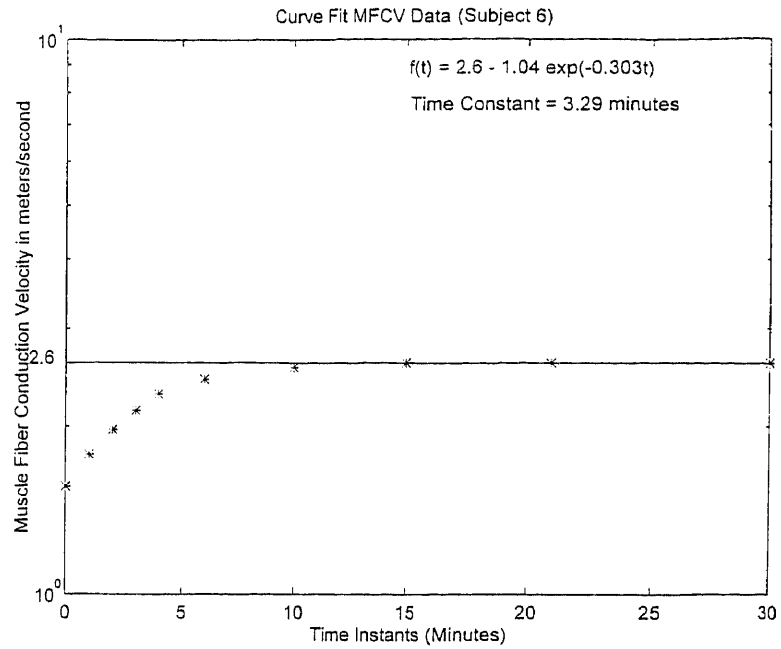


Figure 3.9
Curve Fitted MFCV Data (Subject 6)

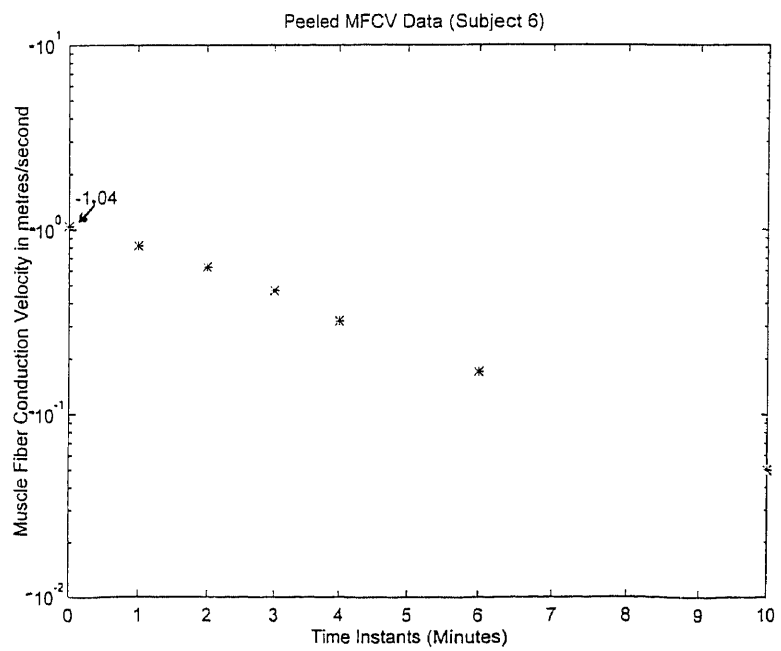


Figure 3.10
Peeled MFCV Data (Subject 6)

3.2 Precision Decomposition of the EMG Signal (Preliminary Results)

The second study involved the decomposition of the myoelectric signal. As mentioned in section 1.5 the objective of this study was to recover as much morphological and temporal information as possible from the myoelectric signal (ME). Precision decomposition therefore involves the decomposition of the ME into its constituent motor units and the templates (signatures) of each motor unit.

3.2.1 Discussion of results

The EMGs from four subjects (different from the MFCV study) were decomposed and the results obtained are discussed in this section. Figure 3.11 shows us three channels of the typical EMG signal recorded from subject A. This signal was obtained from the raw EMG signal and was digitally filtered (low pass, cut off frequency: 300 Hz) so that high frequency noise could be eliminated.

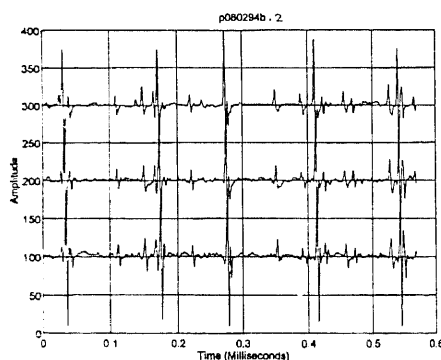


Figure 3.11
Original Filtered Signal
(Channels increase from bottom to top)
Subject A (0.58 msec)

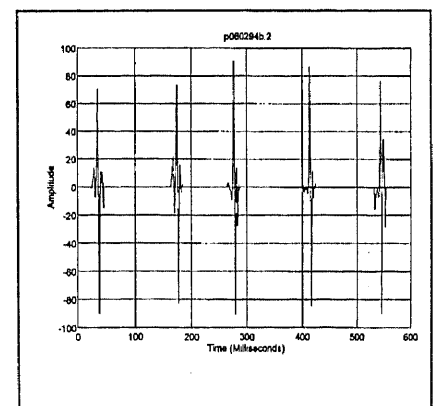


Figure 3.12
Amplitude Thresholded Signal
Channel 1

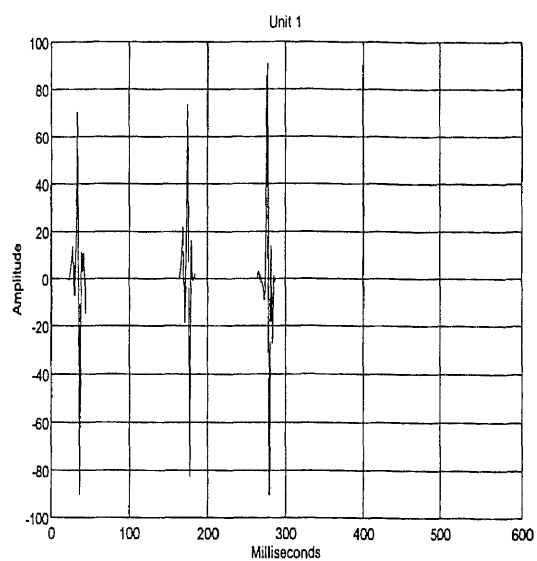


Figure 3.13
Decomposed Signal (Unit I)
Threshold (55 mV) and Decision Criterion (0.15)

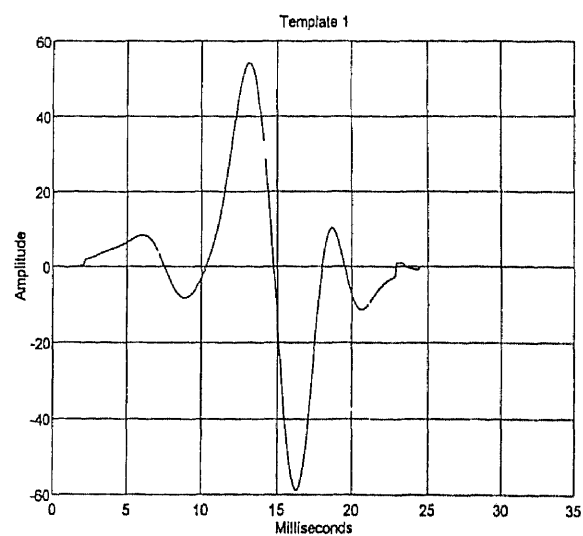


Figure 3.15
Template (Unit I)

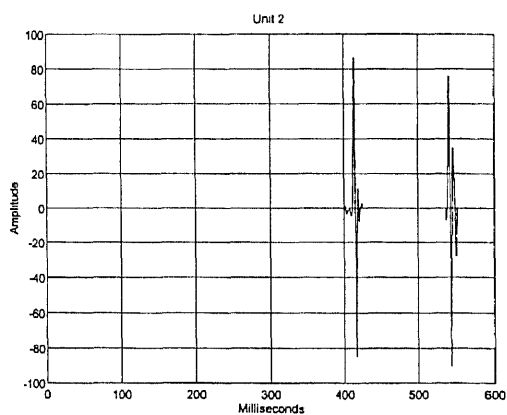


Figure 3.14
Decomposed Signal (Unit II)
Threshold: 55 mV, Decision Criterion: 0.15

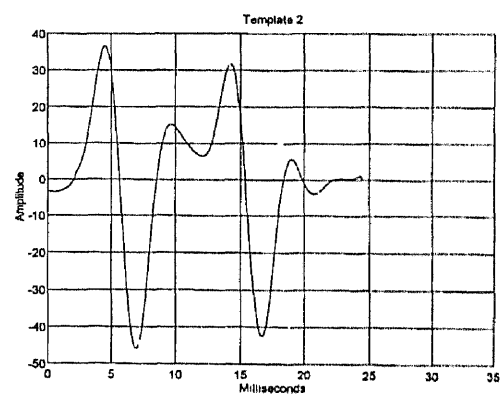


Figure 3.16
Template (Unit II)

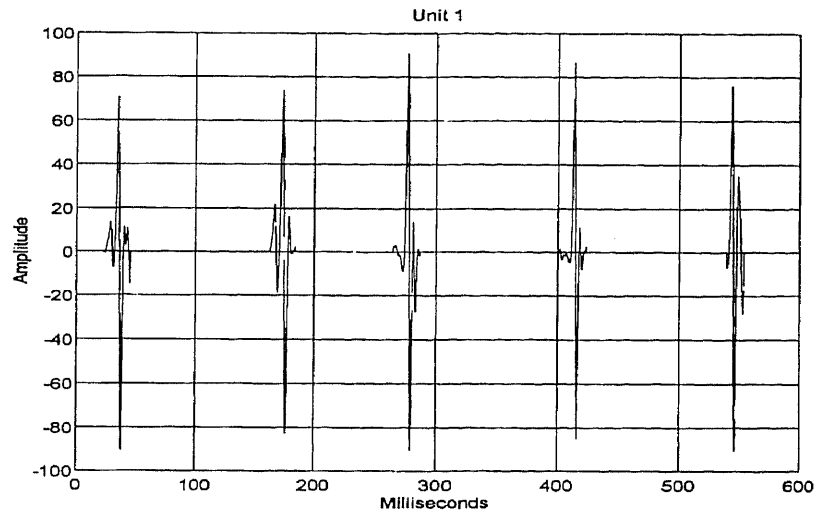


Figure 3.17
Decomposed Signal (Unit I)
Threshold (55 mV), Decision Criteria (0.35)

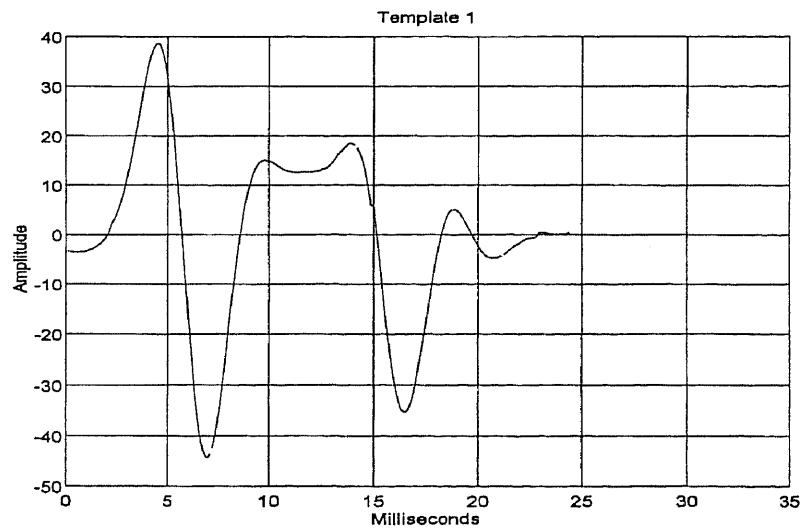


Figure 3.18
Template (Unit I)
Threshold (55 mV), Decision Criterion (0.35)

Channel 1 of this filtered signal was given as an input to the amplitude thresholding software, and the signal was amplitude thresholded (TS) (55 mV) and reconstructed. The reconstructed signal is shown in figure 3.12. The TS was then given as an input to the decomposition software and was separated into its constituent units based on a decision criterion of 0.15 [11]. Figures 3.13 and 3.14 show us the constituent motor units of the TS. Figures 3.15 and 3.16 are the templates of these units, which were formed during the decomposition. The decision criterion (0.15) which was used for the decomposition of the TS was based on the value reported by Deluca et al.[11] and this value was chosen for a fine wire EMG recording.

An important characteristic of a motor unit is its firing rate/ frequency. Each motor unit fires at a given frequency unique to itself and this factor influenced the selection of the decision criterion by the author. Looking at the TS in figure 3.12 we find that all the action potentials (AP) are spaced at nearly equal intervals. The author's observations were confirmed after consultation with an experienced neurophysician at Kessler Institute for Rehabilitation. It was hence believed that all the five action potentials in the TS in figure 3.12 were from the same unit.

Thus the decision criterion was changed by the author from 0.15. Various values of the decision criterion were tried by the author, beginning at a value of 0.15 and proceeding in increments of 0.05. It was found that when the criterion was set to 0.35 all the APs in figure 3.12 were assigned to one unit. Furthermore, decision criteria above the value of 0.35 also yielded the same result. The results obtained due to this change are indicated in figures 3.17 and 3.18. It can be observed that the template in figure 3.18 is a

combination of the templates formed (decision criterion 0.15) in figures 3.15 and 3.16.

This was because the decision criterion was relaxed from 0.15 to 0.35.

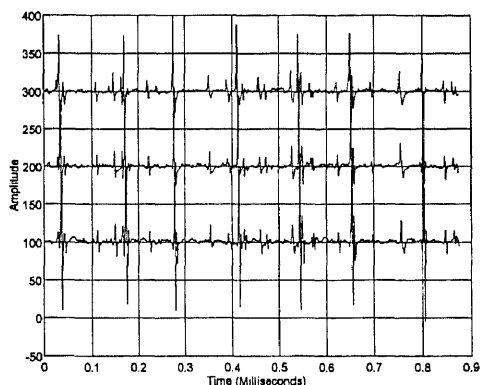


Figure 3.19
Three Channels of the Filtered Original Signal
Subject A (0.85 secs)

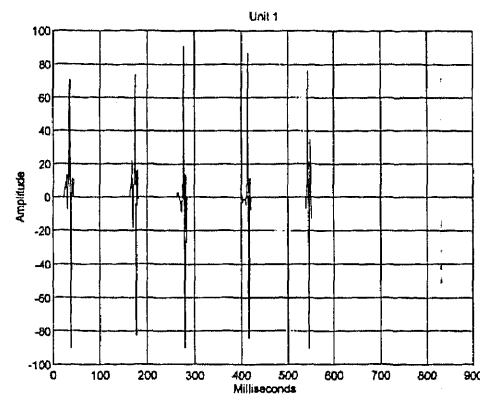


Figure 3.21
Decomposed Signal (Unit I)
(Subject A)

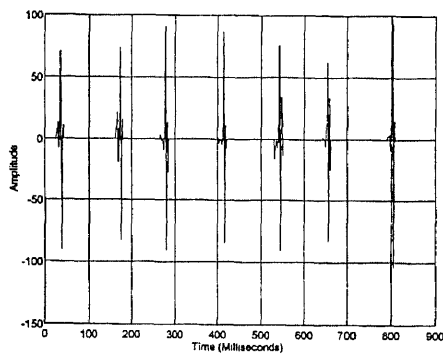


Figure 3.20
Amplitude Thresholded Signal (TS)
(Subject A)

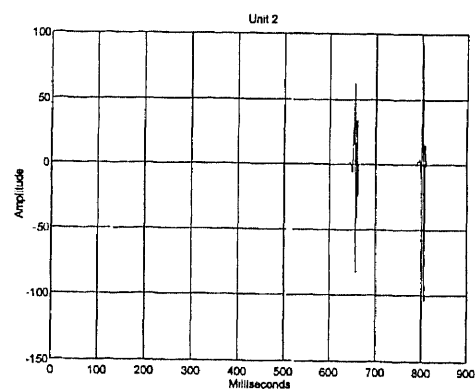


Figure 3.22
Decomposed Signal (Unit II)
(Subject A)

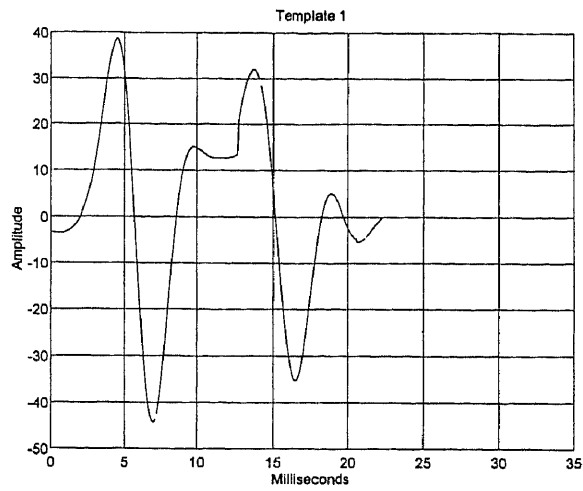


Figure 3.23
 Template (Unit I)
 Threshold (55 mV), Decision Criterion (0.35)

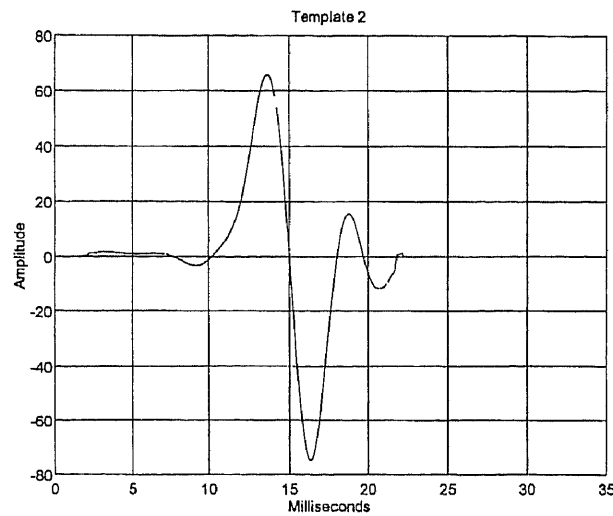


Figure 3.24
 Template (Unit II)
 Threshold (55 mV), Decision Criterion (0.35)

Figures 3.19 to 3.24 show us the decomposition of the EMG of subject A. However this time a longer section of EMG (0.85 seconds) was taken for decomposition. Figure 3.19

represents the filtered EMG signal (0.85 seconds) of subject A. As mentioned earlier a digital low pass filter having a cut off frequency of 300 Hz was used. The (TS) is shown in figure 3.20. The TS was then decomposed and the constituent units of the TS are shown in figures 3.21 and 3.22. The templates of the corresponding units are indicated in figures 3.23 and 3.24. Looking at the templates in figures 3.23 and 3.24 and comparing these with the template in figure 3.18 we may infer the following.

The templates in figures 3.23 and 3.24 were obtained as a result of the decomposition of the EMG signal in figure 3.19, which was of greater duration than the EMG signal in figure 3.11. The TS in figure 3.20 shows seven APs as compared to that in figure 3.12 where there were five APs. As mentioned earlier in this section the decision criterion was changed from 0.15 to 0.35. This was done to obtain a decomposition of the EMG signal in figure 3.11, such that it conforms with our expectations regarding the firing rate of a motor unit. The same decision criterion was used for the decomposition of this extended (in time) TS (figure 3.20). We find that the first five APs in figure 3.20 have been assigned to one motor unit (same as in figure 3.19), while the two new action potentials which are seen in figure 3.20 (and not in 3.12) are assigned to another unit.

Keeping in mind the earlier discussion about the firing rate of the motor units it is once again believed that owing to the near periodic firing interval between the APs in figure 3.20, they should belong to the same motor unit. However the results of the program do not agree with our expectations and these are explained as follows. The first five APs are assigned to the same motor unit and this is done by comparing each AP with its corresponding template. The decision criterion of 0.35 was used in each of these

comparisons. When the sixth AP is encountered (fig. 3.20), the template for the first unit (in figures 3.23 and 3.18) has been sufficiently distorted so that the next comparison results in it being assigned to another motor unit, which is contrary to our expectations.

It can be inferred from the above discussion that owing to the superposition of adjacent motor units in the original EMG signal (fig. 3.19), the shape of each AP is affected. This is a very important factor in this study, as the decomposition is based on the templates, which are in turn influenced by the shape of the individual APs. Hence the need for an involved superposition algorithm is felt at this juncture.

Figures 3.26 to 3.30 show us the results of the decomposition of the myoelectric signal (ME) of subject B (figure 3.25) using a decision criterion of 0.15 [11]. As in the case of subject A, the filtered ME (low pass: cut off 300 Hz) (0.58 secs.) of subject B was amplitude thresholded (55 mV) and then decomposed into its constituent motor units. Figure 3.26 shows us the amplitude thresholded signal (TS), which was then decomposed to yield two constituent motor units, as shown in figures 3.27 and 3.28. Figures 3.29 and 3.30 show us the templates obtained as a result of decomposition of the TS.

We find that the TS (figure 3.26) contains two action potentials (APs). It was believed that these two APs were from the same motor unit as their firing rate were almost equal. Hence the decision criterion was changed to 0.35 (for reasons stated earlier) and the motor unit and its corresponding template are shown in figures 3.31 and 3.32.

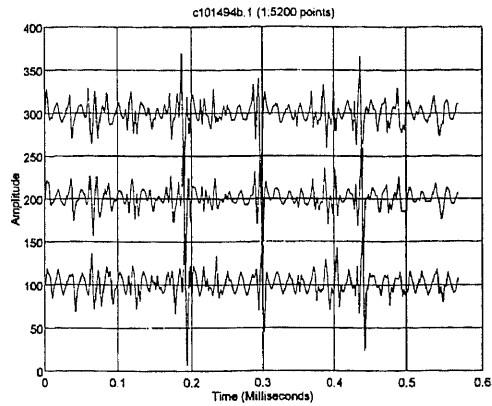


Figure 3.25
 Filtered Original EMG Signal (Subject B)
 (low pass filter: cut off : 300 Hz)

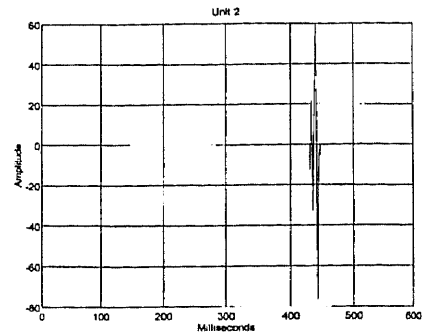


Figure 3.28
 Decomposed Signal (Unit II)
 (decision criterion: 0.15)

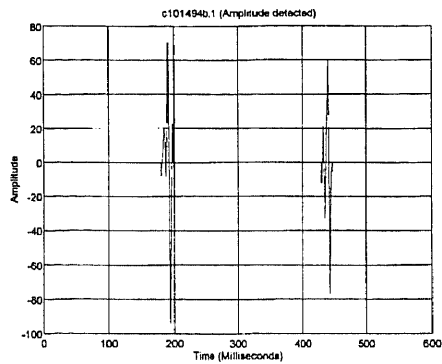


Figure 3.26
 Amplitude Thresholded Signal (Subject B)
 Threshold (55mV), Decision criterion (0.15)

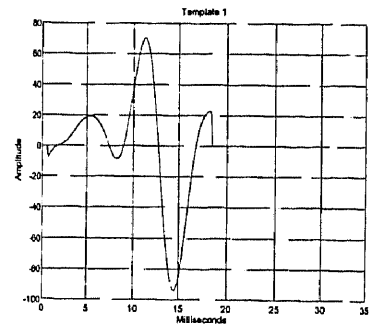


Figure 3.29
 Template 1 (Unit I)

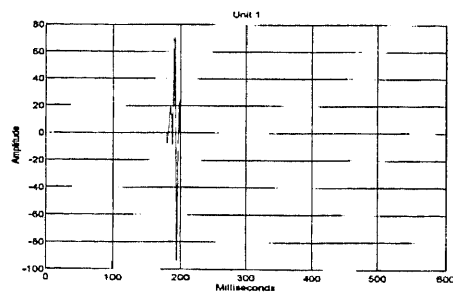


Figure 3.27
 Decomposed Signal (Unit I)
 (Decision criterion : 0.15)

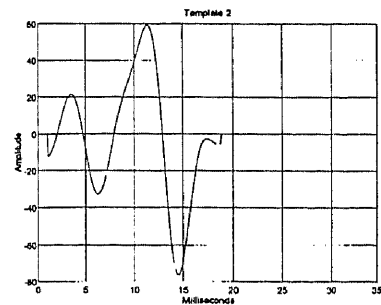


Figure 3.30
 Template 2 (Unit II)
 (Decision criterion: 0.15)

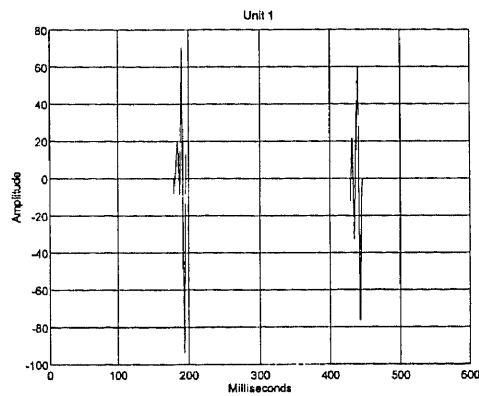


Figure 3.31
Decomposed Signal (decision criterion: 0.35)
(Unit I)

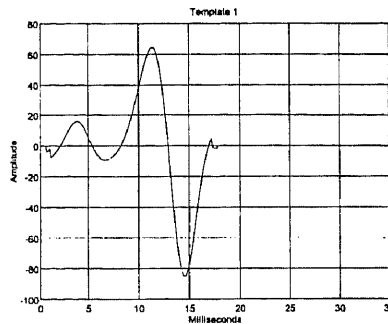


Figure 3.32
Template I (Unit I)
(decision criterion: 0.35)

Figure 3.33 shows us the same EMG signal as in figure 3.25, however a longer section of the EMG signal (1.024 secs) is analyzed in this case. The original EMG signal in figure 3.33 is amplitude thresholded (55mV), as described earlier in this section, to give TS as indicated in figure 3.34. This signal is then decomposed into its motor unit based on the decision criterion of 0.35 which was chosen for reasons mentioned earlier in this section. The decomposed signal obtained from the TS is indicated in figure 3.35. The template

corresponding to this unit is indicated in figure 3.36. Figure 3.37 shows us the same EMG signal as in figure 3.33. However in this case we have a longer section (1.35 secs.) of the

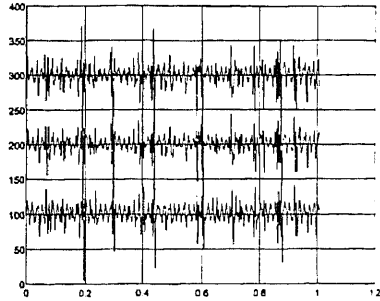


Figure 3.33 (Subject B)
Original Filtered Signal (1.024 secs.)
(low pass cut off : 300 Hz)

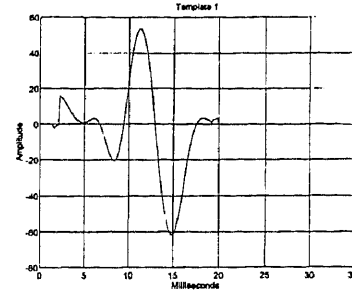


Figure 3.36
Template I (Unit I)

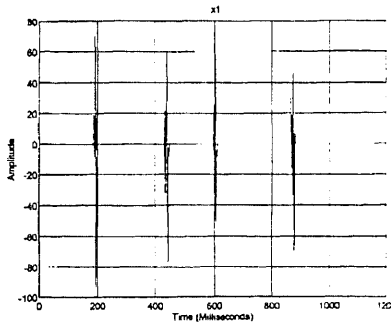


Figure 3.34
Amplitude Thresholded Signal (TS)

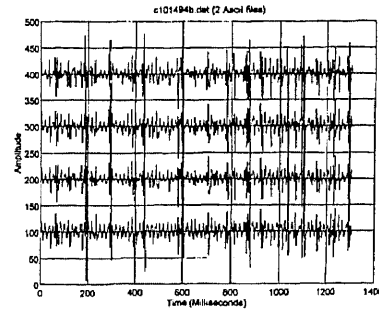


Figure 3.37
Original Signal (1.35 seconds)

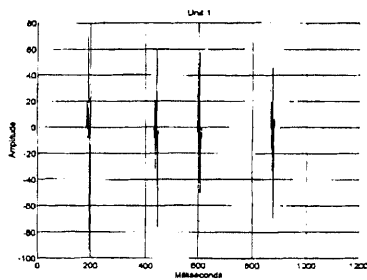


Figure 3.35
Decomposed Signal (Unit I)

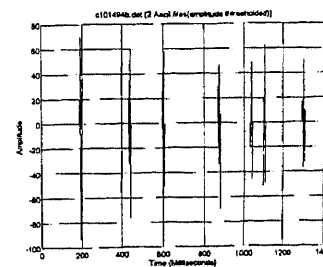


Figure 3.38
Amplitude Thresholded Signal
(TS)

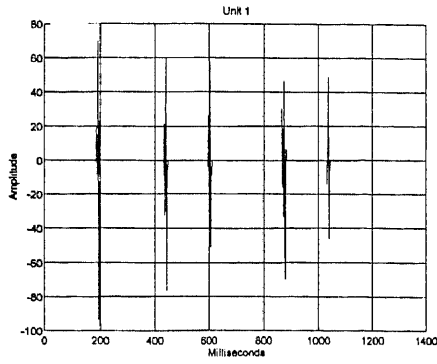


Figure 3.39
Decomposed Signal (Unit I)
Decision Criterion : 0.35

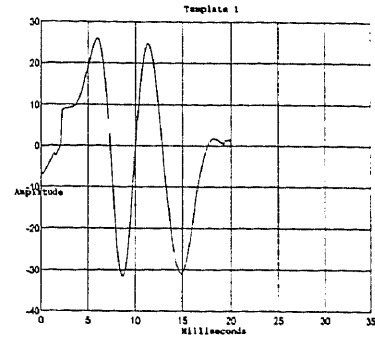


Figure 3.42
Template I (Unit I)

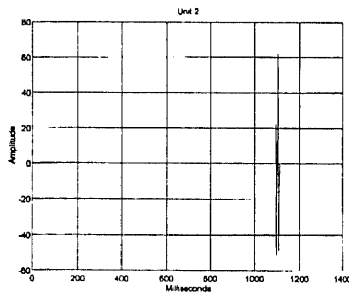


Figure 3.40
Decomposed Signal (Unit II)
Decision Criterion: 0.35

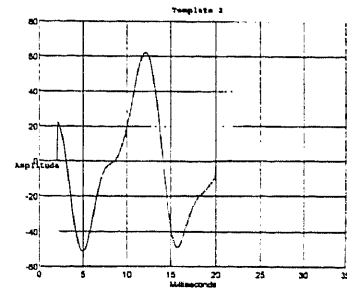


Figure 3.43
Template II (Unit II)

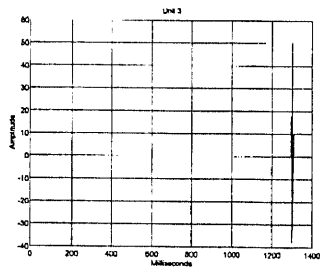


Figure 3.41
Decomposed Signal (Unit III)
Decision Criterion: 0.35

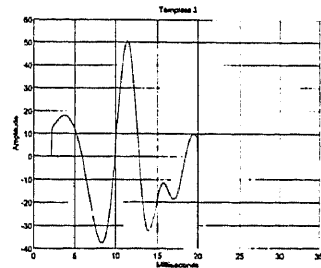


Figure 3.44
Template III (Unit III)

same. Figure 3.38 is the TS obtained from the original filtered EMG in figure 3.37. Figure 3.38 has 7 action potentials (APs) as compared to the TS of figure 3.34 which has four APs. Looking at the TS (figure 3.38) we find that the fifth AP occurs after a time period which is nearly the same as that of the first four APs. Hence it is believed that this belongs to the same motor unit as the other four APs and therefore it is assigned to the same motor unit as indicated in figure 3.39. However the sixth AP fires close to the fifth AP and based on our discussion regarding the firing rate of a motor unit, it is believed that it does not belong to the same motor unit. Therefore it is assigned to another motor unit as indicated in figure 3.40. The seventh AP fires at a much later time as compared to the fifth and the sixth AP. Hence following the same reasoning as before, it is assigned to another motor unit, which is shown in figure 3.41. Figures 3.42 to 3.44 show us the templates corresponding to these motor units. We find that the shapes of these templates also show a significant difference hence justifying our decomposition based on the firing rate of motor units.

This discussion suggests that a decision criterion of 0.35 be used for the decomposition of the surface EMG, using this algorithm/software. Furthermore it has been observed that the superposition of APs from adjacent motor units could reduce the accuracy of this decomposition technique by distorting the shape of the individual APs and hence the template, and therefore an involved superposition algorithm is required to eliminate these superpositions. Appendix A.3 contains the results of two more subjects whose EMG were decomposed using the decision criterion of 0.35.

CHAPTER 4

CONCLUSIONS

4.1 Muscle Fiber Conduction Velocity (MFCV)

As discussed in section 3.1 this study had two objectives, first to determine if MFCV could be used as a reliable indicator of fatigue and second, to study and characterize the recovery of the MFCV after a 20% MVC up to the endurance limit. This section brings out certain important conclusions that were obtained as a result of this study.

4.1.1 MFCV (Fatigue)

The results of this study have already been presented in section 3.1.1. It was found that in all the 6 subjects who were tested, the MFCV declined with the progression of fatigue. As seen in the plots of MFCV vs time instants (minutes) in figures 3.1 and 3.3 (section 3.1.1), the decline of MFCV has been modelled using a simple linear regression. The slope of the regression line tells us the extent to which the subject is fatigued. The decline of MFCV with fatigue in all the 6 subjects tested may be attributed to the following factors.

In the initial stages of a contraction, the type I muscle fibers (smaller diameter, faster firing rate and fatigue resistant) are recruited. These fibers are low twitch fibers i.e. they contract very slowly. However in order to maintain a 20% MVC the subject recruits type II muscle fibers (larger diameter, slower firing rate, fatiguable). This recruitment of type II fibers explains the initial rise (0 min.: fatigue) of MFCV found in

all the 6 subjects tested. However type II fibers are fatiguable and hence as they contract there is a buildup of metabolites viz. lactic acid. Furthermore some of the type II fibers may not be able to produce sufficient force during the course of the fatiguing contraction and may therefore drop out, while the slower type I fibers still contract.

The buildup of lactic acid reduces the excitability of the cell membranes of the muscle fibers and hence the MFCV goes down with fatigue. Another effect that is produced due to the buildup of lactic acid is that the action potentials get broader in shape. This reduces the frequency of the myoelectric signal and this is manifested as a decline in the median frequency.

As discussed in section 3.1.1 the percent decline in median frequency (MF) and MFCV were compared for 4 out of the 6 subjects tested. It was found in 3 out of 4 subjects, that the percent decline in the MF was more pronounced than that of the MFCV. This indicates that the decline of MF is also influenced by other factors like synchronization, recruitment and firing rate of motor units and not by the MFCV alone.

We find that the MFCV declines for all the 6 subjects tested and that this decline of the MFCV corresponds to the decline of MF for 4 out of the 6 subjects tested. Hence we may say that MFCV can also be used as a reliable indicator of fatigue, although it is only one of the factors that can be used to explain fatigue.

4.1.2 MFCV (Recovery)

The results of this study have been presented and discussed in section 3.1.2. The recovery curve of the MFCV has been characterized and a possible explanation for the recovery of the MFCV has been suggested. As described in section 3.1.2 the MFCV of all the nine subjects at (1 min.: post fatigue) rose above the MFCV value at (0 min.: postfatigue). This could be due to the recovery of strength of the type II muscle fibers, which were earlier exhausted, due to the fatigue contraction (20% MVC). The rise in the MFCV at (1 min.: post fatigue) in all subjects could be due to the commencement of the breakdown of lactic acid in the interstitial fluid surrounding the muscle cell membranes, thereby increasing the excitability of the cell membranes, consequently increasing the MFCV. All subjects except subjects 1 and 2 recovered and overshoot their original value of MFCV within 4 minutes.

A stabilized overshoot in the MFCV was observed in all subjects, except subjects 2, 7 and 9. One possible explanation for the overshoot of the MFCV is the increase in the muscle fiber diameter caused by an increase in water content during dynamic exercise conditions.

An increase in temperature is accompanied by an increase in MFCV. However in this study this association between temperature and MFCV were observed only in subjects 3, 6 8 and 9 (between 2-6 min. post fatigue). However a subsequent decline in temperature produced no significant effect on the MFCVs. A clear association between temperature and MFCV was lacking in subjects 1, 2, 4, 5 and 7.

The recovery curves of the MFCV of all nine subjects were curve fit to an exponential using the exponential peeling technique. All recovery curves consisted of a dc component and an exponential component. As discussed in section 3.1.2, the time constants were calculated for all the 9 subjects. It was found that in 8 out of the 9 subjects, the time constants were between 2 - 4 minutes, indicating that the recovery process had a similar response in these subjects. Hence a possible explanation of the recovery process of the MFCV has been provided.

4.2 Precision Decomposition of the EMG

As discussed in section 3.2.1 the aim of the precision decomposition technique was to extract as much morphological and temporal information as possible from the myoelectric signal. The EMG data from four subjects were decomposed using the software developed by the author. The preliminary results of two subjects were discussed in detail in section 3.2 and one more interesting result will be discussed in section 4.3. These results bring out certain deficiencies in the existing software and in the type of recording, namely the surface EMG.

As described in section 3.2, the firing rate is an important characteristic of a motor unit. This fact influenced the selection of a decision criterion of 0.35 for decomposition of the surface EMG signal as against 0.15 for the fine wire EMG signal.

It has been observed that this value of the decision criterion yielded decompositions for the two subjects namely, A and B, which conformed with our expectations, based on the firing rate of motor units. However further research is needed

to validate these preliminary results. The superposition of action potentials (APs) from adjacent motor units distort the APs of a motor unit of interest. Hence an algorithm that eliminates the superposition of the APs is required for decomposing surface EMGs so that the accuracy of this technique may be enhanced.

4.3 Suggestions for the Future

4.3.1 Muscle Fiber Conduction Velocity (MFCV)

The accuracy of the cross correlation technique may be improved by sampling the analog EMG signal at frequencies of 10 - 50 KHz per channel. Such a high sampling rate ensures a lesser spacing between the samples improving the resolution and hence the accuracy of this technique. Data acquisition in this study was done using ordinary wires. It is recommended to use instrumentation cables/wires to minimize the interference due to noise and electromagnetic fields.

As mentioned in section 2.1, the force maintained by the subjects during a contraction was measured in this study. However there were variations in force and hence a criterion has to be established for limiting the deviations of the force of contraction of the subject. Lastly, more subjects have to be tested using the same protocol to confirm the existing results.

4.3.2 Precision Decomposition

Appendix A.3 shows us the results of the remaining two subjects whose EMGs were decomposed using the precision decomposition technique. Referring to Appendix A.3 (subject C) we observe that the original filtered EMG signal (figure A.3.1) is amplitude thresholded (55 mV). The amplitude thresholded signal (TS), in this case contains 4 dominant action potentials (APs) which need to be decomposed into their respective units. The TS is indicated in figure A.3.2. Bearing in mind the discussion regarding the firing rate of the motor units, we may believe that all the 4 APs come from the same unit.

The decision criterion in this case was set to the recommended value of 0.35 for the surface EMG. However it can be observed that the TS has been decomposed into two motor units which are indicated in figures A.3.3 and A.4.4 in Appendix A.3. The templates corresponding to these motor units are shown in figures A.3.5 and A.3.6 in Appendix A.3.

Keeping the threshold value the same (0.35), the author changed the length of each action potential from a total of 300 points to 120 points and the results are shown in figures A.3.7 to A.3.11 in Appendix A.3. It is observed that in the TS (figure A.3.7 : Appendix A.3), the shape of the APs have changed and the results of the decomposition are also different. Looking at figures A.3.8 and A.3.9 we find that this TS (figure A.3.7) has been decomposed into two motor units as before, the difference being that the first motor unit contains all but the one AP at 200 milliseconds. The templates of the corresponding units are indicated in figures A.3.10 and A.3.11. This decomposition tells us that the number of points and hence the shape of each individual action potential can change the results of the decomposition.

Hence further research is needed to determine the optimum size or a range of sizes i.e. number of points, of each individual AP, so that the results obtained from the decomposition software are consistent for, different lengths of data of, all the subjects tested. Furthermore the decomposition procedure needs to be tested with the decision criterion of 0.35 on several subjects to determine the optimal value of the criterion. Further study is also required to determine the amplitude threshold as a result of which the amplitude thresholded signal (TS) is obtained.

Finally, the decomposition algorithm itself has to be tested for consistency on several fine wire EMG recordings, as it has been reported [11], that the fine wire EMG signal has fewer motor units, with fewer superpositions, meaning that the validation of the results obtained from this algorithm would be much easier. Once this has been accomplished, this technique may then be used to decompose surface EMGs.

APPENDIX A

REMAINING RESULTS

A.1 Muscle Fiber Conduction Velocity (MFCV)

As mentioned in section 3.1 there were two objectives of this study. The first was to evaluate if MFCV could be used as a reliable indicator of fatigue and the second was to characterize the recovery of MFCV after a fatiguing contraction. More results of these studies will follow after this section.

Table A.1.1 MFCV (Fatigue) and Median Frequency (Subject 8)

Subject 8				
Condition	Time minutes	MFCV metres/second	Median hertz	Temperature centigrade
during fatigue	0	3.0	119	25.8
during fatigue	2	2.6	84	25.6
during fatigue	4	2.6	81	25.3
during fatigue	6	2.5	66	25.3
during fatigue	8	2.5	76	25.8
during fatigue	10	2.0	69	26.1
during fatigue	12	2.8	72	27.0

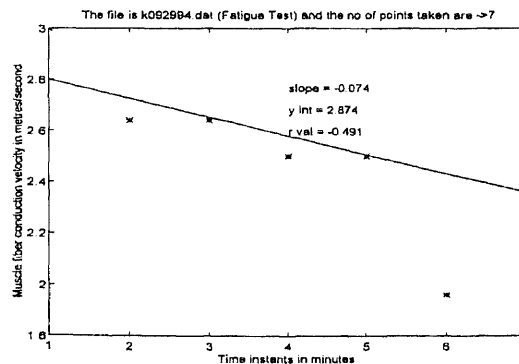


Figure A.1.1
Decline of MFCV with Fatigue (Subject 8)
MFCV vs Time Instants

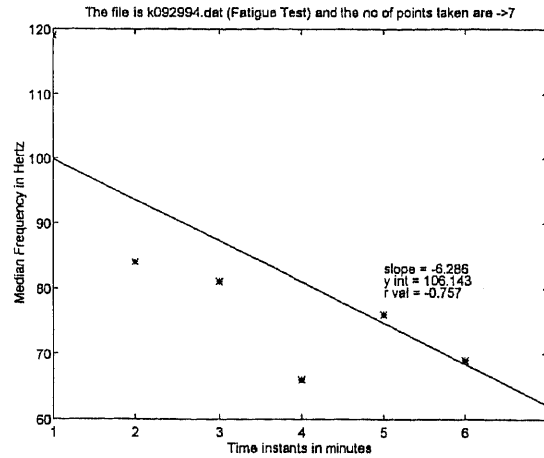


Figure A.1.2
Decline of Median Frequency with Fatigue (Subject 8)
Median frequency vs Time instants

Table A.1.2 MFCV (Fatigue) and Median Frequency (Subject 3)

Subject 3				
Condition	Time minutes	MFCV metres/second	Median frequency Hertz	Temperature centigrade
during fatigue	0	2.4	113	26.3
during fatigue	2	2.5	109	26.3
during fatigue	4	2.4	99	26.2
during fatigue	6	2.3	99	26.4
during fatigue	8	2.1	81	27.0
during fatigue	10	2.1	88	27.4
during fatigue	12	2.1	87	27.8
during fatigue	14	2.1	93	27.8

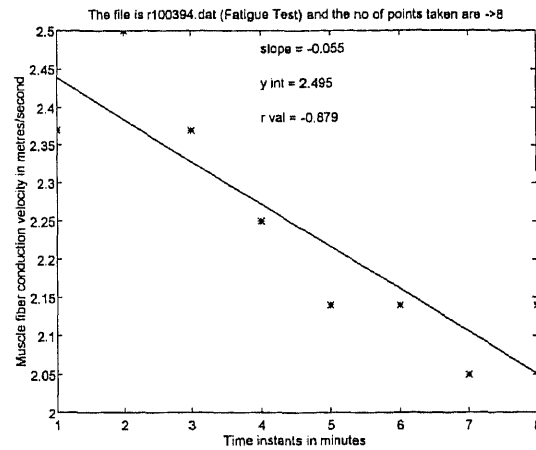


Figure A.1.3
Decline of MFCV with Fatigue (Subject 3)
MFCV vs Time instants

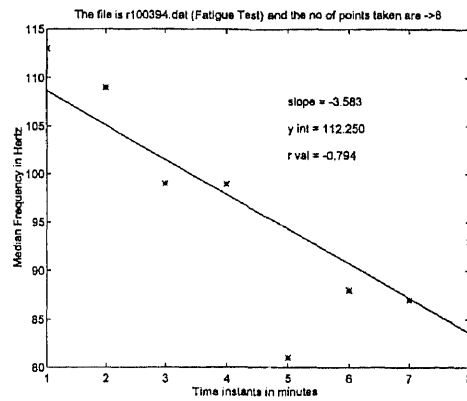


Figure A.1.4
Decline of Median Frequency with Fatigue (Subject 3)
Median frequency vs Time Instants

Table A.1.3 MFCV (Fatigue): Subject 7

Subject 7			
Condition	Time minutes	MFCV metres/second	Temperature centigrade
during fatigue	0	3.5	32.9
during fatigue	2	3.5	32.9
during fatigue	4	3.0	33.1
during fatigue	8	3.0	33.6
during fatigue	10	3.0	33.7

Table A.1.4 MFCV (Fatigue): Subject 2

Subject 2			
Condition	Time minutes	MFCV metres/second	Temperature centigrade
during fatigue	0	2.37	28.5
during fatigue	2	2.14	28.0

A.2 MFCV Recovery**Table A.2.1** MFCV Recovery (Subject 1)

Subject 1			
Condition	Time (minutes) (with respect to fatigue)	MFCV metres/second	Temperature centigrade
prefatigue	before fatigue	3.20	33.4
post fatigue	0	2.40	33.8
post fatigue	1	2.80	33.8
post fatigue	2	3.00	33.8
post fatigue	3	2.80	33.8
post fatigue	4	3.00	33.7
post fatigue	6	3.00	33.6
post fatigue	10	3.20	33.7
post fatigue	15	3.20	33.6
post fatigue	21	3.20	33.4
post fatigue	30	3.50	33.2

Table A.2.2 Smoothed MFCV Data Plotted using the Exponential Peeling Technique (Subject 1)

Subject 1 Recovery										
F(t)	2.58	2.69	2.81	2.91	2.97	3.07	3.2	3.2	3.2	3.2
F1(t)	-0.62	-0.51	-0.39	-0.29	-0.23	-0.13				
t minutes	0.00	1.00	2.00	3.00	4.00	6.00	10.00	15.00	21.00	30.00

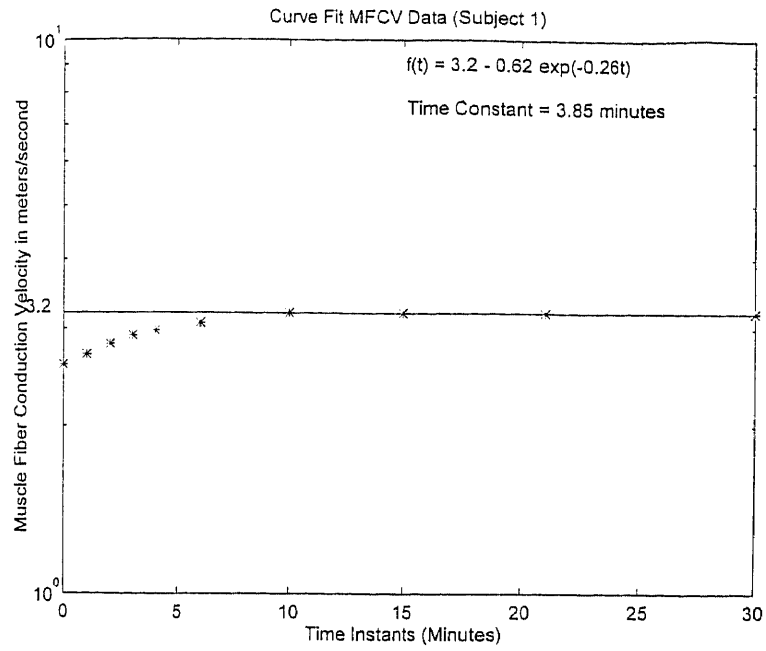


Figure A.2.1
Curve Fitted MFCV Data (Subject 1)

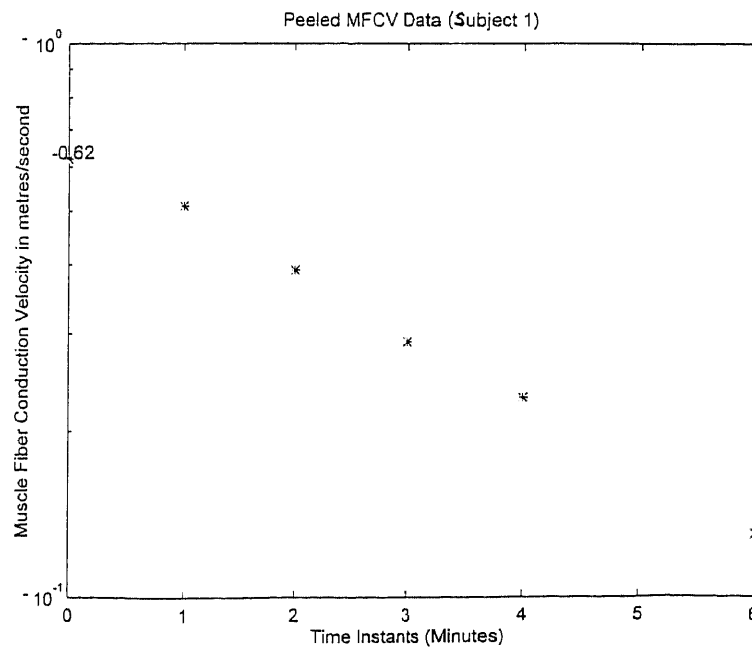


Figure A.2.2
Peeled MFCV Data (Subject 1)

Table A.2.3 MFCV Recovery (Subject 2)

Subject 2			
Condition	Time (minutes) (with respect to fatigue)	MFCV metres/second	Temperature centigrade
prefatigue	before fatigue	3.20	28.3
fatigue	0	1.88	27.9
fatigue	1	2.70	27.9
fatigue	2	2.80	28.4
fatigue	3	2.80	28.3
fatigue	4	3.00	29.2
fatigue	6	2.80	29.0
fatigue	10	2.80	29.3
fatigue	15	3.00	28.8
fatigue	21	3.00	27.9
fatigue	30	2.80	27.7

Table A.2.4. Smoothed MFCV Data Plotted using the Exponential Peeling Technique (Subject 2)

Subject 2 Recovery										
F(t)	2.61	2.7	2.77	2.81	2.83	2.87	2.9	2.9	2.9	2.9
F1(t)	-0.29	-0.2	-0.13	-0.09	-0.07	-0.03				
t minutes	0.00	1.00	2.00	3.00	4.00	6.00	10.00	15.00	21.00	30.00

Table A.2.5 MFCV Recovery (Subject 3)

Subject 3			
Condition	Time (minutes) (with respect to fatigue)	MFCV metres/second	Temperature centigrade
prefatigue	before fatigue	2.14	26.3
post fatigue	0	-	28.3
post fatigue	1	2.14	28.4
post fatigue	2	2.25	28.5
post fatigue	3	2.40	28.6
post fatigue	4	2.40	28.6
post fatigue	6	2.50	28.6
post fatigue	10	2.50	28.4
post fatigue	15	2.50	28.0
post fatigue	21	2.40	27.6
post fatigue	30	2.40	27.0

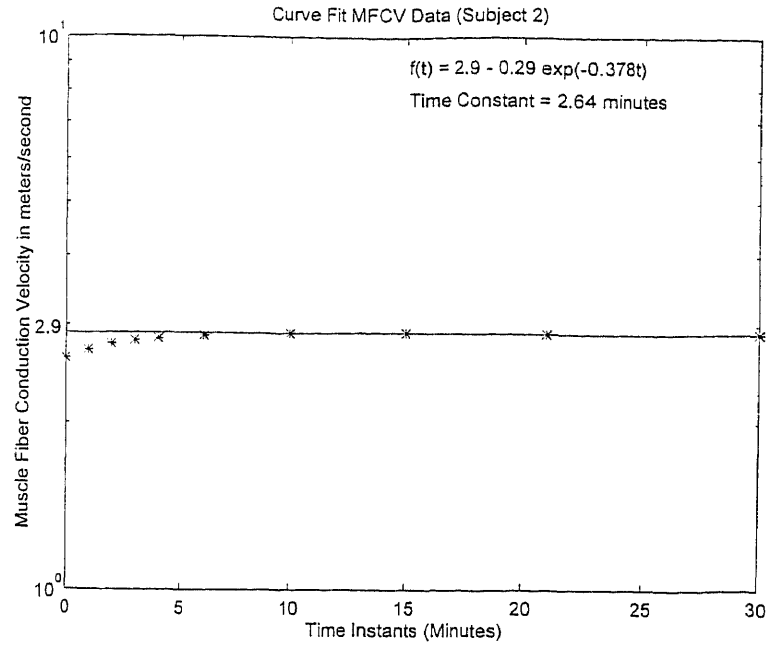


Figure A.2.3
Curve Fitted MFCV Data (Subject 2)

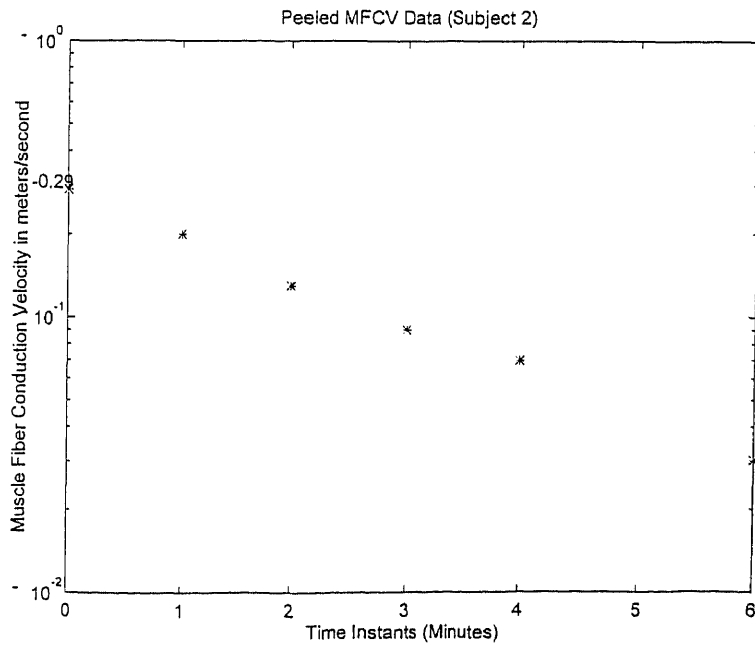


Figure A.2.4
Peeled MFCV Data (Subject 2)

Table A.2.6 Smoothed MFCV Data Points Plotted using the Exponential Peeling Technique (Subject 3)

Subject 3 Recovery										
F(t)	2.1	2.19	2.3	2.37	2.44	2.5	2.5	2.5	2.5	2.5
F1(t)	-0.4	-0.3	-0.2	-0.13	-0.08					
t minutes	0.00	1.00	2.00	3.00	4.00	6.00	10.00	15.00	21.00	30.00

Table A.2.7 MFCV Recovery (Subject 5)

Subject 5			
Condition	Time (minutes) (with respect to fatigue)	MFCV metres/second	Temperature centigrade
prefatigue	before fatigue	3.00	27.3
post fatigue	0	2.40	29.3
post fatigue	1	3.20	29.6
post fatigue	2	3.20	29.8
post fatigue	3	3.50	30.0
post fatigue	4	3.50	30.1
post fatigue	6	3.75	29.8
post fatigue	10	3.75	29.6
post fatigue	15	3.75	29.0
post fatigue	21	3.20	28.6
post fatigue	30	3.75	28

Table A.2.8 Smoothed MFCV Data Points Plotted using the Exponential Peeling Technique (Subject 5)

Subject 5 Recovery										
F(t)	2.96	3.12	3.28	3.41	3.55	3.61	3.75	3.75	3.75	3.75
F1(t)	-0.79	-0.63	-0.47	-0.34	-0.2	-0.14				
t minutes	0.00	1.00	2.00	3.00	4.00	6.00	10.00	15.00	21.00	30.00

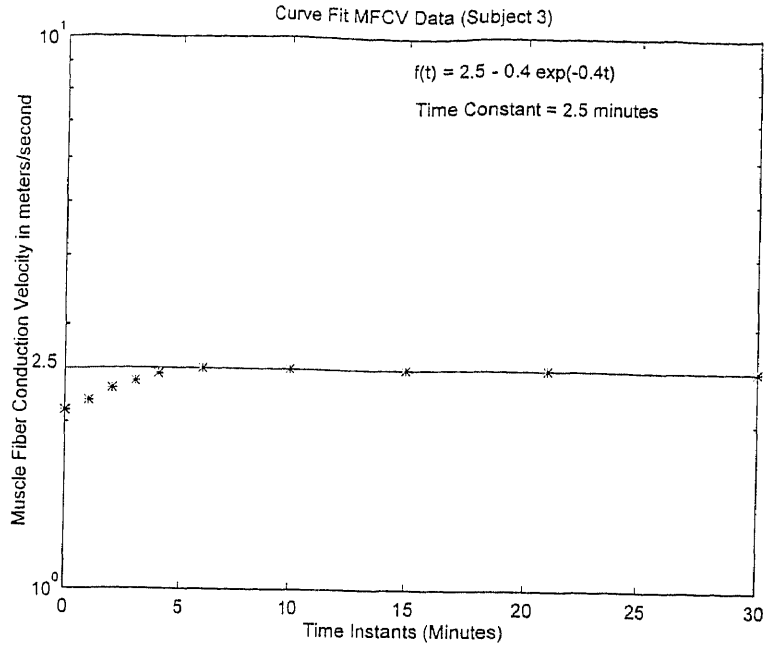


Figure A.2.5
Curve Fitted MFCV Data (Subject 3)

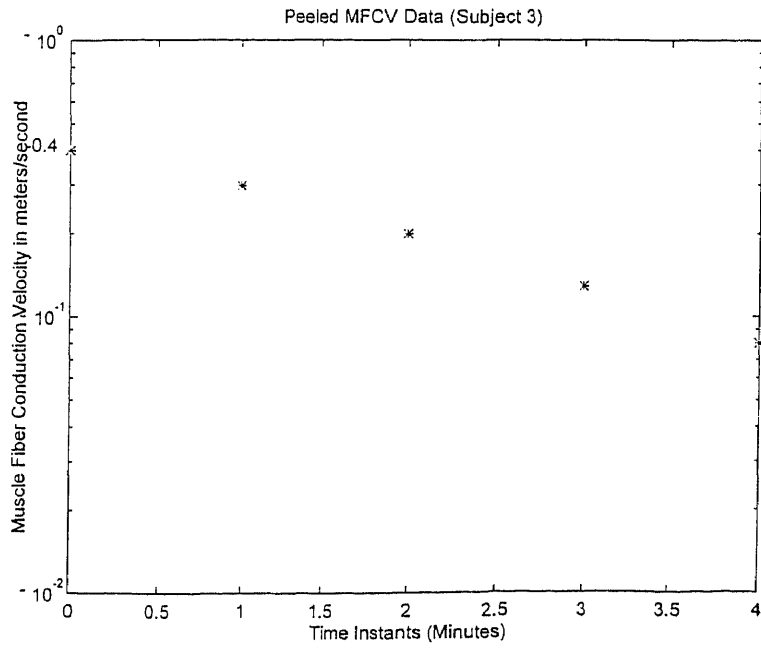


Figure A.2.6
Peeled MFCV Data (Subject 3)

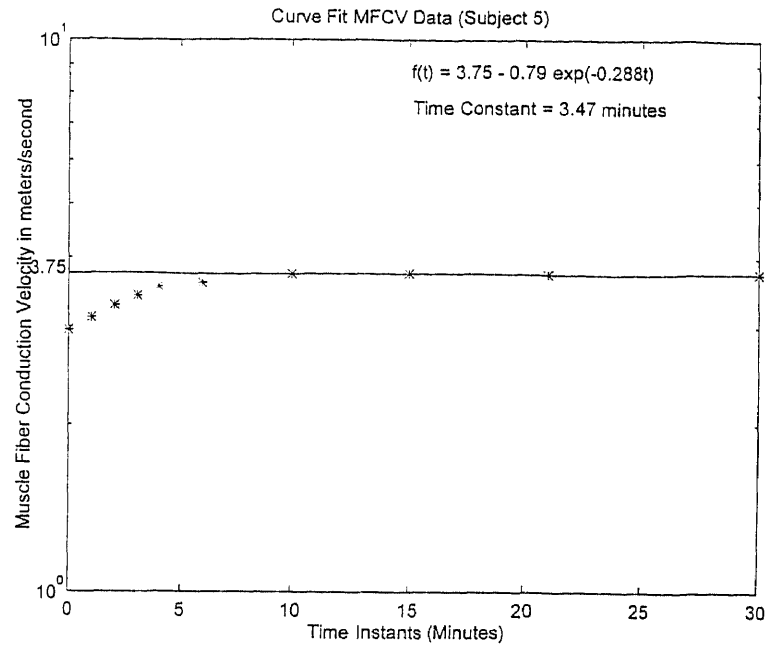


Figure A.2.7
Curve Fitted MFCV Data (Subject 5)

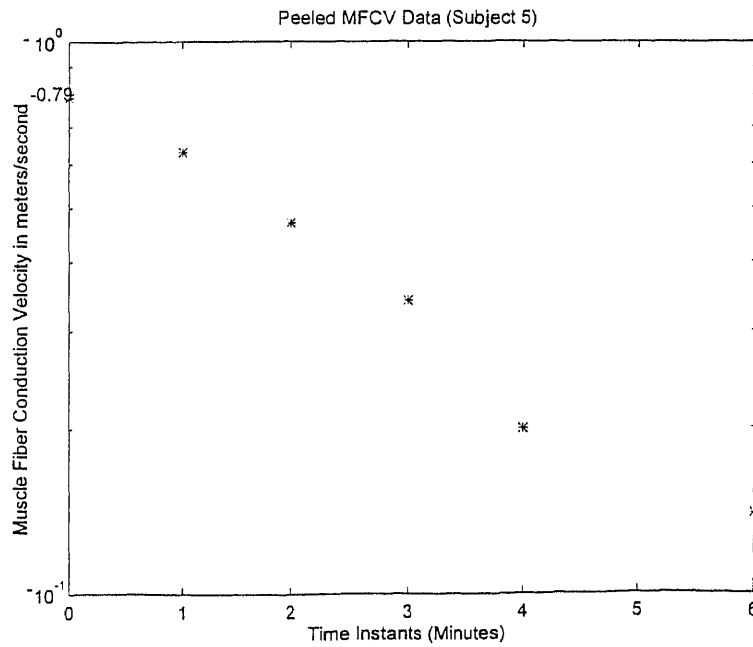


Figure A.2.8
Peeled MFCV Data Points (Subject 5)

Table A.2.9 MFCV Recovery (Subject 7)

Subject 7			
Condition	Time (minutes (with respect to fatigue)	MFCV metres/second	Temperature centigrade
prefatigue	before fatigue	3.5	32.0
post fatigue	0	3.0	33.4
post fatigue	1	3.2	33.4
post fatigue	2	3.8	33.5
post fatigue	3	4.0	33.5
post fatigue	4	3.8	33.5
post fatigue	6	3.5	33.5
post fatigue	10	3.2	33.2
post fatigue	15	3.5	33.3
post fatigue	21	3.5	33.1
post fatigue	30	3.5	31.8

Table A.2.10 Smoothed MFCV Data Points Plotted using the Exponential Peeling Technique (Subject 7)

Subject 7 Recovery										
F(t)	3.08	3.41	3.71	3.85	3.85	3.85	3.85	3.85	3.85	3.85
F1(t)	-0.75	-0.44	-0.14							
t minutes	0.00	1.00	2.00	3.00	4.00	6.00	10.00	15.00	21.00	30.00

Table A.2.11 MFCV Recovery (Subject 8)

Subject 8			
Condition	Time (minutes) (with respect to fatigue)	MFCV metres/second	Temperature centigrade
prefatigue	before fatigue	2.8	25.8
post fatigue	0	2.4	27.0
post fatigue	1	3.0	27.2
post fatigue	2	3.2	27.7
post fatigue	3	3.2	28.2
post fatigue	4	3.5	28.5
post fatigue	6	3.5	28.8
post fatigue	10	3.8	28.5
post fatigue	15	3.8	27.9
post fatigue	21	3.5	27.3
post fatigue	30	3.8	26.8

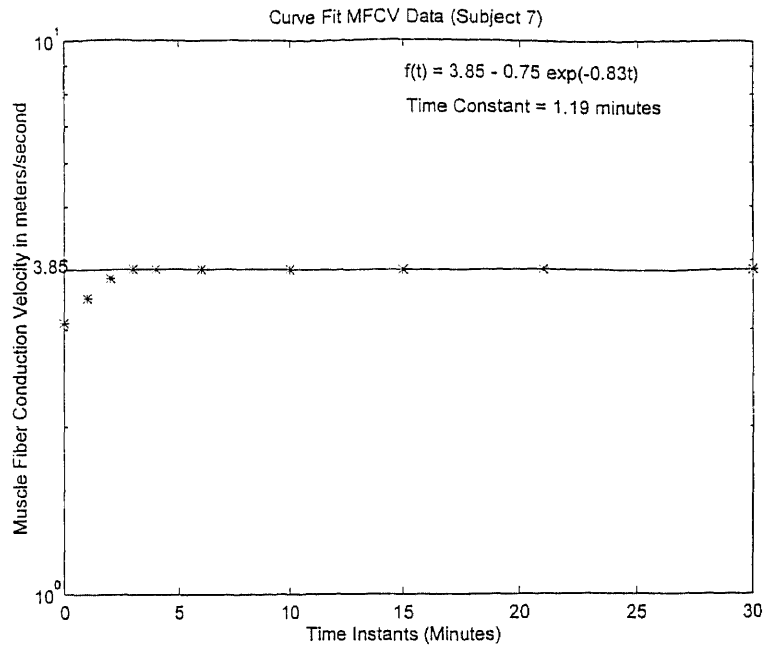


Figure A.2.9
Curve Fitted MFCV Data (Subject 7)

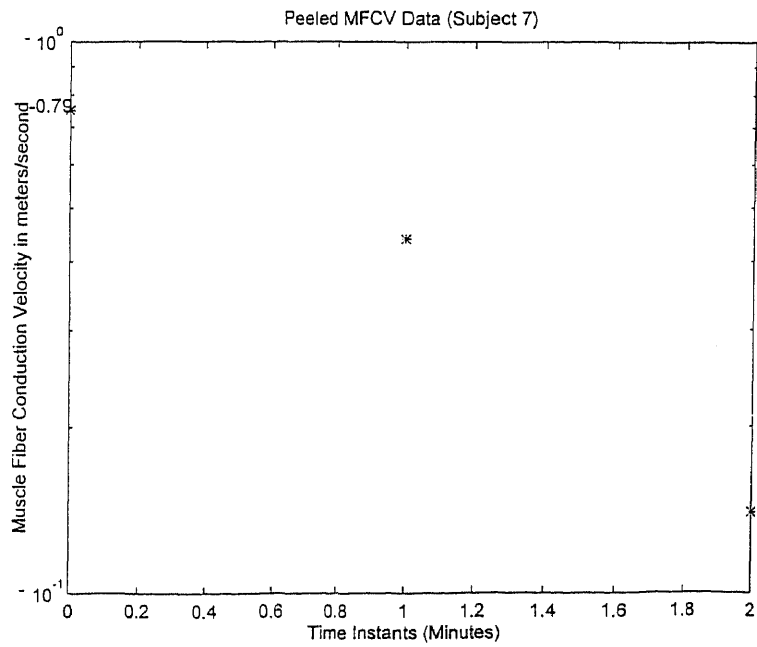


Figure A.2.10
Peeled MFCV Data Points (Subject 7)

Table A.2.12 Smoothed MFCV Data Points Plotted using the Exponential Peeling Technique (Subject 8)

Subject 8 Recovery										
F(t)	2.76	2.94	3.12	3.28	3.43	3.53	3.7	3.8	3.8	3.8
F1(t)	-1.04	-0.86	-0.68	-0.52	-0.37	-0.25	-0.1			
t minutes	0.00	1.00	2.00	3.00	4.00	6.00	10.00	15.00	21.00	30.00

Table A.2.13 MFCV Recovery (Subject 9)

Subject 9			
Condition	Time ((with respect to fatigue)	MFCV metres/second	Temperature centigrade
prefatigue	before	2.8	26.3
post fatigue	0	-	26.7
post fatigue	1	2.5	26.8
post fatigue	2	2.8	27.0
post fatigue	3	2.6	27.3
post fatigue	4	2.8	27.5
post fatigue	6	3.0	27.8
post fatigue	10	2.8	28.4
post fatigue	15	3.0	28.1
post fatigue	21	2.8	27.7
post fatigue	30	2.8	26.7

Table A.2.14 Smoothed MFCV Data Points Plotted using the Exponential Peeling Technique (Subject 9)

Subject 9 Recovery										
F(t)	2.39	2.51	2.63	2.69	2.8	2.8	2.8	2.8	2.8	2.8
F1(t)	-0.41	-0.29	-0.17	-0.11						
t minutes	0.00	1.00	2.00	3.00	4.00	6.00	10.00	15.00	21.00	30.00

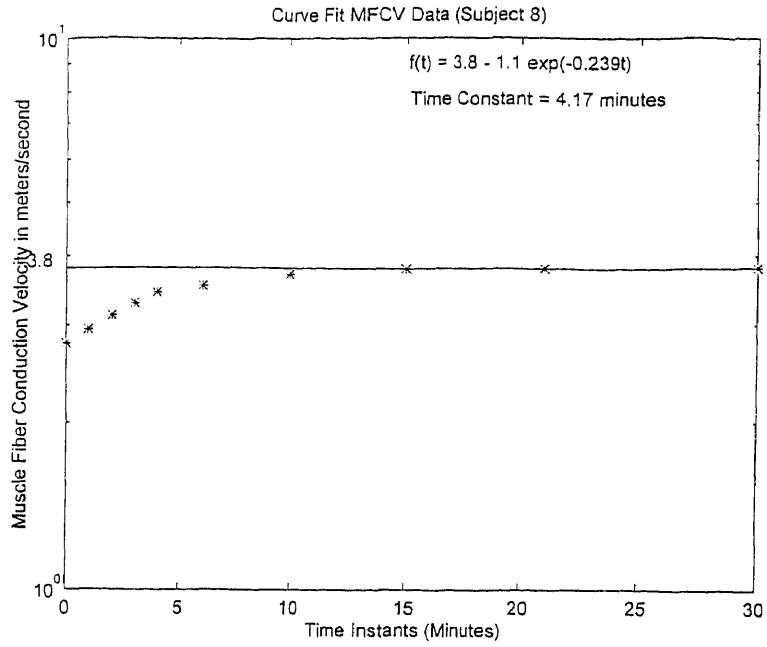


Figure A.2.11
Curve Fitted MFCV Data (Subject 8)

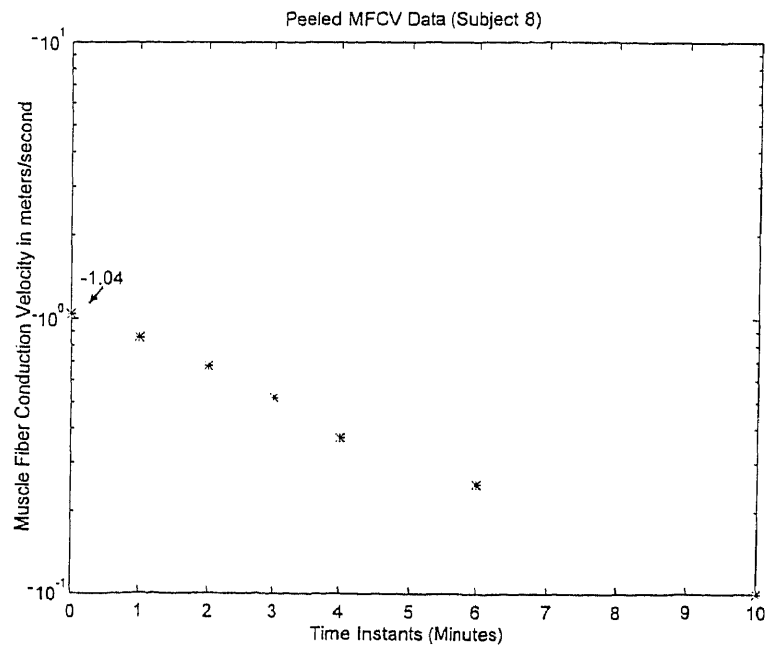


Figure A.2.12
Peeled MFCV Data (Subject 8)

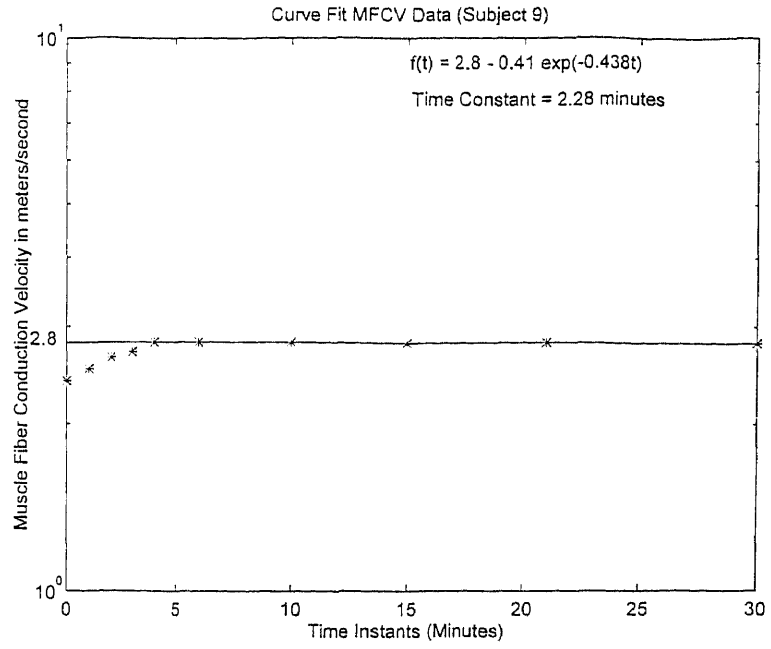


Figure A.2.13
Curve Fitted MFCV Data (Subject 9)

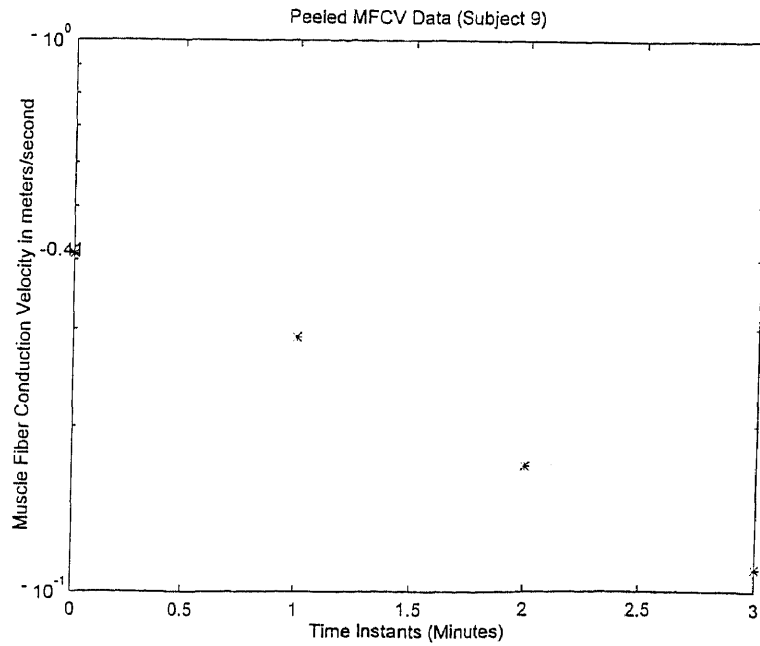


Figure A.2.14
Peeled MFCV Data (Subject 9)

A.3 Precision Decomposition

a) Subject C

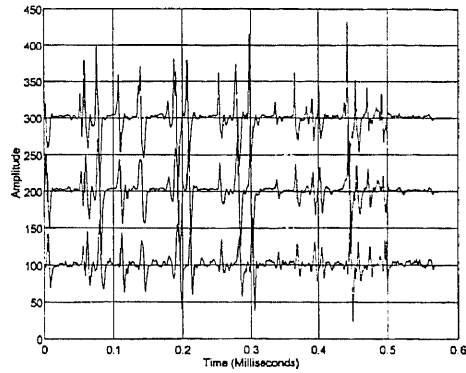


Figure A.3.1
Filtered Original Signal (0.58 secs.)
(low pass: cut off 300Hz)

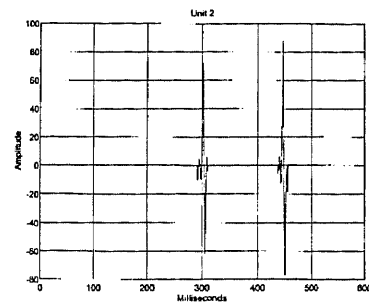


Figure A.3.4
Decomposed Signal (Unit II)
Decision criterion (0.35)

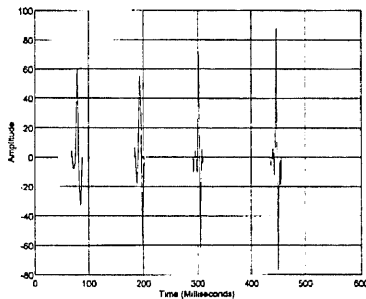


Figure A.3.2
Amplitude Thresholded Signal (55 mV)

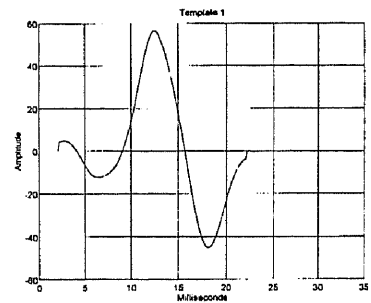


Figure A.3.5
Template 1 (Unit I)

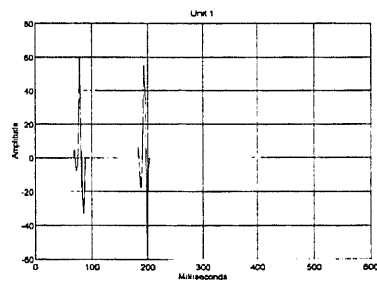


Figure A.3.3
Unit I

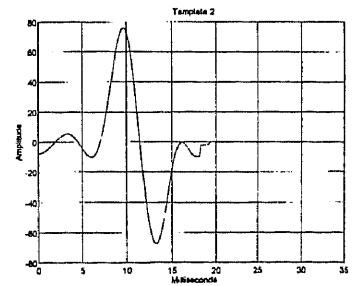


Figure A.3.6
Template 2 (Unit II)

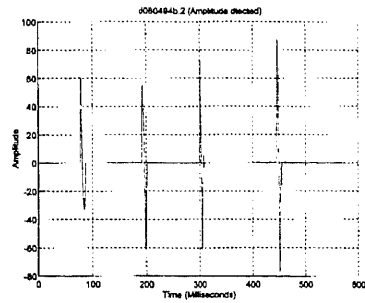


Figure A.3.7
Amplitude Thresholded Signal (55mV)
(120 points of signal)

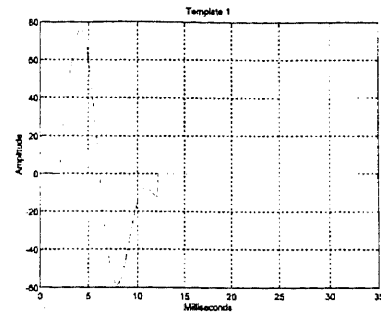


Figure A.3.10
Template I (Unit I)

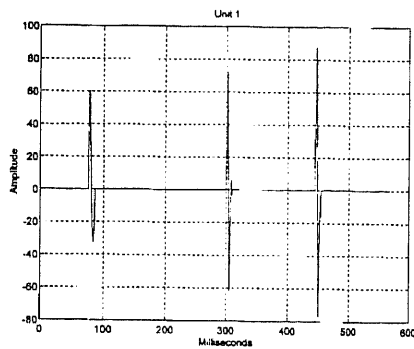


Figure A.3.8
Decomposed Signal (0.35) (Unit I)

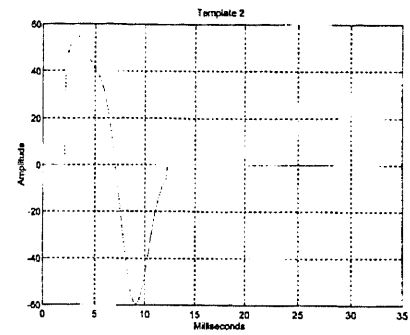


Figure A.3.11
Template II (Unit II)

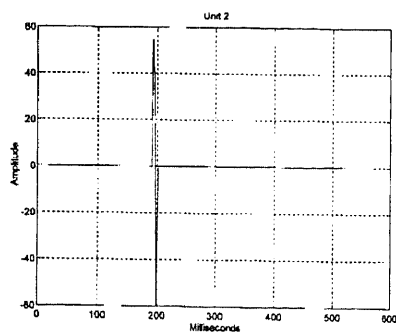


Figure A.3.9
Decomposed Signal (Unit II)
Decision Criterion (0.35)

b) Subject D

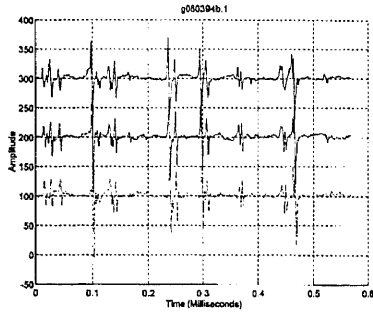


Figure A.3.12
Original Filtered Signal (300 Hz)
(0.58 secs.)

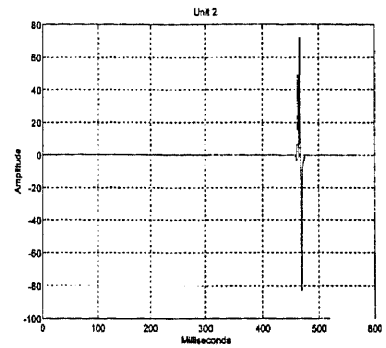


Figure A.3.15
Decomposed Signal (Unit I)
Decision Criterion (0.35)

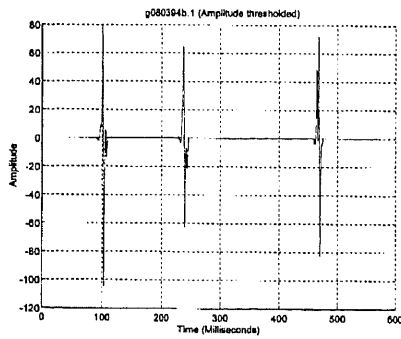


Figure A.3.13
Amplitude Thresholded Signal (55 mV)

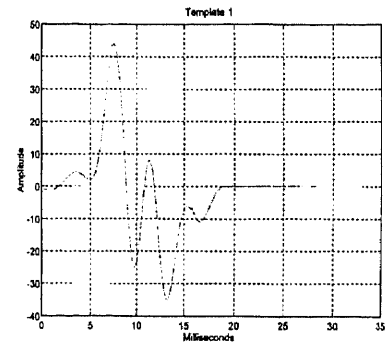


Figure A.3.16
Template I (Unit I)

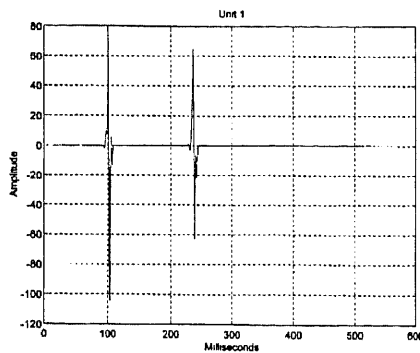


Figure A.3.14
Decomposed Signal (Unit I)
Decision Criterion (0.35)

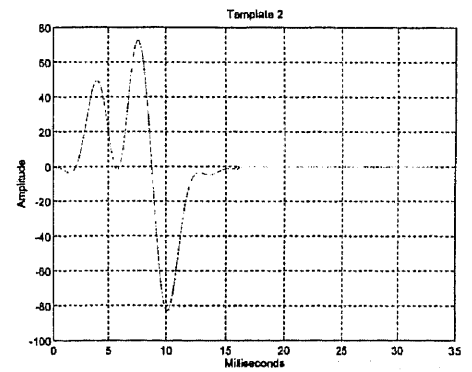


Figure A.3.17
Template II (Unit II)

APPENDIX B

INSTRUMENTATION

This section gives the details of instrumentation equipment that were used in this study.

B.1 Precision load cells

A load cell is in effect a strain gage. It works on the same principle as that of a strain gage. It measures force and pressure. Here the load cell manufactured by SENSOTEC was used. Details regarding the same are given below.

The SENSOTEC's (Model 31) precision load cell was used to measure the force exerted by the subject (i.e. 5% MVC or 20% MVC) figure B.1 shows us the load cell which was used for this study.

The salient features of this load cell are as follows. The model 31 load cell is capable of measuring both tension and compression forces of 50 grams to 10000 lb. This load cell has a stainless steel construction and uses a "tripled" stack design to eliminate the effects of off axis loads. The engineered concepts of larger load cells i.e. precision calibration, stabilizing diaphragms and pressure compensation are built into these miniature load cells.

Finally these load cells are available in several force measurement ranges and for this study only two measurement ranges were used i.e. 1000 grams and 250 lbs.

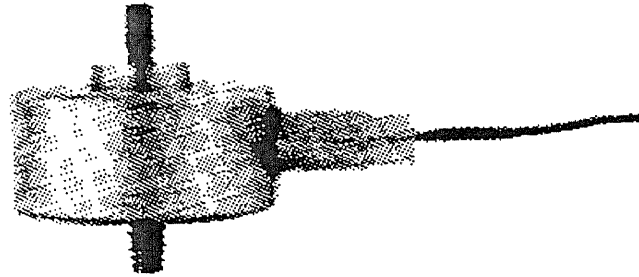


Figure B.1
The SENSOTEC Load Cell (Model 31)

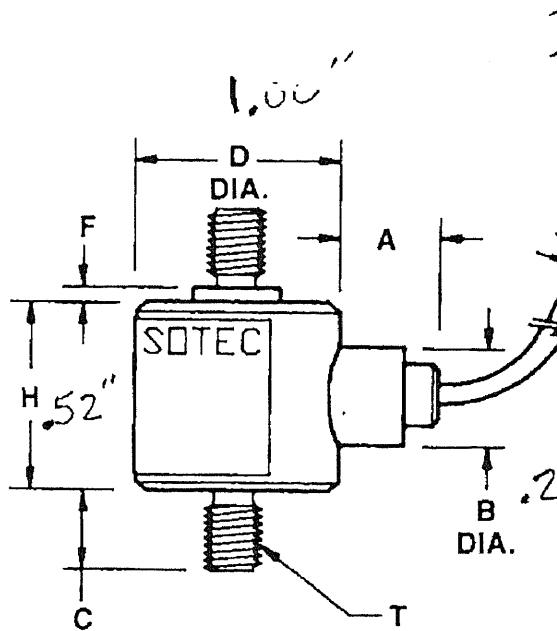


Figure B.2
Dimensions of the SENSOTEC Load Cell

B.2 Instrumentation Amplifier

This study involved the study of the EMG . As mentioned in section 1.3 the amplitude of the EMG varies between 50 microvolts to 500 millivolts. Hence an amplification of the signal is required before digitizing the raw EMG data that is picked up from the electrode

Owing to the small amplitude of the EMG signal an instrumentation amplifier was used in this study. An instrumentation amplifier is an amplifier which has a range of gain settings, filter settings, input buffering, dc offsets and has the ability to amplify input signals of different amplitude ranges.

The GOULD Universal instrumentation amplifier (Model 13 - 4615 -58) was used in this case. This acts as an excellent differential AC or DC signal conditioner and performs as a highly sensitive transducer amplifier. It is a good biophysical amplifier and when utilized with an isolated preamplifier provides excellent isolation. High input impedance, wide bandwidth, low noise, low drift and transducer excitation have all been incorporated in this amplifier to produce good signal conditioning . Figure B.2a gives shows us the various settings available in the amplifier. Figure B.2b gives us one possible configuration in which this amplifier can be used.

The key features of this amplifier are listed below.

Measurement range -----	2.5mV - 10 V full scale or 25 μ V - 250 mV full scale
Excitation voltage-----	5.0 volts \pm 5 mV
Notch filter-----	60 Hz reject filter (Adjustable to 50 Hz)

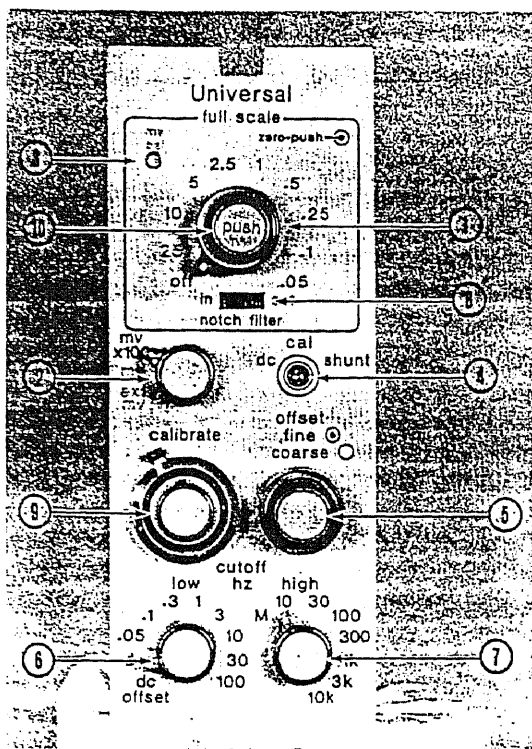


Figure B.2a
Settings available in GOULD amplifier (13-4615-58)

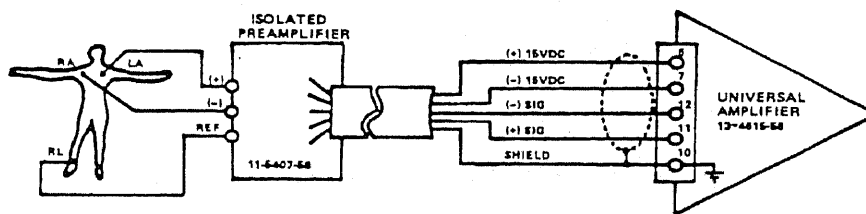


Figure B.2b
A typical experimental configuration of the
GOULD (13-4615-58) amplifier

Impedance-----100 Megaohms(each input
to chassis)

Power requirements-----± 15V

B.3 Isolated Preamplifier (Model 13 - 5407 - 58)

Any study conducted in the biomedical area obviously involves human subjects. Hence a need is felt for an isolation between the subject who is being tested and the electrical circuitry that is being used for the measurements. The GOULD isolated preamplifier was used in this study for the purposes of isolation, buffering and amplification

Figure B.3 shows us the isolation amplifier that was used in this study.

The key features of the isolation amplifier are indicated below.

Impedance-----	DC to 60 Hz
Between inputs-----	> 10 megaohms with common mode signals
Input to chassis-----	> 50 megaohms each input to chassis.

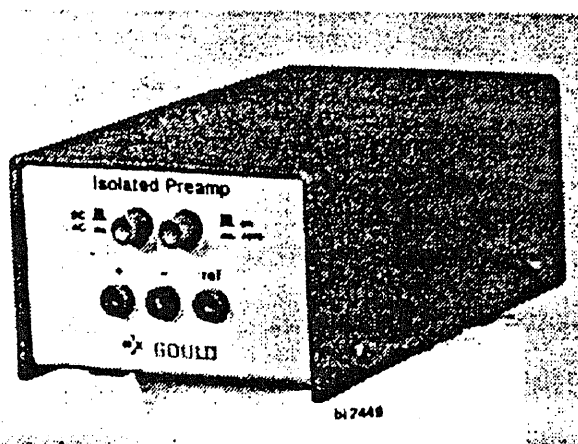


Figure B.3
The Isolated Preamplifier
GOULD (13-5407-58)

B.4 Data Acquisition Board (Keithley Das 1601)

The raw EMG signal that was acquired from the electrodes was sampled and digitized using the DAS 16 data acquisition board. The DAS 16 is a high speed data acquisition board which has the following features. It can sample at a rate of 100 Ks/s. It can be in an 8 channel bipolar mode configuration or in a 16 channel unipolar mode. In this study the DAS 16 was used in the 8 channel bipolar configuration as the EMG input signals were acquired differentially.

APPENDIX C

DATA ACQUISITION

The first step in the data acquisition process was setting up the files for storage of the digital raw EMG data, which was to be picked up by the electrodes. Streamer's™ make file utility was used to create the data files of appropriate size.

The make file utility provided by the Streamer™ software allocates contiguous memory locations for the binary (digitized) data to be stored. This utility is invoked by saying MKFILE at the dos prompt. The mkfile utility provided by streamer requires two inputs. One, being the name of the data file with an extension of '.dat' and second, the size of the data file in kilobytes. A typical command line is indicated below.

eg. C:\> mkfile test.dat 450

The above command informs the mkfile utility to create a contiguous data file of 450 kilobytes for storage of the digitized data.

As mentioned above the mkfile utility requires the size of the data file to be specified as one of its input arguments. Hence we need to determine the exact size of the data file and this is done as follows.

$$Size = \#ch * SR / ch * time * 2 \quad (A.1)$$

where

Size - Size of the data file (kilobytes)

#ch - Number of channels which need to be sampled and digitized.

SR/ch - Sampling rate per channel in kilohertz (khz)

time - Specifies the duration of the experiment (seconds)

We observe from A.1 that the above mentioned variables are multiplied by a factor of 2. This is because each digitized sample takes up 2 bytes and a data file consists of several sample points.

The data file was then converted (“unpacked”) into ASCII files for subsequent handling by the data analysis softwares like MATLAB™ and S Plus™. The unpack program provided by KEITHLEY™ was used for converting the binary dat files into ASCII data files. The unpack program was modified at our R&D lab so that channel numbers were not printed before the digitized values of each channel. This program was renamed as kunpack2.exe and this was the unpacking program used for this study.

Batch files

a) **Unpacking:-** The 2 and 5 seconds of data were unpacked using batch files developed by the author. These batch are attached below for reference.

1) File name - **fchan.bat** (unpacks the five second data file into 5 ASCII files)

This program is copyright protected

Satheesh Kumar Swaminathan

kunpack2 %1.dat,%1.1,0-46079/b/das16

kunpack2 %1.dat,%1.2,46080-92159/b/das16

kunpack2 %1.dat,%1.3,92160-138239/b/das16

kunpack2 %1.dat,%1.4,138240-184319/b/das16

```
kunpack2 %1.dat,%1.5,184320-230400/b/das16
```

Each ASCII file contains 1.024 seconds of data.

2) File name - **sat.bat** (unpacks the two second data file into 2 ASCII files)

```
kunpack2 %1.dat,%1.1,0-46079/b/das16
```

```
kunpack2 %1.dat,%1.2,46080-92159/b/das16
```

Each ASCII file contains 1.024 seconds of data.

It is to be noted that das16 refers to the Analog to Digital converter board which is used to digitize the raw EMG signal.

b) MKFILE (batch mode)

```
satemg1.bat ( calls satemg.bat )
```

```
satemg.bat ( uses mkfile to make twenty data files of specified size )
```


APPENDIX D

FLOWCHARTS AND PROGRAMMING DETAILS

D.1 Muscle Fiber Conduction Velocity (MFCV)

As mentioned in section 1.3 the MFCV was estimated using the cross correlation technique. Details regarding the technique and the explanation of the technique, are available in section 1.3. However the actual algorithm and the MATLAB™ source code for computing the MFCV are provided below.

Figure D.1 gives us the flow chart which outlines the steps involved in the computation of muscle fiber conduction velocity. The details of the various programs used in the calculation of the MFCV are given below.

kscorr.m (script file)

command line: - kscorr

% Main script file wherein values are supplied to the variables by the user.%

```
disp('Please supply the appropriate variables');
s = input('Enter the ascii filename without extension ->','s');
i = input('Enter the extension of the Ascii File ->');
x = sprintf('%s.%d',s,i);
eval(['load ' x]);
p = eval(s);
SR = input('Please enter the Sampling frequency ->');
string1 = 'Yes';
string2 = 'Yes';
while(strcmp(string1,string2))
    snewsat(SR,p,x)
    string2 = input('Would like to take a look at the data again? [Yes/No] ->','s');
end;
disp('Continuing execution of kscorr.m .....');
pause(1);
disp('The following determine which channels are to be correlated');
```

```

disp('Enter the channels which you want to correlate as numbers');
ch1 = input('Enter a number for the first channel..->');
ch2 = input('Enter a number for the second channel..->');
disp('Please note enter the start point of the section');
disp('as 101 or 201 etc keep note of the 1 extra point');
disp('Note channel which is supplied as channel 1 should fire after the channel 2 !!');
disp('The signal supplied as channel 1 should be atleast the length of channel 2 + shift
value');
st1 = input('Enter the start point of the section of channel 1 ->');
ed1 = input('Enter the end Point of the section of channel 1 ->');
st2 = input('Enter the start point of the section of channel 2 ->');
ed2 = input('Enter the end Point of the section of channel 2 ->');
chan1 = p( :,ch1);
chan2 = p( :,ch2);
test1 = chan1(st1:ed1);
test2 = chan2(st2:ed2);
disp('Enter the amount by which the channels are to be shifted');
shift = input('Enter the shift value -> ');
distance = input('Pl. enter the spacing between the electrodes in Metres!! -> ');
ret = kfindcorr(SR,test1,test2,shift,distance,x);

```

snewsat.m (script file)

```

command line: - snewsat
%Script file calling cvnewsat.m %

```

function snewsat(SR,p,x)

```

disp('Make Sure that you load the file before running the script file');
pause(2);
disp('Please enter the values for the function in the following order');
pause(2);
i = input('Please enter the start channel from which to start display ->');
start = input('Please enter the start pt. from which you wish to view -> ');
end1 = input('Please enter the end pt. upto which you wish to view ->');
order = input('Please enter the order of the filter in case you need it ->');
cutoffreq = input('Please enter the cutoff frequency in hertz that you want ->');
[var1 var2]=cvnewsat(SR,p,x,i,start,end1,order,cutoffreq);

```

cvnewsat.m

```

command line : - [ret1, ret2] = cvnewsat(SR, x, test, I, start, end1, order, cutoffreq)
Displays 'n' channels of a file after digital filtering.
function [ret1,ret2] = cvnewsat(SR,x,test,i,start,end1,order,cutoffreq)

```

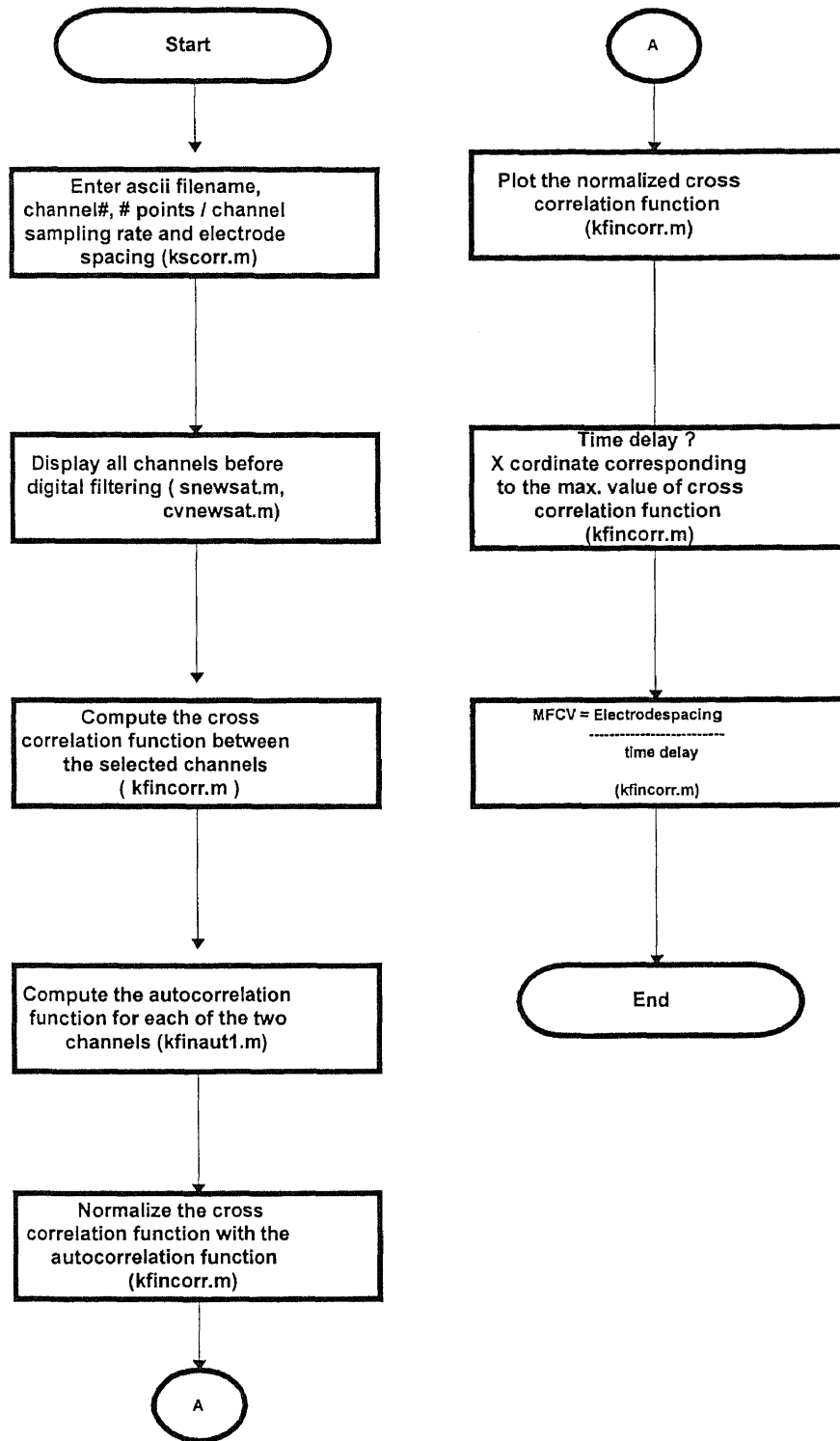


Figure D.1
Flowchart Showing the Steps Involved in the Computation of MFCV

```

colors = ['g','r','b','c','m','y'];
sx = size(x);
fchan = zeros(sx(1), 4);
chan = zeros(sx(1),4);
j = 1;
count = 1;
index = 1;
i2 = 1;
figure
hold
    while ( i <= 4)
        ch = x( :,i);

        if( order > 0 & cutofffreq >0)
            hsfreq = SR/2;
            cfreq = cutofffreq/hsfreq;
            [b,a] = butter(order, cfreq);
            fch=filter(b,a,ch);
            count = count + 1;

            if(count > 2)

                if(j <= 6)
                    plot((fch(start:end1)+(i*100)),colors(j));
                    j = j + 1;
                    i = i + 1;
                    if(i2 <= 4)
                        fchan( :,i2) = fch;
                        i2 = i2 + 1;

                    end;
                else
                    j = 1;
                    plot((fch(start:end1)+i*100),colors(j));
                    j = j + 1;
                    i = i + 1;

                    if(i2 <= 4)
                        fchan( :,i2) = fch;
                        i2 = i2 + 1;

                    end;
                end;
            end;

        else

            plot((fch(start:end1)+(i*100)),colors(j))

```

```

        j = j + 1;
        i = i + 1;
            if(i2 <= 4)
                fchan( :,i2) = fch;
                i2 = i2 + 1;
            end;
        end;
else
        count = count + 1;
        if( count > 2)

            if(j <= 6)

                plot((ch(start:end1) + i*100), colors(j));
                i = i + 1;
                j = j + 1;
                if( i2 <= 4)
                    chan( :,i2) = ch;
                    i2 = i2 + 1;
                end;

            else
                j = 1;
                plot((ch(start:end1)+ i*100), colors(j));
                i = i + 1;
                j = j + 1;
                if( i2 <= 4)
                    chan( :,i2) = ch;
                    i2 = i2 + 1;
                end;
            end;
        end;
else
        plot((ch(start:end1) + i*100),colors(j));
        j = j + 1;
        i = i + 1;
        if(i2 <= 4)
            chan( :,i2) = ch;
            i2 = i2 + 1;
        end;
    end;
end;
end;
hold off
grid
title(sprintf('%s',test))
ylabel('Amplitude');

```

```

xlabel('Index Points');
keyboard
ret1 = fchan;
ret2 = chan;

```

kfincorr.m

command line: - ret = kfincorr(SR, signal1, signal2, shift, distance, str)
 % Performs the correlation between two input signals %

```
function ret = kfincorr(SR,test1,test2,shift,distance,str)
```

```

x = test1;
y = test2;
shift1 = shift;
len2 = length(test2);
corr = zeros(shift1,1);
ret = zeros(shift1,1);
counter = 1;
i = 1;
j = 1;
count = 1;
jcount = 1;
sum = 0;
i2 = 1;
% Both lengths should not be equal ! %

```

```
while(counter <= shift1)
```

```

    while(j <= len2 )
        sum = sum + x(i) .* y(j);
        i = i + 1;
        j = j + 1;

```

```

    end;
    corr(i2,1) = sum;
    i2 = i2 + 1;
    sum = 0;
    counter = counter + 1;
    icount = icount + 1;
    i = icount;
    j = jcount;

```

```
end;
```

```

sauto1 = kfinaut1(x,len2);
sauto2 = kfinaut1(y,len2);
norm = sauto1 .* sauto2;
corr = corr/norm;

```

```

ret = corr;

[maximum,I] = max(corr);
Timedelay = I/SR;
MFCV = distance/Timedelay;

% Scaling the Correlation Plot %
indx = 1:1:length(corr);
taxis = (indx/SR) .* 1000; % Time in Milliseconds %
figure;
pause;
plot(taxis,corr,'r');
grid;
title(sprintf('The value of Conduction Velocity is %f metres/second for
              %s',MFCV,str));
ylabel('Amplitude');
xlabel('Time in Milliseconds');

```

kfinaut1.m

```

command line: - kfinaut1.m
% Performs the auto correlation of a signal %
function sauto = kfinaut1(x, len2);
sig1 = x;
i = 1;
count1 = len2;
count = 1;
sum1 = 0;
    while(count <= count1)
        sum1 = sum1 + sig1(i) .* sig1(i);
        i = i + 1;
        count = count + 1;
    end;
sauto = sqrt(sum1);

```

function satldraw(x,filename)

```

% linedraw.m
% Creates a new vector based on linear regression
% and plots data with best-fit line, slope, intercept,
% and correlation coefficient.
% USES data in workspace: x
% USES data in workspace: plotfitfilename
% CREATES 1x3 vector P=[slope, intercept,coeff]
% CALLS Function LineFit for regression calculations
%
last=length(x)

```

```

P=linefit(x(1:last))
newx=1:1:last;
newpfity=P(2)+P(1).*newx;
figure
plot(x(1:last),'c*')
hold
plot(newpfity,'r')
hold off
tstring1=sprintf('slope = %4.3f,P(1));
tstring2=sprintf('y int = %4.3f,P(2));
tstring3=sprintf('r val = %1.3f,P(3));
text(4,min(x(2:last))+0.95.*(max(x(2:last))-min(x(2:last))),tstring1)
text(4,min(x(2:last))+0.85.*(max(x(2:last))-min(x(2:last))),tstring2)
text(4,min(x(2:last))+0.75.*(max(x(2:last))-min(x(2:last))),tstring3)

title(sprintf('The file is %s and the no of points taken are ->%d',filename,last));
xlabel('Time instants in minutes ')
ylabel('Muscle fiber conduction velocity in metres/second');

%print

%clean up
clear newx
clear newpfity
clear tstring1
clear tstring2
clear tstring3
clear P

```

Linefit.m

```

function lineFit=fit(y)
% Determine coefficients of a least-squares fit to
% data vector passed in y, storing parameters in
% 1x3 vector P[ slope intercept coeff]
%-----
% USES data passed in y
% CREATES 1x3 vector P=[slope, intercept, coeff]
% CALLS non
%
x=1:1:length(y);
Mnum=sum(x.*y)-sum(x)*sum(y)/length(x);
den=sum(x.*x)-sum(x)^2/length(x);
Mslope=Mnum/den
%Bintercept
Bnum=[sum(x.*x)*sum(y)-sum(x)*sum(x.*y)]/length(x);

```



```

Bintercept=Bnum/den;
rcoeff=Mnum/sqrt(den*[sum(y.*y)-sum(y)^2/length(x)]);
lineFit=[ Mslope Bintercept rcoeff];
%cleanup
%done

```

D.2 Precision decomposition

As described in section 1.3.2 the objective of the precision decomposition technique was to decompose the myoelectric signal into its constituent motor units. The actual algorithm and the software implementation of the algorithm are described below. Figure D.2 gives us a flow chart which explains the algorithm for performing the decomposition.

Programs

sampl1.m (script file)

command line: - sampl1

% Script file that calls amplitdet1.m %

```

disp('pl.follow the instructions as given below');
str = input('Enter the name of the ascii file without extension ->','s');
ext = input('Enter the extension of the file ->');
x = sprintf('%s.%d',str,ext);
eval(['load ',x]);
p = eval(str);

i = input('Enter the start channel ->');
start = input('Enter the start point from which to view ->');
end1 = input('Enter the end point upto which you have to view ->');
order=input('Enter the order of the filter in case you need it ->');
frequency = input('Enter the required cutoff freq. for the filter ->');
samplefreq = input('Enter the frequency at which the signal was sampled ->');
[var1,var2] = spnewsat(p,i,start,end1,order,frequency,samplefreq);

pause(1);
disp('Pl. note down the section of the signal');
disp('Entering the Amplitude Detection Section.....');
chnum=input('Enter the desired channel ->');
st1 = input('Enter the start point of the channel ->');
en1 = input('Enter the end point of the selected channel ->');
th = input('Enter the Threshold value ->');
fch = var1( :,chnum);
signal = fch(st1:en1);

```

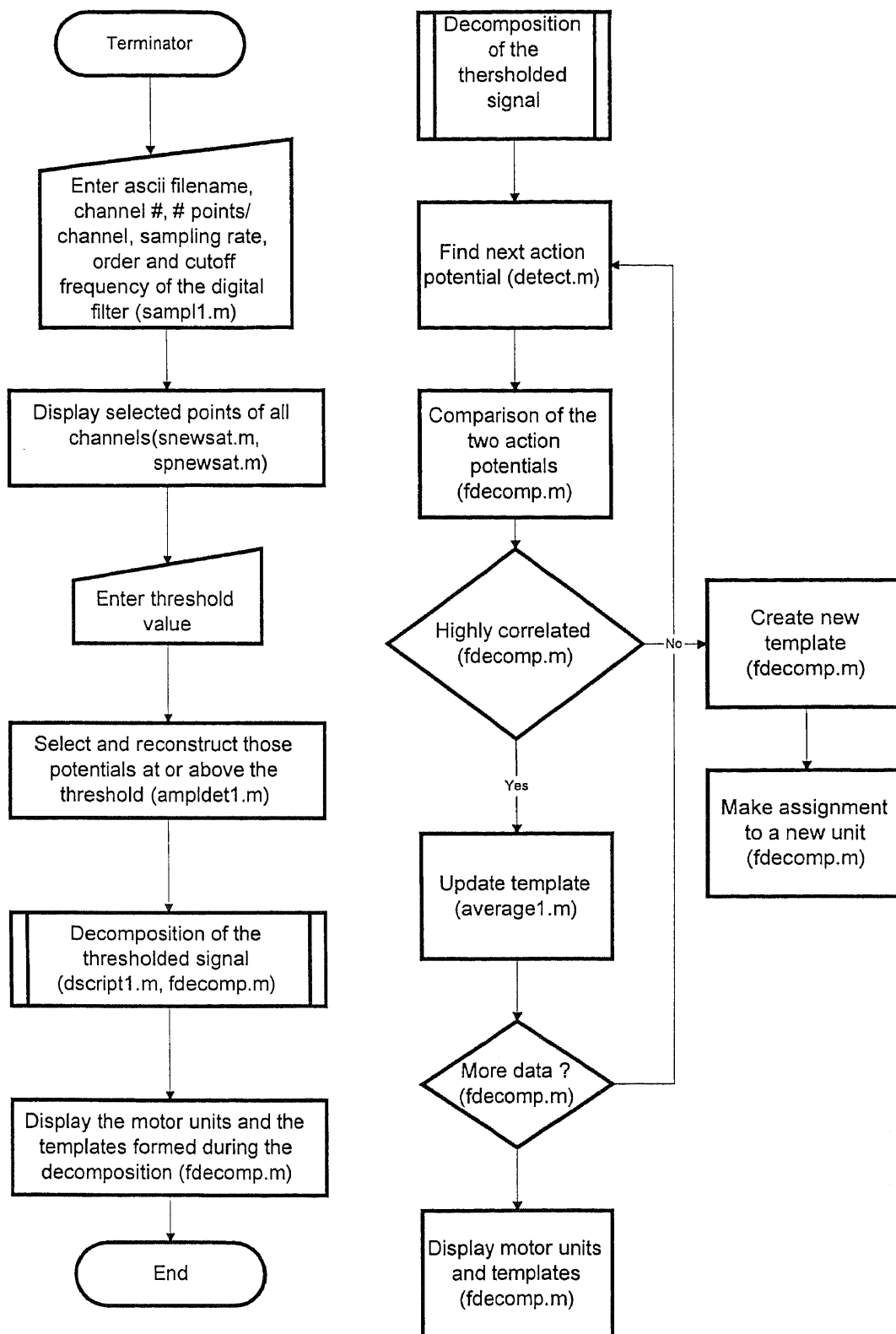


Figure D.2
Flowchart Outlining the Steps to be Carried Out during Precision Decomposition

```
detsig = ampldet1(signal,th,samplefreq);
```

ampldet1.m

```
command line : - ampldet1( signal, th, SR)
```

```
% Reconstructs only those action potentials above a certain amplitude threshold %
```

```
sigvector = signal;
```

```
thresh = th;
```

```
j = 1;
```

```
indx = 1;
```

```
beginindex = 1;
```

```
len = length(sigvector);
```

```
store = zeros(len,1);
```

```
counter =1;
```

```
count = 1;
```

```
count1 = 1;
```

```
while(j <= len)
```

```
    if(sigvector(j) >= thresh)
```

```
        reconstruct = (j - beginindex) + 1;
```

```
        % reconstructing the left hand side of the signal %
```

```
        s1 = sprintf('The no. of points available are -> %s',  
                    num2str(reconstruct));
```

```
        disp(s1)
```

```
        if(reconstruct > 30)
```

```
            disp('Enter the reconstruction number judiciously');
```

```
            recon = input('Enter the number of pts. on the left to be  
                          reconstructed > 30');
```

```
            newindx = (j - recon) + 1;
```

```
            indx = newindx;
```

```
            while(counter <= recon)
```

```
                store(indx) = sigvector(newindx);
```

```
                indx = indx + 1;
```

```
                newindx = newindx + 1;
```

```
                counter = counter + 1;
```

```
            end;
```

```
            counter = 1;
```

```
        else
```

```
            newindx = (j - reconstruct) + 1;
```

```
            indx = newindx;
```

```

while(count <= reconstruct)

    store(indx) = sigvector(newindx);
    indx = indx + 1;
    newindx = newindx + 1;
    count = count + 1;
end;

count = 1;

end;

% end of the reconstruction of the left hand side of the signal %

% reconstruction of the right hand side of the signal %
% this can proceed normally as you have more points to the right than to
the left%
% When you start %

count1 = 1;
j = j + 1;

while(count1 <= 80)

    store(indx) = sigvector(j);
    indx = indx + 1;
    j = j + 1;
    count1 = count1 + 1;

end;
count1 = 1;
beginindex = j;

% end of the case wherein the value of the signal is higher than the
threshold in the early stages %
% end of the first if condition %

else

    store(indx) = 0;
    j = j + 1;
    indx = indx + 1;

end; % end of the if statement %

```

```

end;

detsig = store;
figure;
hold;
t1 = 1:length(signal);
taxis1 = (t1/SR) .* 1000;

ylabel('Amplitude');
xlabel('Time (Milliseconds) ');
plot(taxis1,store,'r');
grid;
tit1=input('Pl. enter the title for the graph','s');
title(tit1);

```

dscrip1.m (script file)

command line :- dscrip

```

%Script file for decomposing the myoelectric signal into its Units %
[t,u] = fdecomp(detsig);

```

```

t1 = 1:length(detsig);
taxis = (t1/9000) .* 1000;

```

```

t2 = 1:200;
taxis1 = (t2/9000).* 1000;

```

```

r1 =20;
counter =1;

```

```

while(counter <= 9)

```

```

    if((t(r1,counter) == 0))

```

```

        counter = counter - 1;
        break;

```

```

    else

```

```

        counter = counter + 1;

```

```

    end;

```

```

end;

```

```

for i = 1:1:counter
    figure;

```

```

        plot(taxis,u(:,i),'b');
        title(sprintf('Unit %s',num2str(i)));
        ylabel('Amplitude');
        xlabel('Milliseconds');
        grid;

end;

disp('***** test*****')

for j = 1:1:counter
    figure;
    plot(taxis1,t(:,j),'g');
    title(sprintf('Template %s',num2str(j)));
    ylabel('Amplitude');
    xlabel('Milliseconds');
    grid;
end;

```

fdecomp.m

Command line :- [template1, units1] = fdecomp(detsig)

```

function [template1,units1] = fdecomp(detsig)
% Performs precision decomposition of the Myoelectric Signal %

    len1 = length(detsig);
    template = zeros(200,8);
    template1 = zeros(200,8);
    units = zeros(len1,8);
    units1 = zeros(len1,8);
    subtract = zeros(200,1);
    searchindx = 1;
    uendindx = ones(1,8);
    flg1 = ones(1,8);
    beginindx = 1;
    endindx = 1;

    % Loops to create empty two dimensional arrays %
    for j = 1:8
        for i = 1:200
            template(i,j)= 0;
        end;
    end;
    sigvector = detsig;

```

```

signal = detsig;
while(searchindx <= len1)

    [beginidx,endindx]=detect(detsig,searchindx);

    if(beginidx == [])
        break;
    else
        searchindx = endindx + 1;
        % This section moves the signal into the Template Array %
        % Search for empty spaces in the array %
        m = 20;
        l = 1;
        while(l <= 8)
            if(template(m,l) == 0)
                templno = l; % Gives the position of the current template %
                break;
            else
                l = l + 1;
            end;
        end;

        % Loading the signal into the template array %
        idx = beginidx;
        var1 = 1;
        while(var1 <= 200)
            template(var1,templno) = detsig(idx);
            var1 = var1 + 1;
            idx = idx + 1;
        end;
        var1 = 1;
        idx = 1;
        y = 1; % used in the program for comparison %
        count3 = 1;
        if(templno == 1)
            a = 1;
            b = 1;
            c = 1;
            ctr1 = 1;
            zeropad1 = (beginidx-1) + 1;
            while(ctr1 <= zeropad1)
                units(a,templno) = 0;
                a = a + 1;
                ctr1 = ctr1 + 1;
            end;
            flg1(templno) = flg1(templno) + 1;

```

```

while(count3 <= 200)

    units(a,b) = template(c,templno);
    a = a + 1;
    c = c + 1;
    count3 = count3 + 1;
end;
uendindx(templno) = a;
else
y = 1;
% comparing the two signals using the distance measure %
while(y < templno)
    [max1,I1] = max(template( :,y));
    [max2,I2] = max(template( :,templno));
    p = I1;
    q = I2;

    if(I1 > I2)

        % Subtracting LHS of signal %
        indx1 = I2;
while(q >= 1)
    subtract(indx1) = template(p,y) - template(q,templno);
    indx1 = indx1 - 1;
    p = p - 1;
    q = q - 1;
end;
% End of Subtraction %
% Subtracting RHS of Signal %

    p = I1;
    q = I2;
    diff1 = (200 - I1);
    indx1 = I2 + 1;
    count = 1;
    p = p + 1;
    q = q + 1;
    while(count <= diff1)
        subtract(indx1) = template(p,y) -
        template(q,templno);
        indx1 = indx1 + 1;
        p = p + 1;
        q = q + 1;
        count = count + 1;
    end;
else

```



```

indx1 = I1;
while(p >= 1)
    subtract(indx1) = template(p,y) -
        template(q,templno);

    indx1 = indx1 - 1;
    p = p - 1;
    q = q - 1;
end;

p = I1;
q = I2;
diff1 = 200 - I2;
indx1 = I1 + 1;
p = p + 1;
q = q + 1;
count1 = 1;
while(count1 <= diff1)
    subtract(indx1) = template(p,y) -
        template(q,templno);
    p = p + 1;
    q = q + 1;
    count1 = count1 + 1;
end;
    % End of Subtraction of the signal %
end;
% End of the if condition for aligning the peaks %
subtract1 = subtract.^2;
numtr = sum(subtract1);
numtr = sqrt(numtr);
snumtr = numtr.^2;
den = template(:,y);
dentr = den.^2;
dentr = sum(dentr);
dentr = sqrt(dentr);
sdentr = dentr.^2;
res = snumtr/sdentr;

if( res < 0.15 )
    flag = 't';
    temp = uendindx;
    new = begindx;
[reindx,template,units] = average1(template,units,templno,y,new,temp);
    uendindx(y) = reindx;
    break;
else

```

```

        flag = 'f';
        y = y + 1;
        end;
    end;
% End of the while loop which does the comparison of 2 signals using the template %
    if(flag == 'f')
        if(flag1(templno) == 1)
            zeropad1 = (begindx -1) + 1;
            ctr2 = 1;
            while(ctr2 <= zeropad1)
                units(uendindx(templno),templno) = 0;
                uendindx(templno) = uendindx(templno) + 1;
                ctr2 = ctr2 + 1;
            end;
            flg1(templno) = flg1(templno) + 1;
            end;
            a1 = 1;
            ctr = 1;
            while(ctr <= 200)
                units(uendindx(templno),templno) = template(a1,templno);
                uendindx(templno) = uendindx(templno) + 1;
                a1 = a1 + 1;
                ctr = ctr + 1;
            end;
        end;
    end; % end of the if loop checking if the signal is the first
one %
    end;
clear beginindx endindx;
end; % end of the main while loop that goes upto length of the signal %
disp('end of signal bye!');
template1 = template;
units1 = units;

```

detect.m

command line :- [ret1, ret2] = detect (detsig, searchindx)

% Returns the beginindex and the endindex of a single action potential %

```
function [ret1,ret2] = detect(sig,searchindx)
```

```
search = searchindx;
```

```
len2 = length(SIG);
```

```
while(search <= Len)
```

```
    if(sig(search) >= 1)
```

```
        newindx = search - 1;
```

```
        eindx = newindx + 199;
```

```

        break;
    else
        search = search + 1;
    end
end;

```

```

    ret1 = newindx;
    ret2 = eindx;

```

average1.m

command line : -

```
function [rindx,tplte,uts1] = average1(templ,uts,templno1,y1,begindx1,temp)
```

```
% This function performs the average of two signals %
```

```
% In this application it performs an updation of the template %
```

```

    template2 = templ;
    units2 = uts;
    templ2 = templno1;
    y = y1;
    begindx2 = begindx1;
    ueidx1 = temp;          % Temporary variable for storing the endindex of each unit
                           % array %

    counter = 1;
    m = 1;
    while(counter <= 200)
        template2(m,y) = (template2(m,templ2) + template2(m,y))/2;
        m = m + 1;
        counter = counter + 1;
    end;

    % Which unit should I move to ?? %
    % I need to pad zeros between beginindex and uendindex %
    % This section pads zeros %
    newcount = 1;
    nindx = (begindx2 - ueidx1(y)) + 1;
    while(newcount <= nindx)
        units2(ueidx1(y),y) = 0;
        ueidx1(y) = ueidx1(y) + 1;
        newcount = newcount + 1;
    end;
    % this section reconstructs the signal after zeros have been padded %
    m = 1;
    count = 1;
    while(count <= 200)
        units2(ueidx1(y),y)=template2(m,templ2);
        m = m + 1;
    end;

```

```
    ueidx1(y) = ueidx1(y) + 1;
    count = count + 1;
end;
% This Section clears the template corresponding to the Template Number %
j = templ2;

for i = 1:200
    template2(i,j) = 0;
end;

rindx = ueidx1(y);
tplte = template2;
uts1 = units2;
```

REFERENCES

- [1] A. J. Vander, J. H. Sherman and D. S. Luciano, "*Human Physiology*," 5th Edition, New York, McGraw-Hill Company, 1990.
- [2] A. C. Guyton, "*Textbook of Medical Physiology*" 8th Edition, Philadelphia, W. B. Saunders Company.
- [3] M. Knaflitz, and B. Gabriella, "*Computer Analysis of the Myoelectric Signal*," IEEE Micro., 10: 12-15, 48-58.
- [4] W. H. Hollinshead and C. Rosse, "*Textbook of Anatomy*," 4th Edition, New York, Harper and Row publishers, 1985.
- [5] J. V. Basmajian and C. J. Deluca, "*Muscles Alive*," 5th Edition, Baltimore, Williams and Wilkins Publishers.
- [6] L. Cromwell, F. J. Weibell, and E. A. Pfeifer, "*Biomedical Instrumentation and Measurements*," 2nd Edition, New Delhi, Prentice Hall of India, 1990.
- [7] E. N. Marieb, "*Muscles and Muscle Tissue*," Human Anatomy and Physiology, 2nd Edition, California, The Benjamin/Cummings Publishing Company Inc., 246-269.
- [8] C. J. Deluca, "*Precision Decomposition of EMG Signals*," Methods in Clinical Neurophysiology, vol. 4; number 1, pp 1-28, 1993.
- [9] G. L. Gerstein and W.A. Clark, "*Simultaneous studies of firing patterns in several neurons*," Science, vol.143, pp 1325 - 1327, 1964.
- [10] D. G. Keehn, "*An iterative spike separation technique*," IEEE Trans. Biomed. Eng., vol.13, pp 19-28, 1966.
- [11] S. L. Ronald, and C. J. Deluca, "*A procedure for decomposing the myoelectric signal into its constituent action potentials (Part I : Technique, Theory and implementation)*," IEEE Trans. on Biomed. Eng., vol.29, pp 149 - 157, 1982.
- [12] A. N. Lars, R. M. Kerry and F. Allan, "*Changes in Muscle Fiber Conduction Velocity, Mean Power Frequency and Mean EMG voltage during prolonged submaximal contractions*," Muscle and Nerve, vol.12, pp 493-497, 1985.
- [13] B. Holger, G. Biloto, and C. J. Deluca, "*A note on the non invasive estimation of muscle fiber conduction velocity*," IEEE Trans. Biomed. Eng., vol. 32, number 5, pp 341 - 343, 1985.

- [14] P. Hilfiker and M. Meyer, "Normal and Myopathic Propagation of Surface Motor Unit Action Potentials," *Electroencephalography and Clinical Neurophysiology*, vol. 57, pp 21-31, 1984.
- [15] H. Broman, G. Biloto, and C. J. Deluca, "Myoelectric signal conduction velocity and spectral parameters : influence of force and time," *The American Physiological Society*, pp 1428-1436, 1985.
- [16] M. Naije, and H. Zorn, "Estimation of the action potential conduction velocity in the human skeletal muscle using the surface EMG cross correlation technique," *Electromyogr. clin. Neurophysiology*, vol. 23, pp 73-80, 1983.
- [17] S. Andreassen, "Computerized analysis of motor unit firings," *Computer Aided Electromyography*, pp 150-163, 1983.
- [18] P. Guiheneuc, J. Calamel, J. Doncarli, C. D. Gitton and C. Michel, "Automatic detection and pattern recognition of single unit motor unit potentials in needle EMG," *Computer Aided Electromyography*, pp 73-127, 1983.
- [19] K. C. McGill, and L. J. Dorfman, "Automatic Decomposition Electromyography : Validation and normative data in brachial biceps," *Electroenceph. Clin. Neurophy.*, vol.65, pp 453-461, 1985.
- [20] D. Stashuk and H. Debruin, "Automatic Decomposition of Selective Needle Detected Myoelectric Signals," *IEEE Trans. Biomed. Eng.*, vol.35, number 1, pp 1-10, 1988.
- [21] S. Nishimura, Y. Tomita and T. Horiuchi, "Clinical Application of an active electrode using an operational amplifier," *IEEE Trans. Biomed. Eng.*, vol. 39, number 10, pp 1096-1099, 1992.
- [22] R. Merletti, M. Knaflitz and C. J. Deluca, "Myoelectric Manifestations of Fatigue in voluntary and electrically elicited contractions," *J. Appl. Physiology*, vol. 69, number 5, pp 1810-1820, 1990.
- [23] L. R. Brody, M. T. Pollock, S. H. Roy, C. J. Deluca and B. Celli, "pH induced effects on median frequency and conduction velocity of, the myoelectric signal," *J. Appl. Physiology*, vol. 71, number 5, pp 1878-1885, 1993.
- [24] J. H. Van Der Hoeven, T. W. Van Weerden and M. J. Zwarts, "Long-Lasting Supernormal conduction velocity after sustained contraction in human muscle," *Muscle and Nerve*, vol. 16, pp 312 - 320, 1993.

- [25] H. J. Wim. P. Linssen, D. F. Stegeman, M. G. Ed Joosten, R. A. Binkhorst et al., "Fatigue in type I fiber predominance: A muscle force and surface EMG study on the relative role of type I and type II muscle fibers," *Muscle and Nerve*, vol. 14, pp 829 - 837, 1991.
- [26] T. Moritani, M. Muro and A. Nagata, "Intramuscular and surface electromyogram changes during muscle fatigue," *American Physiological Society*, pp1179-1185, 1986.
- [27] T. Moritani, A. Nagata and M. Muro, "Electromyographic manifestations of muscle fatigue," *Medicine and Science in Sports and Exercise*, vol. 14, no.3, pp198 - 202, 1982.
- [28] S. D. Nandedkar, E. V. Stalberg, D. B. Sanders, "Simulation techniques in electromyography," *IEEE Trans. Biomed. Eng.*, number 32, pp 775 - 785, 1985.
- [29] S. K. Alverstrand, R. Brandt, E. Hultman, "Intracellular pH and bicarbonate concentration in human skeletal muscle during recovery from exercise," *J. Appl. Physiol.*, number 45, pp 474 - 480, 1978.
- [30] R. Maniar, "Time Domain and Frequency Domain Analysis of the EMG," Masters Thesis, New Jersey Institute of Technology, January 1994.